Université de Montréal

Le rôle des rivières dans les dynamiques du carbone, de l'azote, et du phosphore selon des gradients d'utilisation du territoire et des contrastes climatiques

Par

Stéphanie Shousha

Département de sciences biologiques, Faculté des arts et des sciences

Thèse présentée en vue de l'obtention du grade de Philosophiae Doctor (Ph. D.)

en sciences biologiques

Avril 2022

Université de Montréal

Unité académique : Département de sciences biologiques, Faculté des arts et des sciences

---

Cette thèse intitulée

Le rôle des rivières dans les dynamiques du carbone, de l'azote, et du phosphore selon des gradients d'utilisation du territoire et des contrastes climatiques

Présenté par

Stéphanie Shousha

A été évaluée par un jury composé des personnes suivantes

Marc Amyot
Président-rapporteur

Jean-François Lapierre
Directeur de recherche

Roxane Maranger
Codirectrice de recherche

Matthew Bogard
Membre du jury

Nora Casson
Examinatrice externe

Résumé

Les rivières sont des écosystèmes dynamiques qui reçoivent, transforment, et exportent de la matière organique comprenant du carbone (C), de l'azote (N), et du phosphore (P). De par leur grande surface de contact entre l'eau et les sédiments, elles offrent un potentiel élevé pour les processus de transformation de ces éléments, dans lesquels ils sont souvent conjointement impliqués. Ces transformations peuvent retirer les éléments de la colonne d'eau et ainsi diminuer leurs concentrations pour améliorer la qualité de l'eau. Par contre, les conditions climatiques (débit, température, luminosité), la configuration du territoire (forêt, urbanisation, agriculture), et la durée des activités humaines sur terre affectent la quantité, composition, et proportion de C, N, et P livrés aux cours d'eau receveurs. Dans un contexte où un surplus de nutriments (N, P) peut surpasser la capacité des rivières à retirer les éléments de l'eau, et où les extrêmes climatiques s'empirent à cause des changements climatiques, cette thèse met en lumière le rôle des rivières dans les dynamiques de C, N, et P pour une meilleure compréhension de la réponse des écosystèmes lotiques aux pressions actuelles et futures.

La Rivière du Nord draine séquentiellement des régions couvertes de forêt, d'urbanisation, et d'agriculture, et oscille entre quatre saisons distinctes, l'exposant à des utilisations du territoire et conditions climatiques contrastées. Nous avons échantillonné les formes de C, N, et P à 13 sites le long du tronçon principal (146 km), une fois par saison pour trois ans. De façon générale, les concentrations de N et P totaux ont augmenté d'amont vers l'aval, concordant avec l'activité humaine plus importante dans la deuxième moitié du bassin versant, mais les concentrations de C organique total sont restées constantes peu importe la saison et l'année. La stœchiométrie écosystémique du C : N : P était donc riche en C comparé au N et P en amont, et s'est enrichie en nutriments vers l'aval. L'étendue (2319 : 119 : 1 à 368 : 60 : 1) couvrait presque le continuum terre – océan à l'intérieur d'une seule rivière. Des formes différentes de C, N, et P dominaient la stœchiométrie totale dépendamment des saisons et de l'utilisation du territoire. En été, la composition du N était dominée en amont par sa forme organique dissoute et par le nitrate en aval, tandis qu'en hiver, l'ammonium et le P dissous avaient préséance sur l'entièreté du continuum. Malgré une concentration constante, la proportion des molécules composant le C différait aussi selon la saison et l'utilisation du territoire. L'été était dominé par des formes dégradées par l'action microbienne et l'hiver par des formes bio- et photo-labiles. Ceci fait allusion au potentiel de transformation de la rivière plus élevé dans la saison chaude plutôt que

sous la glace, où les formes plus réactives avaient tendance de s'accumuler. La composition du C en amont était aussi distincte de celle en aval, avec un seul changement abrupt ayant lieu entre la section forestière et la section d'utilisation du territoire urbaine et agricole. Ces changements de compositions n'étaient pas présents durant le printemps de crue typique échantillonné, mais dans l'inondation de fréquence historique nous avons observés des apports nouveaux de molécules provenant soit des apports terrestres normalement déconnectés du réseau fluvial ou de surverses d'égouts. L'influence des facteurs naturels et anthropiques s'est aussi reflétée dans les flux historiques riverains de C, N, et P (1980 – 2020). La précipitation explique le plus les flux de C et les flux de N dans la section pristine. Les apports historiques au territoire de N anthropique (nécessaires pour soutenir la population humaine et les activités agricoles) expliquent fortement la tendance temporelle à la hausse des flux riverains de N dans la section urbaine. Durant les quatre dernières décennies, un peu plus du tiers des apports de N au territoire sont livrés à la rivière annuellement, suggérant que la source urbaine de N anthropique est encore peu gérée. Le manque de corrélation entre les flux de P dans la rivière et les précipitations ou les apports au territoire de P anthropique peut être expliqué par les usines de traitement des eaux usées installées dans la région vers la fin des années 1990 qui ont fait diminuer presque de moitié le P livré à la rivière. La variation de ces flux s'est reflétée dans la stœchiométrie écosystémique historique, qui varie de 130 : 23 : 1 en 1980 à 554 : 87 : 1 en 2007-08 après l'effet de l'usine d'épuration et du N qui a augmenté.

À travers les axes historiques, spatiaux, et saisonniers, cette thèse contribue à la compréhension du rôle des rivières dans la réception, la transformation, et l'export du C, N, et P. Combinée aux concentrations, l'approche de stœchiométrie écosystémique propose une façon d'intégrer apports et pertes des éléments pour les étudier de pair au niveau du bassin versant. Puis, comme certaines formes de C, N, et P sont associées à des sources terrestres spécifiques, ou à certains types de transformations, les inclure dans un cadre conceptuel combinant des extrêmes climatiques et des utilisations du territoire différentes offre un aperçu sur le résultat des sources et transformations des éléments. Enfin, les tendances décennales de C, N, et P riverains montrent l'influence des facteurs naturels et anthropiques sur la stœchiométrie écosystémique historique d'une rivière.

Mots-clés : rivière, stœchiométrie écosystémique, carbone, azote, phosphore, utilisation du territoire, saisons

Abstract

Rivers are dynamic ecosystems that receive, transform, and export organic matter that includes carbon (C), nitrogen (N), and phosphorus (P). Their high surface of contact between water and sediments offers important potential for transformation processes to occur, which usually include all three elements together. These transformations can remove elements from the water column, thus decreasing their concentrations and leading to improved water quality. However, climatic conditions (discharge, temperature, light), landscape configuration (forest, urbanisation, agriculture), and length of human activities on land affect the quantity, composition, and proportion of C, N, and P delivered to receiving waters. In a context where a surplus of nutrients (N, P) can surpass a river's capacity to remove elements from the water column, and where climatic extremes are worsening because of climate change, this thesis shines a light on the role of rivers in the dynamics of C, N, and P for a better understanding of lotic ecosystems' responses to present and future pressures.

The *Rivière du Nord* sequentially drains forested, urban, and agricultural regions, and oscillates between four distinct seasons, exposing it to contrasting land use changes and climatic conditions. We sampled forms of C, N, and P at 13 sites along the mainstem (146 km), once per season for three years. Overall, concentrations of total N and P increased downstream, concurrent with higher human activities in the lower half of the watershed, but total organic C concentrations remained constant regardless of season or year. As a result, C: N: P ecosystem stoichiometry was rich in C compared to N and P upstream, but became enriched in nutrients downstream. Within a single river, the range spanned by the ratios (2319: 119: 1 to 368: 60: 1) almost covered the land – ocean continuum. Different forms of C, N, and P dominated overall stoichiometry depending on season and land use. In summer, upstream N composition was dominated by dissolved organic N and shifted to nitrate downstream. In winter, ammonium and dissolved P were dominant throughout the continuum. Despite constant concentrations, C composition also differed as a function of season and land use. Summer was dominated by microbial humic-like components and winter by bio- and photolabile ones, hinting at the river's higher transformation potential in the warm season rather than under the ice, where more reactive forms tended to accumulate. Upstream C composition was also distinct from the downstream one, with a unique sharp change between the forested pristine section and the downstream impacted one. This marked shift in composition was not observed in the typical high spring flow, but in the historical flood sampled, we observed new inputs of molecules coming from either previously

disconnected terrestrial sources or sewage overflows. The influence of natural and anthropogenic factors was also reflected in the historical riverine loads of C, N, and P (1980 – 2020). Precipitation explained more than half of C loads, and some N loads from the pristine section. Historical anthropogenic N inputs to land (necessary to sustain human population and agricultural activities) strongly explained the increasing trend in riverine N loads from the urban section. In the last four decades, just over a third of anthropogenic inputs to land are loaded to the river annually, suggesting that the urban source of N is still largely uncontrolled. The lack of correlation between riverine P loads and precipitation or anthropogenic P inputs to land could be explained by the installation of wastewater treatment plants in the region at the end of the 1990s, which reduced almost half the amount of P loaded to the river. The variation in riverine loads was reflected in the historical ecosystem stoichiometry, which varied from 130: 23: 1 in 1980 to 554: 87: 1 in 2007-08 due to both the impact of wastewater treatment and increasing N use.

With its historical, spatial, and seasonal axes, this thesis contributes to the understanding of the role of rivers on C, N, and P loading, transformation, and export. In combination with concentrations, ecosystem stoichiometry represents an approach to study elements together and integrate their loadings and losses at the watershed scale. Because certain forms of C, N, and P are associated with specific land use sources or certain types of transformation pathways, including them in a conceptual framework that combines climatic extremes and gradients of land uses allows for insight on the net effect of sources of transformations. Lastly, decadal trends of riverine C, N, and P loads will reveal the influence of natural and anthropogenic factors on the historical ecosystem stoichiometry of a river.

Keywords: river, ecosystem stoichiometry, carbon, nitrogen, phosphorus, land use, seasons

Table des matières

Liste des tableaux

Chapitre 1

Chapitre 2

Chapitre 3

Liste des figures

Introduction générale

Chapitre 1

Chapitre 2

Chapitre 3

Conclusion

Liste des sigles et abréviations

L'anglais est en italique.

ACP : analyse en composantes principales | *PCA : principal component analysis*

ARIL : *average of the relative 95% prediction interval lengths*

β:α : indice de fraîcheur | *freshness index*

BQMA : Banques de données sur la qualité du milieu aquatique

°C : degrés Celsius | *degrees Celsius*

C : carbone | *carbon*

C1 – C5 : composante 1 à 5 | *components 1 to 5*

CH_4 : méthane | *methane*

CO_2 : dioxyde de carbone | *carbon dioxide*

COD : carbone organique dessous | *DOC : dissolved organic carbon*

COT : carbone organique total | *TOC : total organic carbon*

COP : carbone organique particulaire | *POC : particulate organic carbon*

CRSNG : Conseil de recherches en sciences naturelles et en génie du Canada | *NSERC : Natural Sciences and Engineering Research Council of Canada*

cv : coefficient de variation | *coefficient of variation*

EEM : matrices d'émission et excitation | *emission and excitation matrices*

Fe^{3+} : fer | *iron*

FI : indice de fluorescence | *fluorescence index*

Fig. : figure | *figure*

FONCER : Programme de formation orientée vers la nouveauté, la collaboration et l'expérience en recherche | *CREATE : Collaborative Research and Training Experience program*

FRQNT : Fonds de recherche du Québec : Nature et Technologie

g : gramme | *gram*

GFF : filtres en fibres de verre | *glass fiber filters*

GRIL : Groupe de recherche interuniversitaire en limnologie | *Interuniversity Research Group in Limnology*

h : heure | *hour*

HCl : acide chlorhydrique | *hydrochloric acid*

HIX : indice d'humification | *humification index*

jr : jour | *d : day*

kg : kilogramme | *kilogram*

km : kilomètre | *kilometer*

L : litre | *liter*

LULC : utilisation du territoire | *land use – land cover*

m : mètre | *meter*

mg : milligramme | *milligram*

ml (ou mL) : millilitre | *milliliter*

mm : millimètre | *millimeter*

MOD : matière organique dissoute | *DOM : dissolved organic matter*

MODC : matière organique dissoute colorée | *CDOM : coloured dissolved organic matter*

MODF : matière organique dissoute fluorescente | *FDOM : fluorescent dissolved organic matter*

Mn_4^+ : manganèse | *manganese*

MST : matière en suspension totale | *TSM : total suspended matter*

µg : microgramme | *microgram*

µm : micromètre | *micrometer*

µmol : micromole | *micromole*

°N : degrés Nord | *degrees North*

N : azote | *nitrogen*

N_2 : diazote | *dinitrogen (nitrogen gas)*

NANI : apport anthropique d'azote net | *net anthropogenic nitrogen input*

NAPI : apport anthropique de phosphore net | *net anthropogenic phosphorus input*

NH_3 : ammoniac | *ammonia*

NH_4^+ : ammonium | *ammonium*

NID : azote inorganique dissous | *DIN : dissolved inorganic nitrogen*

NO : monoxyde d'azote | *nitrogen monoxide*

NO_2^- : nitrite | *nitrite*

NO_3^- : nitrate | *nitrate*

N_2O : oxyde nitreux | *nitrous oxide*

NOD : azote organique dissous | *DON : dissolved organic nitrogen*

NT : azote total | *TN : total nitrogen*

NTD : azote total dissous | *TDN : total dissolved nitrogen*

O_2 : oxygène | *oxygen*

P : phosphore | *phosphorus*

PARAFAC : analyse en facteurs parallèles | *parallel factor analysis*

Pg : petagramme (10^{15} grammes) | *petagram*

PO_4^{3-} : phosphate | *phosphate*

PSR : phosphore soluble réactif | *SRP : soluble reactive phosphorus*

PT : phosphre total | *TP : total phosphorus*

PTD : phosphore total dissous | *TDP : total dissolved phosphorus*

PTP : phosphore total particulaire | *TPP : total particulate phosphorus*

QC : Québec | *Quebec*

RKm : kilomètre de rivière | *river kilometer*

RRMSE : *relative root mean square error*

RU : unite Raman | *Raman units*

s : seconde | *second*

sd : écart type | *standard deviation*

SO_4^{2-} : sulfate | *sulfate*

Tg : teragramme (10^{12} grammes) | *teragram*

U.S. : États-Unis | *United States*

UV : ultraviolet | *ultraviolet*

vs: versus

°W : degrés Ouest | *degrees West*

WWTP : usine d'épuration (ou de traitement) des eaux usées | *wastewater treatment plant*

yr : an | *year*

Une rivière coule perpétuellement.

Est-ce alors la même rivière qu'on étudie si on y retourne?

Remerciements

J'ai entamé un doctorat car je trouvais attirant le mélange de terrain, laboratoire, lecture et écriture. Je n'ai pas été déçue. Mise à part la science, à laquelle le reste de ma thèse est dédié, j'ai eu l'opportunité de rencontrer plusieurs personnes magnifiques.

Avec mes directeurs de thèse, Jean-François et Roxane, j'ai pu développer des belles relations individuellement, et leur complémentarité scientifique m'a permis d'avoir une meilleure compréhension et profondeur sur mon projet. Merci.

Lisa, nous avons fait toutes (ou presque) nos campagnes d'échantillonnage ensemble. Nous avons ri, pleuré un peu à cause de la préparation de matériel et du froid en automne, et crû côte à côte. Merci pour cette amitié soutenue et au plaisir de partager ces moments continuellement. Et combien de gens nous ont aidées sur le terrain! Merci Phil, Amélie, Jade, Andréanne, Chris, Caro, Richard, Morgan, Charles, et Anna pour votre enthousiasme à nous suivre dans des conditions climatiques parfois douteuses. Ensuite merci à Gabriel Lanthier pour le support technique, à l'équipe de la Station de biologie des Laurentides, et à Dominic Bélanger pour le support analytique. Sans vous, il n'y aurait probablement pas eu de terrain ni d'analyses en laboratoire.

Morgan, Jean-Olivier, Richard : trio de force quand je suis rentrée au doctorat. Merci pour les amitiés, la musique, la grimpe. J-O, merci de ta patience sans fin face à mes questions de NANI-NAPI. Maintenant c'est bon, je ne crois pas qu'il y en ait d'autres. Morgan, parcourir la fin du doctorat en ta compagnie était une bénédiction à laquelle je ne m'attendais pas. Je suis reconnaissante de tes points de vue honnêtes. Ça fait du bien. Aussi, j'ai hâte au spa.

J'ai passé trois mois dans le laboratoire de Gabriel Singer, à Berlin dans le temps. Gabriel, thanks for welcoming me in your group and trusting me to be part of an intense field campaign in Albania. It was surprisingly easy to fit in. Franzi, Matt, Lukas, Selin, Jan : you made my time in Berlin enjoyable and I almost considered staying longer.

Marie, Marion, Simon : je suis fière du travail « parascolaire » que nous avons accompli ensemble. S'il y a une chose que je considère peut être mon lègue aux étudiant.es du département, c'est bien l'amélioration de la condition étudiante financière que nous avons fait votée et acceptée en AD.

Morgan, Manu, Andrew : nos rencontres de bookclub m'ont apportée la perspective qu'il manquait à mon parcours. Les discussions de philosophie des sciences, accompagnées de bière et de bonne nourriture, c'est facile. Merci! Et puis, le Ph. D. sans philosophie… c'est quoi?

Charles, ta patience, ton écoute, et ton intérêt continu sur mes sujets scientifiques sempiternels sont inestimables. J'ai beaucoup de chance de pouvoir échanger avec toi quand je veux. Merci pour le support que tu m'offres et les directions que tu m'encourage à prendre pour poursuivre mes intérêts.

Finalement, chère famille, Ev, Flo, Papa, Maman, merci d'avoir été à mes côtés pendant cette aventure et de m'avoir encouragée à terminer.

Introduction générale

L'importance des rivières et du carbone, de l'azote, et du phosphore

Les rivières sont des écosystèmes dynamiques qui transportent de la matière organique (MO) comprenant du carbone (C), de l'azote (N), et du phosphore (P), ainsi que la forme inorganique de ces nutriments, vers les écosystèmes aquatiques situés en aval. Les trois éléments ont une provenance et un destin parfois similaires, parfois contrastés, et sont sujets à des transformations qui maintiennent le fonctionnement des écosystèmes, comme la production primaire, la respiration, la décomposition, et le recyclage de nutriments ou polluants (von Schiller et al., 2017). Ces transformations retirent le C, N, et P de l'environnement aquatique de façon permanente ou temporaire. Un retrait temporaire sous-entend que les éléments peuvent être remobilisés et retournés à l'écosystème aquatique tandis qu'un retrait permanent indique une perte ultime de ces éléments de l'écosystème. Un aspect clé des écosystèmes lotiques se trouve dans le potentiel de transformation offert aux organismes qui effectuent ces processus de par l'interaction de l'eau avec les sédiments, comme avec la présence de zones hyporhéiques (Boano et al., 2014), de structure de biofilms (Battin et al., 2016), et par le mouvement de l'eau à travers ces substrats (Krause et al., 2022). Par leur nombre et grande connectivité[1] au milieu terrestre, les ruisseaux de tête sont souvent considérés comme les écosystèmes ayant un potentiel de transformation élevé (Alexander et al., 2000), mais les plus grandes rivières peuvent contribuer au fonctionnement des écosystèmes de façon plus importante par unité de territoire que les plus petits ruisseaux (Wollheim et al., 2022). Dans le contexte actuel de variations climatiques et changements d'utilisation du territoire, comprendre où, quand, et comment les rivières reçoivent, transforment et exportent le C, N, et P reste critique, car le retrait de ces éléments mène à une eau de meilleure qualité, service écologique non-négligeable pour les humains.

Les processus menant à la rétention de C, N, et P

Les transformations de C, N, et P menant ultimement au retrait de ces éléments impliquent plusieurs processus influencés par la forme du réseau hydrographique, des conditions environnementales

[1] Une grande connectivité peut être définie par un ratio élevé de « périmètre du cours d'eau : aire de surface du cours d'eau ».

différentes, et les formes de ces éléments elles-mêmes (dissoutes, particulaires, organiques, inorganiques).

Le retrait temporaire des éléments implique le processus de production primaire, car les organismes qui fixent le dioxyde de carbone (CO_2) et qui nécessitent conjointement le N et le P pour leur croissance (préférentiellement sous forme inorganique) peuvent relâcher de la matière organique dissoute (MOD) au courant de leur vie ou à leur mort, ou encore pendant le *sloppy feeding* du zooplancton (Thornton, 2014). Dans les écosystèmes lotiques, ce processus est majoritairement effectué par les macrophytes, planctons et bactéries dans les biofilms sur les roches et le lit de la rivière. Ici, les trois éléments sont utilisés conjointement : le C sous forme de CO_2, le N sous forme d'ammonium (NH_4^+), nitrate (NO_3^-) ou encore N organique dissous soluble (NOD/acides aminés), et le P sous forme de phosphate (PO_4^{3-}). De façon générale, la production primaire dans les ruisseaux de tête est limitée par la canopée recouvrant les cours d'eau, et par une forte rétention de nutriments dans les écosystèmes terrestres peu perturbés comme les forêts (Vitousek & Howarth, 1991; Vitousek et al., 2010). La production primaire peut aussi être limitée dans les plus grandes rivières par une atténuation plus forte de la lumière via les particules en suspension ou couleur de l'eau foncée. Le contraire sera aussi vrai. Ensuite, les particules dans l'eau (production primaire algale ou autre) sédimentent lorsque le temps de résidence de l'eau augmente et le leur permet. Les lacs et les réservoirs sont critiques pour la sédimentation (Von Wachenfeldt & Tranvik, 2008; Harrison et al., 2009; Maavara et al., 2015), particulièrement les lacs pour le P et les réservoirs pour le N (Goyette et al., 2019). Sans remobilisation, cette perte est permanente. La variabilité de la rétention dépend donc de l'agencement du réseau hydrographique. Un réseau comprenant plus de lacs et de réservoirs exportera des concentrations de C, N, et P plus basses qu'un réseau de taille et morphologie équivalents n'en comprenant pas.

Une autre perte permanente implique les transformations de C et N en gaz. Le P n'a pas de perte gazeuse significative. Ces transformations ont lieu durant la minéralisation complète de la MOD, soit en milieu oxique (respiration, perte en CO_2) ou anoxique (dénitrification, perte en diazote (N_2)), souvent à l'interface eau-sédiment ou dans les sédiments. La minéralisation du N et du P subvient aux besoins énergétiques et en nutriments des organismes hétérotrophes (Kritzberg et al., 2004). Un excès de ces formes inorganiques peut être produit par les hétérotrophes (Heath, 2004; Arnosti, 2011; Castagno et al., 2021), utilisé par des organismes adjacents, ou transporté vers l'aval avec le courant où les prochains organismes pourront en bénéficier. La minéralisation du C, ou respiration, fournit de

l'énergie aux hétérotrophes et relâche du CO_2 comme sous-produit, forme utilisée à nouveau dans la production primaire ou émise vers l'atmosphère selon la pression partielle de CO_2 dans l'eau versus l'air et selon la vélocité d'échange gazeux. Cette transformation mène donc à la perte permanente de C. Pour clore la respiration, l'oxygène (O_2) est utilisée comme accepteur final d'électron. Cette transformation doit se passer dans des environnements oxiques.

Dans les environnements anoxiques, le NO_3^-, puis le manganèse (Mn^{4+}), le fer (Fe^{3+}), le sulfate (SO_4^{2-}), le CO_2, et le méthane (CH_4) peuvent remplacer l'O_2 comme accepteurs finaux d'électron (Sikora et al., 2017). Lorsque le NO_3^- est utilisé, il est réduit en N_2 gazeux suivant quatre réactions chimiques passant par le nitrite (NO_2^-), le monoxyde de N (NO), et l'oxyde nitreux (N_2O) pour arriver au N_2 (Skiba, 2008). C'est la perte permanente de N, aussi appelée dénitrification. Cette transformation dépend de conditions anoxiques et de présence de NO_3^-, qui préalablement est produit par des bactéries chimio-autotrophes faisant la nitrification du NH_4^+ en zone oxique.

La perte permanente de C implique aussi des réactions photochimiques qui agissent préférentiellement sur les molécules de MOD de provenance allochtone terrestre plutôt qu'autochtone où l'action des rayons UV peut transformer la MOD en CO_2 (Cory & Kling, 2018).

Bref, les processus de rétention agissent sur des formes différentes de C, N, et P, parfois conjointement, parfois non, et diminuent leurs concentrations dans la colonne d'eau. Lors de la remise en circulation des éléments retirés temporairement, et ce plus loin dans la rivière à cause du courant, les transformations auront de nouveau la possibilité de les retirer, cette fois-ci en permanence (Newbold et al., 1981). Ainsi, dans un écosystème hypothétiquement stable, les concentrations de C, N, et P devraient diminuer d'amont vers l'aval à travers plusieurs cycles de transformations.

Rétention au niveau de l'écosystème

Les taux de retraits de C, N, et P (temporaires et permanents) varient largement, mais peuvent être attribués à une certaine gamme de valeurs. Le C serait retiré de l'écosystème à un taux variant entre ~1 et ~8 g-C m^{-2} jr^{-1} pour les ruisseaux et rivières de Suède (Humborg et al., 2010), avec une moyenne de 6.5 g-C m^{-2} jr^{-1} pour les rivières aux États-Unis (Butman & Raymond, 2011) et une moyenne de 2.6 g-C m^{-2} jr^{-1} pour seize rivières mondiales (Luo et al., 2019). Globalement, cela équivaudrait environ 1.5 – 2.1 Pg-C an^{-1} émis vers l'atmosphère pour tous les ruisseaux et rivières (Raymond et al., 2013), auquel il faudrait rajouter un autre 0.2 – 0.55 Pg-C an^{-1} pour inclure la respiration nocturne qui est en générale

27% plus élevée que les taux quotidiens (Gómez-Gener et al., 2021). Du CO_2 total émis, un tiers viendrait de la minéralisation aquatique tandis que le reste serait fourni par la respiration des sols, apporté aux écosystèmes aquatiques via l'eau souterraine (Hotchkiss et al., 2015). La majorité de la minéralisation aquatique serait produite par l'oxydation microbienne plutôt que photochimique (Koehler et al., 2014). Ces émissions représenteraient 72% du C organique total entrant dans les écosystèmes lotiques (Maranger et al., 2018), contribuant à la baisse de C le long du continuum.

Les taux de retraits de N sont plus variables et plus faibles que le C, allant de ~1 à 1500 mg-N m^{-2} jr^{-1} pour 72 ruisseaux répartis dans 8 régions distinctes des États-Unis (Hall et al., 2009), avec une moyenne de 97 ± 86 mg-N m^{-2} jr^{-1} pour 24 rivières aux États-Unis et en Europe lors du mois de l'année ayant l'eau la plus chaude (Piña-Ochoa & Álvarez-Cobelas, 2006). La proportion de N retirée par l'assimilation ou la dénitrification variera dépendamment du nombre de plantes, d'apports de MOD, et de concentration de NO_3^- et d'O_2, (Saunders & Kalff, 2001; Ashkenas et al., 2004). Par exemple, la dénitrification peut être responsable de 0.5% à 100% des retraits de N totaux, le reste étant retiré via l'assimilation (Mulholland et al., 2009). Ces retraits équivalent à proche ou plus de la moitié des intrants de N, soit 49 Tg-N an^{-1} (Galloway et al., 2004; Maranger et al., 2018).

Le P n'a pas de phase gazeuse significative, donc la voie de perte de P est l'assimilation biologique ou la liaison avec des composés minéraux et sédimentation subséquente. Les taux de retraits ont été mesurés à 52 mg-PO_4-P m^{-2} jr^{-1} (ruisseaux tempérés aux État-Unis, Davis & Minshall, 1999), à 86 mg-PO_4^{3-} m^{-2} jr^{-1} (ruisseaux et rivières aux États-Unis, Newbold et al., 2006), et à 65 ± 16 et 253 ± 99 mg-P m^{-2} jr^{-1} pour deux ruisseaux en Espagne (Martí & Sabater, 1996). Des retraits plus élevés pourraient être attendus dans les rivières de plus grand ordre, car un courant plus lent et une luminosité plus élevée faciliterait un retrait sédimentaire et assimilatoire, respectivement. Combinant les écosystèmes aquatiques lotiques, cette perte serait de 5 Tg-P an^{-1} et représenterait environ la moitié des intrants totaux (Maranger et al., 2018).

Au niveau du continuum terre – océan, les écosystèmes lotiques peuvent donc être considérés comme réacteurs et transformateurs de C, N, et P, retirant ces éléments de l'eau. Par contre, considérer ces éléments séparément ne permet pas de déterminer s'ils sont retirés de l'écosystème ensemble ou non, ou encore dans les mêmes proportions.

La stœchiométrie écosystémique

La stœchiométrie[2] écosystémique est une approche qui balance les apports et les pertes des éléments de façon nette (Maranger et al., 2018). Le mot stœchiométrie fait référence au ratio de deux ou plusieurs éléments qui démontre combien plus un élément qu'un autre se retrouve dans l'écosystème. Le mot écosystémique défini l'échelle à laquelle la stœchiométrie est étudiée. Dans l'étude de ruisseaux et rivières des États-Unis, Maranger et al. (2018) ont observé pour la première fois que le C était préférentiellement perdu vers l'atmosphère comparé au N, et que le P était préférentiellement perdu vers les sédiments comparé au C et au N. Tirée de leur article, la Figure 1 démontre ce résultat.

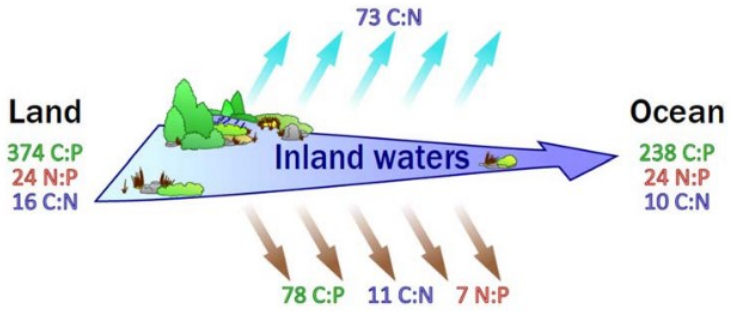

Figure 1 Estimés des ratios molaires C : N, C : P, et N : P des ruisseaux et rivières inclus dans l'article de Maranger et al. (2018).

Au niveau du continuum terre – océan, les écosystèmes lotiques peuvent donc être considérés comme réacteurs et transformateurs de C, N, et P, retirant ces éléments de l'eau, où les différences dans la rétention surviendraient dépendamment de la biogéochimie contrastée des éléments. L'étendue des taux de rétention reportée ici et des ratios peut être justifiée par l'influence proportionnelle qu'ont certains contrôles physiques (débit), chimiques (concentration des éléments), et biologiques (assimilation de la production primaire) sur la rétention des éléments dépendamment du temps qu'ils ont à agir dans un écosystème aquatique lotique. Identifier les périodes clés de transformation s'avère donc utile pour comprendre quand une rivière a le plus grand potentiel de rétention.

[2] Stœchiométrie, du grec ancien *stoekheîon* pour élément et *métron* pour mesure, est un terme qui a été déterminé par Jeremias Benjamin Richter en 1792.

L'influence du climat

Dû au temps de résidence de l'eau[3] élevé, les périodes de faible débit des rivières promeuvent les transformations du C, N, et P. Les saisons chaudes et lumineuses d'été (dans l'hémisphère nord) favorisent aussi l'assimilation biotique des nutriments, et la dégradation (photo ou bio) du C. Lors des périodes de fort débit, comme les pluies ou la fonte des neiges (des régions tempérées), le temps de résidence de l'eau diminue et offre moins de temps aux processus de rétention d'agir. L'intensité des transformations et conséquemment de la rétention du C, N, et P est donc influencée par les conditions climatiques environnantes. Généralement, les périodes de forts débits sont comparés à aux périodes de faibles débits, car le potentiel de transformation des éléments varie selon le débit. Par exemple, la composition du C, N, et P demeurera plus similaire le long d'un continuum fluvial lors de forts débit occasionnés par des précipitations ou par la fonte des neiges, car le temps qu'ont les processus de transformation à agir sur les éléments sera diminué (Hendricks & White, 2000; Saunders & Kalff, 2001; Weyhenmeyer et al., 2012). Comparativement, la période typique de débit faible est l'été, où le potentiel de transformation est grand grâce au temps de résidence de l'eau élevé, en plus d'une température plus chaude et une luminosité abondante (Doyle, 2005; Catalán et al., 2016). Comme la production primaire, le recyclage, et le retrait de C, N, et P agissent sélectivement sur certaines formes des éléments, on pourrait s'attendre à un regroupement de molécules exporté aux écosystèmes en aval différent de celui en amont. On s'attendrait aussi à moins de particules dans l'eau, car elles auraient le temps de sédimenter (Von Wachenfeldt & Tranvik, 2008; Withers & Jarvie, 2008). Dans les rivières tempérées, l'hiver constitue aussi une période de faible débit et représente un potentiel de transformation différent de celui de l'été à cause d'une disponibilité de lumière faible (glace recouvrant la rivière) et de températures plus basses (allant en bas de 0°C). On pourrait s'attendre à une proportion plus élevée de N et de P inorganique dans l'eau, car leur assimilation serait faible à cause d'une production primaire limitée par la lumière (Hampton et al., 2017). On pourrait aussi s'attendre à une accumulation de molécules plus photodégradables en hiver qu'en été à cause de la barrière physique pour les rayons UV qu'exerce la glace et la neige recouvrant la rivière (Gonsior et al., 2013). Les rivières situées dans les régions avec des forts gradients saisonniers permettent donc d'explorer l'amplitude de l'influence des facteurs environnementaux sur les transformations et cycles du C, N, et P.

[3] Temps de résidence : temps que prend un lac pour renouveler (ou remplacer par de la nouvelle eau) chaque goutte d'eau le composant. Pour les rivières, c'est plus logique de définir le temps de résidence comme le temps que l'eau passe pour se rendre d'un point en amont à un point en aval.

L'influence de l'utilisation du territoire

Presqu'aucun cours d'eau reste intouché par les activités anthropiques, et les processus de rétention des rivières peuvent se voir surpassés (Stutter et al., 2018), menant à des conséquences connues sur la qualité de l'eau. Le type d'utilisation du territoire va influence la composition des formes de C, N, et P entrant dans les écosystèmes aquatiques. Les rivières drainant des bassins versants minimalement perturbés reçoivent en général les formes dissoutes et organiques de C, N, et P (Kortelainen et al., 2006) où les concentrations de N et P sont faibles à cause d'un fort recyclage et effet de rétention des forêts. En comparaison, les rejets des usines de traitement des eaux usées auront tendance à ajouter des formes hautement biodisponible de N et P, soit le NH_4^+ et le P réactif soluble, ou TDP (Haggard et al., 2005; Withers & Jarvie, 2008). L'excès des fertilisants[4] des terres agricoles lessivera plutôt du NO_3^- et du P dissous ou particulaire dépendamment du régime de précipitation (Vanni et al., 2001; Manning et al., 2020). Quant à elle, la composition de la MOD dans les zones urbaines et agricoles est dominée par des molécules de petites tailles et biolabiles, que ce soit à cause d'une production de MOD autochtone *in situ* favorisée par l'apport de nutriments plus élevés ou une production dans les sols agricoles ou dans les bassins de rétention des eaux usées et lessivée à la rivière (Hosen et al., 2014; Parr et al., 2015). L'accumulation et l'enrichissement en NO_3^-, NH_4^+, et en P dissous dans les cours d'eau (eutrophisation[5]) mènent à des proliférations d'algues qui peuvent être toxiques aux animaux (Glibert & Burkholder, 2011). La décomposition subséquente de MOD labile par les organismes hétérotrophes épuise les quantités d'O_2 dans les environnements isolés de nouveaux apports d'O_2 et peut mener à des environnements aquatiques hypoxiques ou même anoxiques, non propices à la survie de beaucoup d'organismes benthiques (Rabalais et al., 2001). Si ce n'est pas la rivière elle-même qui devient eutrophe à cause d'un courant trop rapide ou de turbidité trop élevée, ce seront les écosystèmes receveurs des nutriments excessifs où le temps de résidence de l'eau permet au taux de dédoublage des algues nocives d'avoir lieu (Hilton et al., 2006). L'utilisation du territoire aura donc une influence

[4] Les fertilisants peuvent être minéraux ou organiques. Les fertilisants organiques sont composés de fumier et de composte. Les fertilisants minéraux de N sont composés d'éléments chimiques inorganiques comme l'ammoniac (NH_3), le nitrate d'ammonium (NH_4NO_3) ou l'urée ($CO(NH_2)_2$) et sont le produit du processus Haber-Bosch qui synthétise de façon industrielle le NH_3 à partir des gaz N_2 et H_2. Les expériences de Haber ont eu lieu avant et pendant la première guerre mondiale, où le NH_3 était aussi utilisé dans les bombes allemandes. Le P minéral est extrait de dépôts rocheux sous forme d'apatite ($Ca_5(PO_4)_3X$ ou le X représente du fluor (F), du chlore (Cl) ou de l'hydroxyde (OH). Les dépôts se trouvent majoritairement au Maroc, en Chine, au Moyen Orient, en Russie et aux États-Unis et ont une quantité limitée de P.

[5] L'eutrophisation est un processus naturel des lacs qui reçoivent graduellement du N et du P des écosystèmes terrestres. Ces nutriments favorisent la production algale dans l'eau qui sédimente au fond du lac lorsqu'elle meurt. Les lacs « mourront » lorsqu'ils seront remplis de sédiments, ce qui prend des (centaines de) milliers d'années. L'agriculture et l'urbanisation ont accéléré ce processus, qui peut maintenant prendre seulement quelques dizaines d'années.

sur la quantité et la qualité du C, N, et P livré aux cours d'eau. Inscrire les études des rivières dans un contexte de changements d'utilisation du territoire devient donc nécessaire pour une meilleure compréhension des intrants de C, N, et P, transformations par celles-ci, et exports subséquents, tant au niveau spatial qu'historique.

Certaines utilisations du territoire sont établies depuis longtemps. Dans la vallée du Saint-Laurent, l'agriculture s'est intensifiée à partir du 18e siècle avec l'établissement des colons Français, Anglais, et Irlandais (Laurin, 1989; Russell, 2012). L'utilisation de fertilisants inorganiques a pris de l'ampleur à partir des années 1920 pour le P et 1960 pour le N (Goyette et al., 2016). Étant donné que seulement 15 – 30 % du N et 5 – 15% du P ajouté aux sols agricoles se retrouve dans l'eau, le reste s'accumule sur le territoire (Howarth et al., 1996; Han et al., 2013; Hong et al., 2017). Pour plusieurs décennies, le N et le P ont donc eu la chance de s'accumuler dans les sols. Se liant fortement au sol, le stock de P accumulé dans les sols agricoles est bien quantifié (Van Staden et al., 2021). Bien que beaucoup plus mobile sous sa forme de NO_3^- (Caraco & Cole, 1999), le N organique est aussi un stock important dans les sols, d'autant plus que c'est une source long terme pour la minéralisation du N qui peut contribuer au N inorganique lessivé (Van Meter et al., 2016). L'accumulation de N et P dans les sols agricoles peut mener à des lègues de nutriments aux cours d'eau receveurs sur le long terme, et dans certaines régions, même un arrêt immédiat d'ajouts de fertilisants ne mèneraient qu'à un retour à la normal dans quelques centaines d'années (Goyette et al., 2018). Pour l'urbanisation, son développement à l'extérieur de la vallée du Saint-Laurent (vers le nord) est plus récent à cause de la densité forestière et l'inaccessibilité du Bouclier Canadien qui ont longtemps dissuadé l'établissement de colons, et s'est graduellement[6] effectué le long des rivières pénétrant cette province géologique (Laurin, 1989). L'apport de nutriments pour subvenir aux besoins alimentaires humains dans ces villages et villes est donc plus récent et se traduit en rejet d'égouts ponctuels dans les cours d'eau receveurs.

Certaines sources de N et P aux cours d'eaux sont mieux contrôlées que d'autres. Au Québec en 1978, le gouvernement provincial a lancé le « Programme d'assainissement des eaux du Québec » en 1978 et

[6] L'incitatif d'établissement des colons francophones vs anglophones était encouragé moralement en tant que « course vers le Nord » par le curé Antoine Labelle. C'est le curé Labelle qui a fait pression sur les gouvernements pour construire un train rejoignant Montréal au Nord afin de faciliter le transport de victuailles et matériaux. Plus tard, le ski (de fond et ensuite alpin) a solidifié l'attrait des Laurentides, où le premier remonte-pente mondial motorisé a été installé. Le même train, alors appelé « P'tit train du Nord », amenait les avides de ski vers les Laurentides. Entre 1930 et 1960, 1600 kilomètres de chemins de ski parcouraient la région et l'ont popularisée mondialement.

planifiait subventionner ~85% des coûts de construction d'usines d'épurations dans les municipalités. En 1995, des usines d'épurations ont été établies dans environ 500 municipalités (MELCC, 2022a), et en 2019, 827 exploitants municipaux comptaient une usine d'épuration (MELCC, 2021). Tous types de traitements confondus, les usines retirent presque 80% du P total se rendant à l'affluent des stations (MELCC, 2021). Malheureusement, le N n'est pas pris en compte dans les normes régissant les rejets (MTESS, 2021b). De plus, l'imperméabilisation des surfaces, qui facilite le lessivage de P, est à la hausse dans les deux plus grandes villes du Québec, avec une augmentation de 30.8% des zones urbaines de 2001 à 2021 pour Montréal et 30% pour la ville de Québec (Hobbie et al., 2017; Yang & Toor, 2018; Müller et al., 2020; Bouchard & Shiab, 2022). Pour les régions agricoles, les apports diffus de N et P sont favorisés par les drains agricoles[7] (McIsaac & Hu, 2004). Bien que certains apports soient plus évidents à gérer que d'autres, des cultures hivernales réduiraient l'érosion des sols et donc l'apport de P à l'eau (Kaspar & Singer, 2011; Basche et al., 2016), une manutention de fumier diminuerait les apports de P agricoles (Van Meter et al., 2021), et des installations spécifiques dans les usines d'épurations traiteraient le N (Rahimi et al., 2020). Comprendre d'où (emplacement sur le territoire) et depuis quand (accumulation au sol) le N et le P s'immiscent dans les cours d'eau pourrait aider à déterminer le type de solutions de contrôles à implémenter sur un territoire pour réduire la quantité de nutriments qui atteignent la rivière et améliorer la qualité de l'eau.

Objectifs, approches, et structure

Ma thèse s'appuie donc sur quatre facettes clés, qui comportent chacune des approches d'études typiques. Ces facettes sont les suivantes :

- Le C, N, et P sont utilisés différemment ou conjointement dans plusieurs processus à la base du fonctionnement des écosystèmes.
- Les rivières offrent un potentiel élevé de transformations pour « nettoyer » l'eau.
- Les conditions climatiques influencent ces processus de transformation.
- L'utilisation du territoire (forêt vs urbain vs agricole) et sa gestion historique influencent le C, N, et P livrés aux cours d'eau, qui à leur tour affectent les transformations dans l'eau.

[7] Augmenter les aires de surface cultivables pour augmenter la production agricole a été accompli en drainant des régions (faussement) jugées comme inutiles, tel que des milieux humides. Les drains étaient originalement fabriqués à partir de tuiles d'argile provenant de toitures, d'où l'expression anglophone « tile drainage » traduite à « drains agricoles » en français. Maintenant, la plupart des tuyaux sont sous terre et accélèrent l'écoulement d'eau sous-terrain pour empêcher une stagnation dans les champs agricoles.

Mais ces quatre facettes sont rarement étudiées simultanément. L'objectif général de ma thèse vise donc à utiliser le cadre conceptuel de la stœchiométrie écosystémique combinée aux formes de C, N, et P pour capturer la réponse des rivières aux changements de climat et d'utilisation du territoire au niveau du bassin versant de façon spatiale, saisonnière et historique.

La stœchiométrie écosystémique

Déterminer l'influence des facteurs naturels et anthropiques sur la livraison de C, N, et P vers une rivière, leur transformation, et leur export subséquent de façon spatiale, saisonnière et historique devient possible seulement lorsqu'on utilise la stœchiométrie écosystémique. Ici, la colonne d'eau d'un chenal principal du réseau fluvial constitue l'écosystème, étant l'intégration ultime des activités terrestres et aquatiques d'un bassin versant. La stœchiométrie écosystémique représente donc l'inclusion de toutes les formes des éléments dans la colonne d'eau qui constituent la totalité du C, du N, et du P sauf le C inorganique dissous. La comparaison de ratios d'un écosystème (ou d'un site) aux ratios d'un autre peut dévoiler à quel point l'écosystème gagne ou perd d'un élément comparé à un autre. Par exemple, les ratios C : N, C : P, et N : P resteront stables entre deux sites (amont vs aval) si leurs concentrations baissent ou augmentent dans les mêmes proportions. Ces comparaisons peuvent être spatiales, entre saisons, ou même capturer les tendances historiques de ratios. Combiner la stœchiométrie du C, N, et P à leurs concentrations représente donc une approche innovatrice pour comprendre la réponse finale d'une rivière face aux pressions naturelles et humaines qui ont lieu dans son bassin versant et à travers le temps.

Les formes de C, N, et P et leur proportion

Le C, N, et P proviennent de tous les types d'environnements. Le long d'une rivière, où le courant homogénéise l'ensemble de molécules qui y coulent, déterminer la provenance exacte des molécules peut être plus difficile, mais certaines formes sont associées à une utilisation du territoire spécifique. Quantifier la proportion qu'occupent ces formes sur l'ensemble des molécules de C, N, et P le long de la rivière peut révéler où et quand une utilisation influence disproportionnellement ces éléments dans l'eau. Détailler les formes de C, N, et P est d'autant plus important pour le C. Si l'agriculture et l'urbanisation ont des effets clairs sur les concentrations de N et P (Carpenter et al., 1998; Carey & Migliaccio, 2009), ce n'est pas toujours le cas avec le C (Stanley et al., 2012; Xenopoulos et al., 2021) car c'est plutôt au niveau qualitatif que ces impacts se font sentir. Certaines formes de C, N, et P sont

aussi plus faciles à consommer ou retirer que d'autres dépendamment du processus de transformation. Une période de faible potentiel de transformation comprendrait une plus grande proportion de ces formes dans la colonne d'eau. Un changement dans la composition de l'ensemble des molécules de C, de N, ou de P qui coulent le long d'un continuum aquatique suggérerait un changement dans l'utilisation du territoire ou dans le potentiel de transformation de la rivière.

Le design expérimental

De façon générale, les processus de transformation et les apports de C, N, et P selon l'utilisation du territoire ont lieu de concert et continuellement. Départager l'influence des processus de l'influence des apports devient donc presqu'impossible sans des combinaisons expérimentales de potentiels contraires d'apports et transformations dans une même rivière. Une rivière drainant un bassin versant dont la configuration de l'utilisation est séquentielle et assez distincte devrait permettre de comparer, le long d'un même tronçon, l'influence de ces apports sur la composition des éléments. Une rivière où des données de qualité d'eau existent depuis plusieurs décennies serait nécessaire pour quantifier l'effet à long terme de l'utilisation du territoire. Comparer les périodes de faibles versus forts débits viendra confirmer l'influence du temps de résidence de l'eau sur les transformations, mais comparer deux moments de faible débit mais de disponibilité de lumière et de chaleur opposée, comme l'été versus l'hiver, permettra de quantifier la force des transformations sur les formes de C, N, et P. Ensemble, les contrastes de climat et la configuration du paysage séquentielle et historique enlaçant une seule rivière aideront donc à élucider où, quand, et comment la rivière reçoit, transforme, et exporte les formes de C, N, et P.

Dans ce contexte, la Rivière du Nord, située à environ 100 kilomètres au nord-ouest de Montréal dans la région des Laurentides représente une expérience naturelle pour étudier la stœchiométrie du C, N, et P ainsi que les proportions des formes des éléments à travers l'espace, les saisons, et le temps. La rivière draine en premier une région forestière minimalement développée, passe par quelques zones urbanisées, et fini par drainer les Basses-terres du Saint-Laurent. Le gradient séquentiel d'utilisation du territoire permettra d'explorer les différentes formes livrées au tronçon principal d'un réseau fluvial par une région forestière, urbaine, et agricole. La rivière subit aussi un régime hydrologique prononcé, avec le plus fort débit au printemps à cause de la fonte des neiges. Il y a deux périodes de faibles débits, soit l'été tel qu'attendu, et l'hiver. Des données de C, N, et P dans l'eau existent depuis 1980 pour trois sites le long du tronçon principal. Ces données ont été récoltées, et le sont encore, par plusieurs

organismes et sont archivées dans la banque de données ouvertes, la Banque de données sur la qualité du milieu aquatique du Ministère de l'Environnement et de la Lutte contre les changements climatiques. Finalement, très rapidement ses ruisseaux de têtes se rejoignent et forme un tronçon principal d'ordre Strahler[8] 5, ordre que la rivière maintient jusqu'à son exutoire. Un même ordre de grandeur aide à diminuer la variabilité associée aux échelles différentes des ruisseaux versus rivières.

Structure

Ma thèse comprend trois chapitres (schématisés dans la Fig. 2) qui sont présentés sous formes d'articles scientifiques. Le **Chapitre 1** démontre que selon les saisons et l'utilisation du territoire, des formes différentes de C, N, et P dominent la stœchiométrie écosystémique. Le **Chapitre 2** identifie si les changements brusques d'utilisation du territoire exercent une influence sur la composition du C, dont les concentrations sont restées stables spatialement et temporellement (chapitre 1). Le **Chapitre 3** quantifie les flux de C, N, et P de 1980 à 2020 et explique leurs patrons avec les changements de précipitations historiques, utilisation du territoire, et pratiques de gestions retrouvées dans le bassin versant. Une conclusion résume les contribution clé de la thèse.

[8] L'ordre de Strahler permet de définir la grosseur du ruisseau ou de la rivière basé sur un principe d'hiérarchie. Un ruisseau qui sort de la terre sera assigné un 1. Lorsque deux 1 confluent, le ruisseau devient un 2. Lorsque deux 2 confluent, ils deviennent un 3, mais lorsqu'un 2 et un 1 se rencontrent, l'ordre reste 2. Il n'y a pas d'ordre précis où un ruisseau devient une rivière. La différence entre les deux est plutôt basée sur plusieurs variables comme le pourcentage de canopée recouvrant le cours d'eau, sa largeur et profondeur, son type de substrat, son métabolisme, l'atténuation de la lumière, et j'en manque.

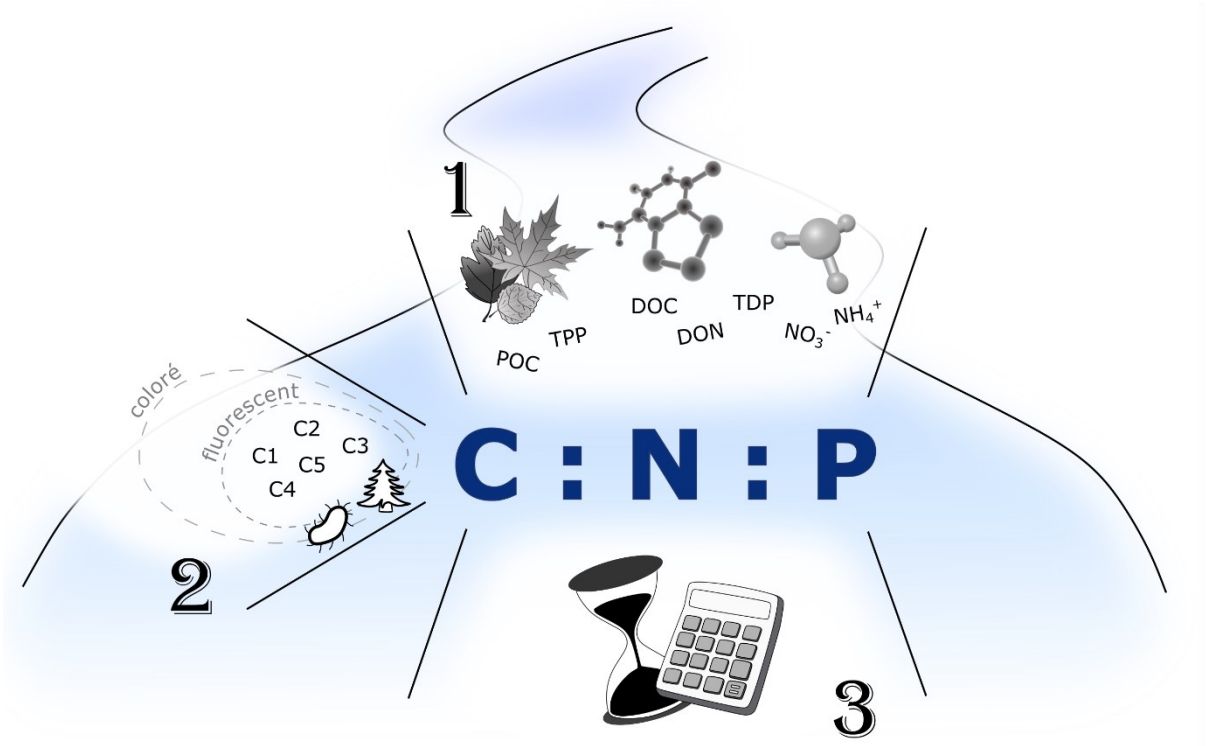

Figure 2 Schéma conceptuel démontrant les trois chapitres de cette thèse s'imbriquant dans la Rivière du Nord. Le **Chapitre 1** explore les formes de C, N, et P inorganiques, organiques, ou particulaires à travers les saisons et l'utilisation du territoire. Le **Chapitre 2** se penche sur les composantes fluorescentes du C qui peuvent démontrer sa provenance et réactivité. Le **Chapitre 3** quantifie de façon historique les flux de C, N, et P à travers les décennies et utilise le climat et le changement d'utilisation du territoire pour les expliquer.

Chapitre 1 : stœchiométrie, saisons, utilisation du territoire

Il y a une riche littérature sur les impacts de l'utilisation du territoire sur la qualité de l'eau, mais peu d'études se penchent à la fois sur le C, N, et P, et sur la proportion d'un élément à un autre. Le **Chapitre 1** vise à combiner les trois éléments en utilisant l'approche de stœchiométrie écosystémique à travers des gradients d'utilisation du territoire et de saisons. Le premier objectif était de capturer l'étendue des ratios que pouvait couvrir une rivière de sa source à son exutoire à travers les saisons. Le deuxième objectif était de déterminer si certaines formes de C, N, et P contribuaient plus que d'autres au ratio C : N : P pendant certaines saisons où à cause de certaines utilisations du territoire.

Chapitre 2 : carbone, composition, extrêmes climatiques

Il n'y a pas encore de consensus sur les tendances de concentrations de C selon l'utilisation du territoire. Un résultat du **Chapitre 1** montre que dans la Rivière du Nord, les concentrations du C sont restées stables. Dans un système naturel, les concentrations devraient diminuer à cause des transformations de rétention. Pour que les concentrations restent stables, soit la rétention doit être minime ou les apports doivent la contrebalancer. Des études comparatives de bassins versants ayant des utilisations du territoire opposées suggèrent des changements plutôt qualitatifs que quantitatifs, mais départager l'influence de l'utilisation du territoire de l'effet des processus de dégradation du C reste à approfondir. Le **Chapitre 2** vise donc à identifier s'il y a un changement dans l'ensemble de molécules qui compose la matière organique dissoute coulant le long de la rivière à travers les saisons. Spécifiquement, l'objectif était de déterminer où, quand, et de combien l'ensemble de molécules composant la MOD changeait le long du tronçon principal à travers des extrêmes de potentiels de dégradation, et si ces changements s'effectuaient aussi soudainement que les changements d'utilisation du territoire observés.

Chapitre 3 : tendances décennales, gestion du territoire, exports

Sur une échelle de temps de trois ans, les **Chapitres 1** et **2** ont montré que certaines formes de C, N, et P sont différentiellement apportées et transformées à l'échelle du bassin versant. Le **Chapitre 3** explore les tendances de C, N, et P sur une échelle de temps de quarante ans, et tente d'expliquer les patrons observés avec l'historique du climat (précipitation, déposition atmosphérique) et de l'utilisation du territoire (budgets de N et P importés sur le territoire). Le premier objectif était de quantifier les flux de C, N, et P le long de la rivière de 1980 à 2020 et utiliser des données climatiques pour expliquer la variation observée. Si les tendances climatiques expliquaient peu la variabilité observée, d'autres facteurs devaient être pris en compte. Le deuxième objectif était donc de quantifier les apports de N et P anthropiques au territoire en utilisant les recensements agricoles et de population, et utiliser ces données pour expliquer le reste de la variabilité observée dans les flux de N et P. Le troisième objectif était d'identifier si, et à quel point, les flux de C, N, et P exportés ont influencé la stœchiométrie écosystémique historique du C : N : P.

Chapitre 1

Différentes formes de carbone, d'azote, et de phosphore influencent la stoichiométrie écosystémique d'une rivière en zone tempérée à travers les saisons et l'utilisation du territoire

Different forms of carbon, nitrogen, and phosphorus influence ecosystem stoichiometry in a north temperate river across seasons and land uses

Stéphanie Shousha[1], Roxane Maranger[1], Jean-François Lapierre[1]

[1] Département de Sciences Biologiques, Université de Montréal, Pavillon MIL, Montréal, Québec H3C 3J7 Canada. Groupe de Recherche Interuniversitaire en Limnologie (GRIL)

Article publié dans *Limnology and Oceanography*, 10.1002/lno.11960

Small edits after thesis evaluation render this version different than the published one.

Abstract

Natural and human features on land result in differential loadings of carbon (C), nitrogen (N), and phosphorus (P) to rivers that influence within ecosystem processing. However, little is known about how land use, together with seasonal changes in climate and hydrology, influence the relative proportions of C, N, and P in rivers. To evaluate the spatial and temporal patterns in ecosystem-level C: N: P stoichiometry, we sampled 13 sites once per season for three years along the mainstem of a north temperate river with winter ice-cover that flows across a gradient of forested, urban, and agricultural landscapes. We found that C concentrations were rather stable along the continuum, whereas N and P rapidly increased downstream due to urban and agricultural land uses. The flow-weighted C: N: P ecosystem stoichiometry ranged from 2319: 119: 1 in the most upstream site to 368: 60: 1 at the outlet. The dominant form of N generally shifted from dissolved organic nitrogen in upstream forested reaches to nitrate in more impacted, downstream reaches, and winter stoichiometry was enriched in inorganic N and dissolved P forms. Concentrations of all three elements were generally lower in spring during year-high flow due to dilution. The spatial and temporal variation in stoichiometry in this north temperate river covered much of the range previously observed between litter ratios and the Redfield ratio. This suggests that even moderate human impacts can have profound effects on riverine ecosystem stoichiometry, and that these effects are modulated by seasonal trends in temperature and hydrology.

Key words: River, Ecosystem, Stoichiometry, Carbon, Nitrogen, Phosphorus, Land use, Season

Introduction

Human activities on the landscape have modified the loadings of carbon (C), nitrogen (N), and phosphorus (P) to aquatic ecosystems. C loadings have changed as a function of agricultural expansion and urbanisation, altering either the magnitude or the type that enters (Wilson & Xenopoulos, 2009; Hosen et al., 2014; Parr et al., 2015). Nutrient inputs to freshwaters are known to increase with urbanisation largely through point source wastewater treatment plants (WWTP) and as diffuse sources from agriculture due to extensive fertilizer use (Carpenter et al., 1998). The proportion of nutrients entering may differ since P is preferentially removed in most WWTPs and the N to P use in crops versus pasture varies (Arbuckle & Downing, 2001; Carey & Migliaccio, 2009). These changes have led to modifications of aquatic ecosystem processes, including increased photosynthesis and decomposition resulting in eutrophication and enhanced greenhouse gas emissions (Carpenter et al., 1998; Smith & Schindler, 2009; Borges et al., 2018). Given that the relative concentrations of these elements have changed due to differential land uses, the proportions entering have therefore also shifted with consequences for ecosystem functioning.

Understanding how an organism maintains its elemental ratios relative to those of its resources is the foundation of ecological stoichiometry (Sterner & Elser, 2002). Ecological stoichiometry has largely focused on the organismal level to assess how physiology changes in response to resource variability. The same approach can be adapted to the watershed scale to assess changes and responses in ecosystem-level stoichiometry as a function of global change (Maranger et al., 2018). For example, riverine ecosystems receive C, N, and P mostly from land in proportions that vary depending on changes in land cover and land use, and on season. Like ecological stoichiometry, the relative proportion of C, N, and P loaded to a riverine ecosystem may differ from its capacity to process the elements via a combination of biogeochemical pathways that can be influenced by hydraulic flow.

The few studies that explicitly considered ratios of C, N, or P in flowing waters have typically focused on pairs of elements. Several have found elevated C ratios in headwater streams which are more closely connected to terrestrial soils and litter, both known to be C rich and nutrient poor (Vitousek & Howarth, 1991; Aitkenhead-Peterson et al., 2003; Vitousek et al., 2010). These generally unimpacted forested exports are dominated by dissolved C, N, and P forms (Kortelainen et al., 2006). However, temporal patterns in precipitation can influence the relative amount of particulate compared to dissolved inputs because of changes in hydrologic flow paths and increased erosion (Meyer & Likens,

1979; Hornberger et al., 1994; Jeong et al., 2012; Inamdar et al., 2015). In disturbed catchments, the concentrations and forms of C, N, and P differ from pristine environments, and their source may be point or nonpoint. For example, concentrations of highly bioavailable ammonium (NH_4^+) and soluble reactive phosphorus (SRP) have been found to increase from 10-100 times and 50 times, respectively, downstream of WWTPs in U.S. rivers (Haggard et al., 2005), and overall loads are higher with larger human populations (Withers & Jarvie, 2008; Carey & Migliaccio, 2009). The dominant N form entering rivers from agricultural nonpoint sources is typically NO_3^-, which is highly mobile in the soil matrix (Caraco & Cole, 1999; Stanley & Maxted, 2008), whereas for P, high dissolved concentrations are typically observed, but precipitation promotes increased particulate mobilization as a function of soil erosion (Vanni et al., 2001; Goyette et al., 2019; Manning et al., 2020). In terms of C, riverine concentrations are dependent on the type of human activity and ecosystem, and have been shown to vary in strength and direction (Stanley et al., 2012; Xenopoulos et al., 2021).

As the elements flow downstream, C and N can be permanently removed from the ecosystem via atmospheric evasion (Mulholland et al., 2009; Cory et al., 2014), while P is nearly only lost from the water column via sedimentation (Vanni et al., 2001). Because of these removal processes, all things being equal, concentrations of all elements should in principle decrease from land to the ocean (Seitzinger et al., 2006; Cole et al., 2007; Withers & Jarvie, 2008) but the differential removal of C, N, and P should alter their ratios (Maranger et al., 2018). Indeed, high variability has been measured in pairs of ratios in rivers worldwide, but this variability is poorly constrained and driven by a multitude of natural and human factors that influence elemental composition. Rivers draining primarily urban and agricultural watersheds would thus be expected to contain high concentrations and proportions of bio-reactive N and P forms compared to more pristine ones, but the consequences for C, N, and P ratios at the ecosystem level across spatial and seasonal gradients remain unknown.

In this study we aim to understand the patterns and drivers of ecosystem-level stoichiometry of a temperate river exposed to large gradients in land cover, land use, and environmental conditions across seasons including ice covered winter. Although winter limnology has grown in popularity, most studies have focused on under-ice dynamics in lakes and the repercussions of ice-loss (Hampton et al., 2017). Studies of winter dynamics in rivers remain rare (Cruaud et al., 2020) but from a stoichiometric perspective, temperate, northern hemisphere winter represents an interesting extreme of low hydrologic flow combined with cold temperatures and limited light. We define ecosystem stoichiometry as the ratio of the sum of all forms of C, N, and P in the water whether they are

particulate or dissolved except inorganic carbon, which should reflect the net result of their gains and losses in the aquatic ecosystem. Our specific objectives were to 1) quantify how riverine ecosystem level C: N: P ratios respond to a sharp shift in land use, and how this response varies across seasons, and 2) determine what elemental forms contribute most to this seasonal ecosystem C: N: P stoichiometry. To do so, we sampled a temperate river along its mainstem that consecutively drains forested, urban, and agricultural regions once every season, for three years. We finally quantified how the observed ecosystem C: N: P stoichiometry varied within terrestrial and marine extremes previously reported in the literature.

Methods

Study area and sampling

The *Rivière du Nord* watershed (Fig. 1) is situated roughly 100 kilometers north-west of Montréal, QC, Canada, in the region of the Laurentians. This region has a temperate climate, with 10-year average seasonal temperatures of -6, 12, 19 and 1°C for winter, spring, summer, and fall, respectively (Government of Canada, 2021a), and mean annual precipitation of 972 mm (Climate Data, 2012). Highest stream discharge occurs in the spring (typically end of April) and lowest discharge can occur either in summer or winter, depending on years (MDDELCC, 2018b). The river drains two different geological provinces. The northern half, or Canadian Shield, is mostly covered by boreal forest growing on metamorphic rocks with very little topsoil (Douglas, 1970). The southern half, the St. Lawrence Lowlands, has supported agriculture with its fertile soil and negligible slope for the past several centuries, with a major shift from crop to dairy farming in the late nineteenth century (Wiken et al., 1996; Russell, 2012). At the intersection of these provinces is the more heavily urbanized area that includes the largest town in the catchment, *Saint-Jérôme*, whose wastewater treatment plant serves a population of just over 77 000 (Statistics Canada, 2017d) and discharges to the river. To estimate the current daily flow of effluent from this WWTP (45° 45' 1.6236" N, 74° 0' 25.0524" W), we modelled 969 WWTP discharge measurements and their associated populations using data from 2011 (MELCC, 2011). This resulted in a strong linear relationship (R^2=0.97) from which we derived a more recent discharge estimate using *Saint-Jérôme*'s latest population count.

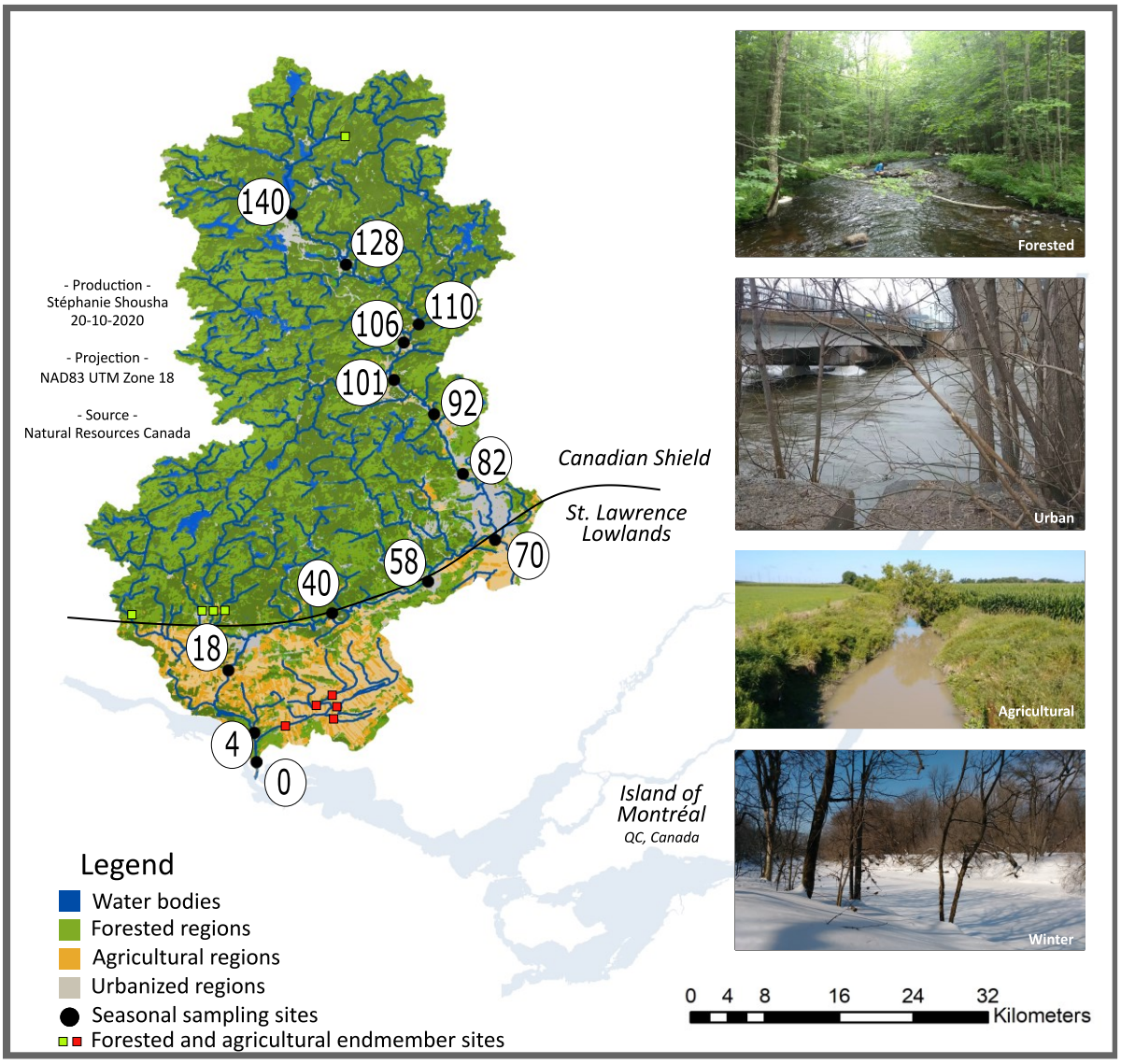

Figure 1 Distribution of the seasonal sampling sites (black circles as river km) along the mainstem of the *Rivière du Nord* watershed, QC, and location of the forested and agricultural endmembers (green and red squares, respectively). The Saint-Jérôme gauging station is situated just upstream of RKm 70, but its effluent is captured by RKm 58. Outlet coordinates are 45.53, -74.33. Photographs show a forested headwater stream (representing green squares on map, summer), the main stem passing through the highly urbanized region (spring), a small stream draining the agricultural subwatershed (red squares on map, summer), and site RKm 70 as an example of winter conditions.

We sampled 13 sites along the main stem of the 146.6-kilometer long *Rivière du Nord* once per season, from summer 2017 to winter 2020, which resulted in 11 field campaigns. The objective was to obtain three full yearly cycles, but the last spring sampling was cancelled due to public health restrictions in April 2020. The site names refer to their position along the river in terms of their distance, in River Km from the outlet, which is Site 0, or "RKm 0". Our most upstream sampling site is located where the river quickly becomes, and remains, Strahler Order 5. We targeted hydrological extremes, with spring, summer, and winter campaigns representing the river's maximum or minimum discharge. In summer 2018, we added 5 additional impacted sites in headwater streams draining landscapes with > 90% agriculture and 5 forested headwater streams draining landscapes with >90% forest. For each campaign, we sampled all the sites within a two-day window to reduce hydrological variability.

Field measurements

At all sites, we measured water temperature, conductivity, pH, and dissolved oxygen with a handheld meter (Yellow Springs Instrument, Ohio, United States). All physical and chemical water measurements were taken just below the surface of the water in the middle of the river. We collected water samples as far as possible from the shore. When possible, we sampled from the middle of the river either by boat or by lowering a Van Dorn from a bridge. When sampling the middle was not possible, we took a grab sample as far as we could from the shore, facing the current. Winter samples were taken from the middle of the river through a hole in the ice bored with an electric ice auger. We conditioned 0.5 and 1 L acid-washed bottles three times with river water before filling them and transporting them back to the lab on ice for further processing.

Sample preparation

We stored unfiltered water samples in the 0.5L opaque bottles in the dark at -20°C for total N (TN) and total P (TP) analyses. On the same day, in the lab, we first filtered water through a 0.7 μm GFF filter using a filtration-tower, then passed the filtrate through 0.45 μm Filtropur S polycarbonate filters using a syringe (Sarstedt, Nümbrecht, Germany) for total dissolved N (TDN), nitrite-nitrate (NO_2^- - NO_3^-) henceforth referred to as NO_3^-, ammonium (NH_4^+), and total dissolved P (TDP), which we stored in 150 ml pre-acid washed HDPE bottles in the dark at -20°C. Dissolved organic carbon (DOC) was filtered using the same procedure into pre-combusted amber bottles, which were then stored in the dark at 4°C. We sampled suspended matter for campaigns 2 to 11, by filtering water through pre-

weighed and pre-burned (450°C for 4h) Whatman GF/F filters with a nominal pore size of 0.7 μm. At the time of analysis, filters were dried at 100°C for 1h and reweighed to estimate suspended matter concentration as the difference in weight. We collected field blanks with Milli-Q water to ensure a lack of contamination due to filtering techniques and bottle effect.

Sample analyses and variable calculations

We analysed TN, TDN, NO_3^- (USEPA-352.3, 1993) and NH_4^+ (USEPA-350.1, 1993) by colorimetry using a Latchat QuickChem 8000 flow injection analyzer (Latchat Instruments, Loveland, United States). Particulate N, as the difference between TN and TDN, represented on average 2.3% of TN and was therefore not considered. We calculated dissolved inorganic N (DIN) by summing NO_3^- and NH_4^+, and subtracted DIN from TDN to estimate the dissolved organic form (DON). We analysed TP and TDP with a segmented flow analyzer USEAP365.1(Astoria-Pacific, Clackamas, United States; We subtracted TDP from TP to get total particulate P (TPP). We analysed DOC concentrations (USEPA-415.1, 1974) with a TOC analyzer (Aurora 1030, IO Analytical Instruments, Texas, United States). The detection limits for TP-TDP, TN-TDN, NO_3^-, NH_4^+, and DOC were 0.7 μg L^{-1}, 4 μg L^{-1}, 0.4 μg L^{-1}, 1.4 μg L^{-1}, and 0.15 mg L^{-1}, respectively. We measured particulate C using an elemental CHNS-O analyzer (Thermo Fisons model EA1108; Zimmermann et al., 1997). For each site, we collected three filters and randomly cut ¼ of each filter to isolate it in a tin foil. We then multiplied the resulting %C by the suspended matter concentrations to obtain POC concentration. We then estimated POC concentrations for campaigns 2 to 7, for which we had suspended matter concentration but no measured %C. To do this, we averaged the measured %C by season and river section. Mean and standard deviation of %C were variable for the agricultural (mean = 7.39, sd = 2.7), urban (mean = 10.53, sd = 4.9), and forested reaches (mean = 23.23, sd = 9.3), but our conclusions are not sensitive to this variation given that DOC generally dominated the TOC pool, hence POC contributed little to TOC (Table 2). We averaged POC in summers 2018 and 2019 to estimate POC in summer 2017. Finally, we summed DOC and POC to estimate total organic carbon (TOC). All analyses have been conducted at the *Université de Montréal*'s GRIL (*Groupe de Recherche Interuniversitaire en Limnologie*) analytical lab. All resulting stoichiometric ratios are molar based.

Geographical analyses

We delineated the *Rivière du Nord* watershed area using 1x1 meter digital LiDAR elevation data (Gouvernement du Québec, 2016b) in the ArcHydro Toolbox of the ESRI ArcGIS version 10.5.1 (ESRI, 2017). We measured river kilometer and Strahler order using the LiDAR data, then delineated individual sites subwatersheds, determined as the area drained between two sites. We obtained daily discharge data for the study years from *Saint-Jérôme*'s gauging station (situated between RKm 70 and 82) operated by the *Centre d'expertise hydrique du Québec* (MDDELCC, 2018b). From this value, we estimated discharge at each site assuming that discharge is proportional to catchment area, which was supported by the low variation in surface runoff at the scale of the catchment (Statistics Canada, 2017a). Using the discharge data, we calculated time spent by water between each site for every season, to be used as a proxy for water retention time, with the WatershedTools package (Talluto, 2020) in R version 3.6.1 (R Core Team, 2019). Because the seasonal differences in discharge in headwater sites compared to downstream sites are so large, we used a discharge-deviation value (discharge-dev), as estimated in Galantini et al., 2021 as a proxy for discharge. We also estimated lake volume per subwatershed following Heathcote et al. (2015). We obtained land use and land cover data from the Center for Topographic Information (Natural Resources Canada, 2009) and intersected this layer in ArcGIS with the subwatershed layer to determine %forest, %urban and %agriculture in each subwatershed.

Statistical analyses

To quantify spatial patterns in ecosystem stoichiometry that are representative of the full study period, we first estimated flow-weighted values. These were calculated as the percentage of water flowing during each season multiplied by the molar concentrations measured at each site. We divided this flow-weighted C and N concentrations by the flow-weighted P concentrations, resulting in flow-weighted C: P and N: P ratios. We then determined the correlations between the contribution of the different C, N, and P forms to total concentrations across seasons and across land uses with a Principal Component Analysis (PCA), using the vegan package (Oksanen et al., 2019). To emphasize seasonal patterns, only chemical variables were used to determine principal components 1 and 2. Then, environmental variables and land use variables, some of which remain fixed among seasons, were passively projected on principal components 1 and 2. We were then able to assess relationships

between C, N, and P forms with environmental properties while focusing on the patterns among elements.

We then quantified the accumulation of the different C, N, and P forms along the continuum by modelling linear regressions using river kilometer as a predictor. These accumulations, in $\mu mol \cdot L^{-1} \cdot km^{-1}$, correspond to a net riverine accumulation rate that depends on the balance between loadings and processing. They were plotted for each season with the vioplot package (Adler & Kelly, 2019). We determined which accumulation rates were significantly different from others with posthoc Tukey HSD tests. In some cases, there was no significant accumulation, or the accumulation appeared non-linear, leading to non-significant slopes. Sampling campaigns with non-significant linear trends resulted in a low slope with a high uncertainty that overlapped with zero, which is taken into account in our analyses.

Finally, we compared our measured ratios within a stoichiometric space that included extreme known values along the land to ocean continuum as well as watershed endmembers. This included the Redfield ratio (Redfield et al., 1963), pristine senesced litter from temperate coniferous and broadleaf forests (McGroddy et al., 2004) as well as forested and highly agricultural sites sampled within the *Rivière du Nord* watershed.

Results

Catchment hydrology and landscape characteristics

The *Rivière du Nord* flows along a gradient of landscapes dominated by forest cover in the upstream reaches (RKms 140 to 92), followed by a moderately urbanized section immediately adjacent to the river (RKms 92 to 70), with agricultural land use dominating downstream (RKms 70 to 0, Fig. 1, Table 1). In particular, the forested section has low urban density and low agriculture: on average every subwatershed from RKm 140 to 92 has < 5% impervious area and < 5% agriculture. The subwatersheds with dense urban areas have up to 37% impervious cover. In subwatersheds from RKm 70 to the outlet, agriculture reaches 74% of coverage and urban areas decrease to < 5%. Averages of three-month seasonal discharge measured at the *Saint-Jérôme* gauging station were 65.5, 11.2, 23.8, and 18.1 $m^3 \cdot s^{-1}$, for spring, summer, fall, and winter, respectively. During our two-day snapshot campaigns, average discharges at this same station were estimated at 195.0, 17.8, 29.0, and

11.1 $m^3 \cdot s^{-1}$. The spring snapshot campaigns deviated most from their seasonal average, which allowed us to capture this season's extreme; our winter campaigns also captured an extreme low-flow period.

Table 1 Percent land cover and land use per subwatershed. RKm refers to the subwatershed drained. Category specifications can be found below the table.

RKm	Forest	Wetlands	Water	Agriculture	Urban	Other
140	87.53	0.06	8.36	0.00	0.20	3.85
128	80.73	0.04	9.16	0.16	4.10	5.80
110	89.28	0.00	3.88	0.30	1.25	5.32
106	89.27	0.11	6.22	0.31	1.09	3.00
101	88.44	0.05	4.59	1.03	1.43	4.47
92	77.53	0.00	1.36	4.80	5.25	11.06
82	61.87	0.44	8.66	5.03	9.94	14.06
70	35.49	0.00	0.44	17.67	37.12	9.33
58	64.88	0.51	2.78	15.98	4.80	11.04
40	65.49	0.71	1.19	14.22	2.33	16.07
18	79.37	0.27	5.23	8.04	1.29	5.80
4	27.86	0.04	1.91	62.54	4.73	2.91
0	18.79	0.00	0.89	73.69	0.81	5.94

Forest: coniferous, broadleaf, mixed wood.
Wetlands: vegetation (coniferous, broadleaf, mixed wood, shrub, herb) combined with a water table near, at, or above the soil surface for a long enough period to promote biogeochemical processes.
Water: lakes, reservoirs, rivers, streams, or salt water.
Agriculture: annual, perennial cropland and pasture.
Urban: impervious areas.
Other: exposed land (example: river sediments, beaches, gravel pits, etc.), low and tall shrubs, and herbs.

Spatial and seasonal patterns in C, N, and P concentrations and stoichiometry

For total C, N, and P, overall concentrations generally increased from upstream to downstream along changes in land cover and land use. This increase was rather linear and much steeper for N and P as compared to C. There also was a significant increase in N and P for all seasons, but not for C. The ranges for the three flow-weighted elements along the continuum were 441.8 to 550.9 $\mu mol \cdot L^{-1}$ (mean = 493.6, sd = 31.2) for C, 26.2 to 89.33 $\mu mol \cdot L^{-1}$ (mean = 51.7, sd = 19.9) for N, and 0.22 to 1.50 $\mu mol \cdot L^{-1}$ (mean = 0.84, sd = 0.47) for P (Fig. 2a). These patterns result in a flow-weighted stoichiometry at the ecosystem level that varies from 2319: 119: 1 in the upstream section to 368: 60:

1 at the river mouth, following a gradual increase in N and P relative to C along the mainstem (Fig. 2b).

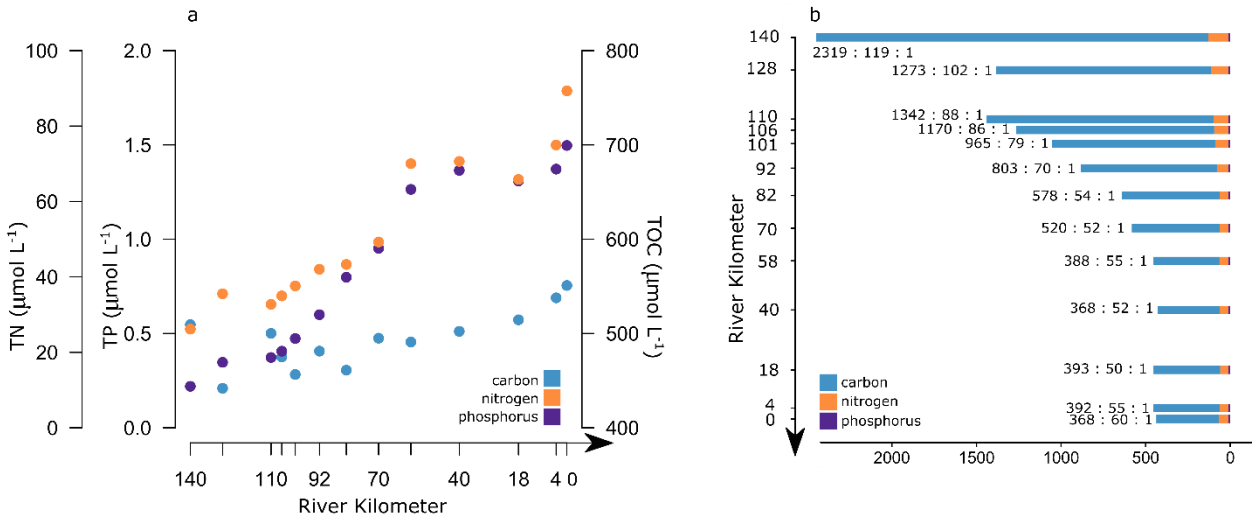

Figure 2 Patterns in C, N, and P concentrations and stoichiometry along the *Rivière du Nord* mainstem. Panel a shows the overall (all sampling dates combined) flow-weighted molar concentrations of TOC, TN, and TP along the river continuum represented by RKm. Panel b shows overall flow-weighted TOC: TN: TP molar ratios also along the continuum. The arrows on the x and y axes of panels a and b respectively indicate flow direction.

There was also considerable seasonal variation in C: N: P ecosystem stoichiometry that varied along upstream to downstream gradient (Table 2). Forested C: P ratios were highest in fall (1887), due to low P concentrations and lowest in summer (1353) coinciding with comparatively high P. Downstream C: N ratios remained highest in spring (11), due to the lowest N concentrations in this season. Winter C: N ratios were lowest in every region (forested: 11, urban: 7, agricultural: 4). N: P ratios were relatively constant in summer along the continuum (forested: 70, urban: 61, agricultural: 64) but more than halved in winter (118 to 53) and spring (98 to 44). These patterns are driven by differences in the concentrations of total C, N, and P, which are in turn dictated by the elements' specific forms. To visualize which C-N-P forms dominated in certain regions and seasons, we plotted them against environmental and geographic properties using a Principal Component Analysis (Fig. 3). Together, principal components 1 and 2 explain 77% of the variance in C, N, and P forms. PC1 is mostly driven by C forms, and PC2 by N, but more specifically NH_4^+, which was higher during the

winter. NO_3^- correlates strongly with % agriculture, whereas suspended matter was higher during the spring.

	Forested region				Urban region				Agricultural region			
	Summer	Fall	Winter	Spring	Summer	Fall	Winter	Spring	Summer	Fall	Winter	Spring
TOC	529	502	411	486	538	501	391	475	578	564	465	505
DOC	487	479	392	446	503	469	360	425	535	510	418	442
POC	42	23	18	41	35	32	31	50	43	54	47	64
TN	28.91	32.05	39.31	30.08	39.21	43.89	59.89	35.79	97.68	86.78	114.02	44.32
NH_4^+	2.55	4.31	9.41	2.11	3.87	6.4	17.58	2.82	16.35	15.2	53.97	4.17
NO_3^-	8.43	9.38	16.64	16.28	16.6	16.68	26.83	19.86	55.1	40.97	40.94	24.14
DON	17.65	17.85	13.06	11.45	16.13	20.19	14.28	12.07	22.94	23.93	16.2	14.17
TDN	28.63	31.55	39.1	29.84	34.02	43.28	58.69	34.75	94.39	80.1	111.11	42.48
TP	0.42	0.28	0.36	0.32	0.67	0.49	0.79	0.75	1.54	1.24	2.16	1.03
TDP	0.21	0.16	0.24	0.12	0.28	0.22	0.55	0.16	0.86	0.57	1.55	0.25
TPP	0.21	0.12	0.12	0.2	0.39	0.26	0.24	0.59	0.68	0.67	0.61	0.78
TSM	1.9	1.1	3.4	2.2	4.3	3.0	2.8	12.7	6.6	11.0	5.6	18.0
TOC: TN: TP	1353: 70: 1	1887: 116: 1	1401: 118: 1	1604: 98: 1	841: 61: 1	1108: 94: 1	537: 80: 1	731: 54: 1	392: 64: 1	470: 71: 1	219: 53: 1	501: 44: 1

Table 2 Concentrations ($\mu mol \cdot L^{-1}$) of C, N, and P elemental forms for different land uses and seasons. Total suspended matter (TSM) concentrations are in $mg \cdot L^{-1}$.

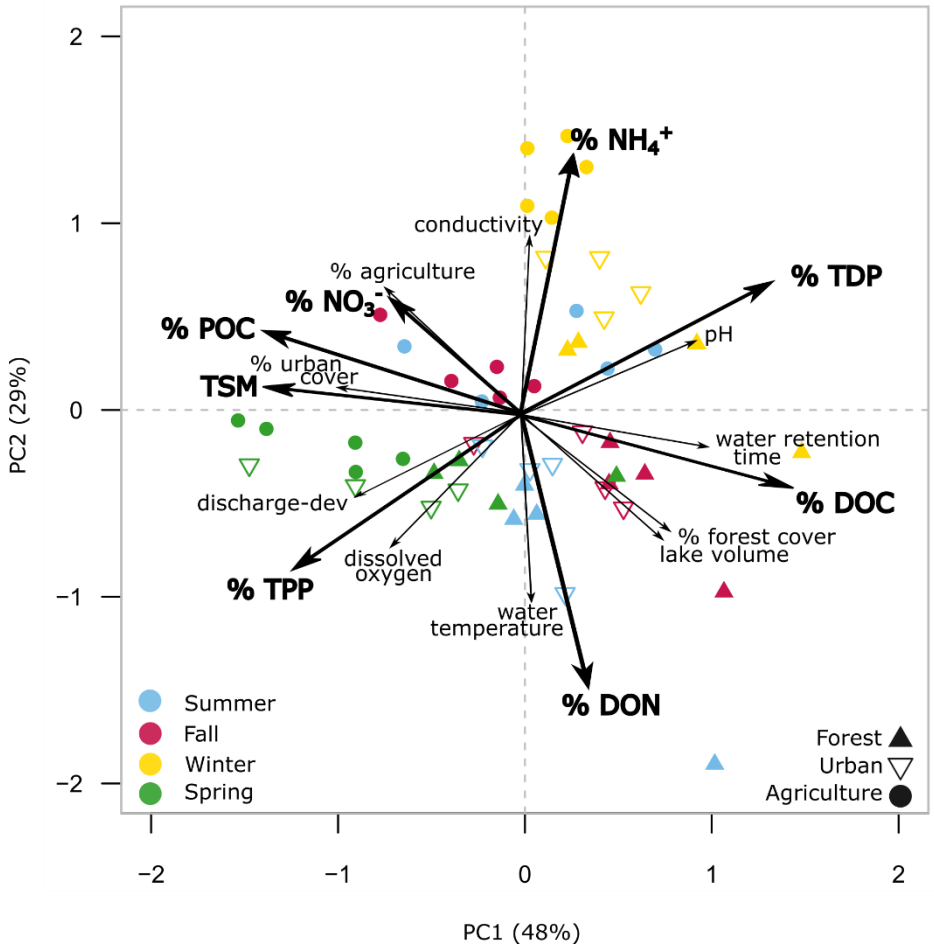

Figure 3 Principal component analysis using the proportion of elemental forms relative to total to define the space (bold black acronyms), while passively superimposing the environmental variables (smaller grey words).

Filled triangles, empty inverted triangles, and circles represent the forested, urban, and agricultural regions respectively, and sites are coloured by season. Acronyms refer to total suspended matter (TSM), particulate organic carbon (POC), nitrate (NO_3^-), ammonium (NH_4^+), total dissolved phosphorus (TDP), dissolved organic carbon (DOC), dissolved organic nitrogen (DON) and total particulate phosphorus (TPP).

Accumulation of elemental forms across seasons and land uses

All forms of C, N, and P tended to accumulate from upstream to downstream at the watershed level, but some accumulated at different rates, influencing riverine stoichiometry (Fig. 4). In particular, TN tended to accumulate 4.6 times slower during the spring high flow period (0.14 $\mu mol \cdot L^{-1} \cdot km^{-1}$) compared to a relatively stable accumulation rate for the other three seasons (0.65 $\mu mol \cdot L^{-1} \cdot km^{-1}$, mean of R^2 of all TN slopes = 0.84). There were also strong, but different, seasonal patterns in TP accumulation, with concentrations accumulating appreciably during winter (0.017 $\mu mol \cdot L^{-1} \cdot km^{-1}$) compared to the other three seasons (0.010 $\mu mol \cdot L^{-1} \cdot km^{-1}$, mean of R^2 of all TP slopes = 0.83). TOC accumulation was significant ($p < 0.05$) in only four out of 11 sampling events, but marginally significant ($p < 0.10$) in four other events. As a result, the average accumulation rates reported in Fig. 4 for TOC are considerably more variable and relatively closer to overlapping with zero than for TN and TP, and there were no seasonal trends in TOC accumulation rates (p-value > 0.05).

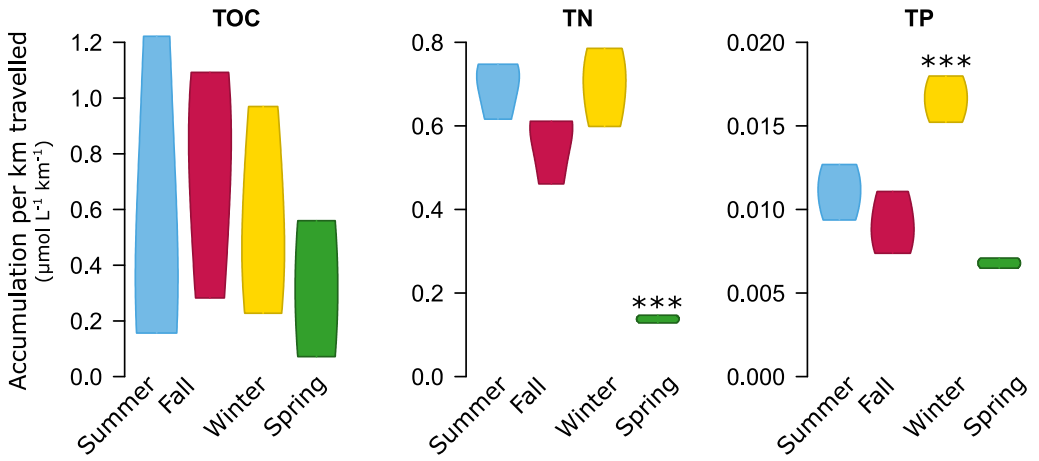

Figure 4 Total organic carbon (TOC), total nitrogen (TN), and total phosphorus (TP) accumulation rates along the continuum, across seasons. Rates were calculated as the slope of elemental concentrations per river km travelled using linear regression models. All rates are in $\mu mol \cdot L^{-1} \cdot km^{-1}$. Summer POC was estimated as the average of POC for summers 2018 and 2019. Posthoc Tukey tests

determine whether rates are different from each other, and significantly different rates are shown with asterisks (p-value < 0.001 = ***)

We further quantified how specific forms of C, N, and P tended to accumulate from upstream to downstream to assess how they may account for patterns in ecosystem stoichiometry. The main forms driving TN accumulation shifted from NO_3^- during summer and fall to NH_4^+ during the winter (Fig. 5a). Concentrations and accumulation rates of NH_4^+ during the winter were as high as NO_3^- accumulation during the two other seasons, emphasizing the disproportionate importance of this bio-reactive form for ecosystem stoichiometry during the winter. Spring concentrations and accumulation rates were lower for all N forms than in any other season. TDP and TPP accumulated at similar rates in summer and fall but had opposite trends in winter and spring (Fig. 5b). Winter TDP accumulated almost three times faster than TPP, analogous to NH_4^+, where the bio-available form tends to disproportionately accumulate in cold and low discharge conditions. Spring had the opposite patterns. TPP accumulated over 4x faster than TDP at annual peak flow. This was coherent with high suspended matter concentrations (spring = 11.5 $mg \cdot L^{-1}$, other seasons = 4.5 $mg \cdot L^{-1}$), and accumulation rates (spring = 0.16 $\mu mol \cdot L^{-1} \cdot km^{-1}$, other seasons = 0.06 $\mu mol \cdot L^{-1} \cdot km^{-1}$). Because POC is a proportion of suspended matter, we expected it to behave similarly. However, while POC accumulated significantly in fall, winter, and spring ($p < 0.05$), rates did not differ among those three seasons (Fig. 5c). Although suspended matter was high in spring, the %C was lowest during this season (Fig. S1). There was no measurable POC accumulation in summer, and DOC accumulation was only observed in the first of the 11 campaigns.

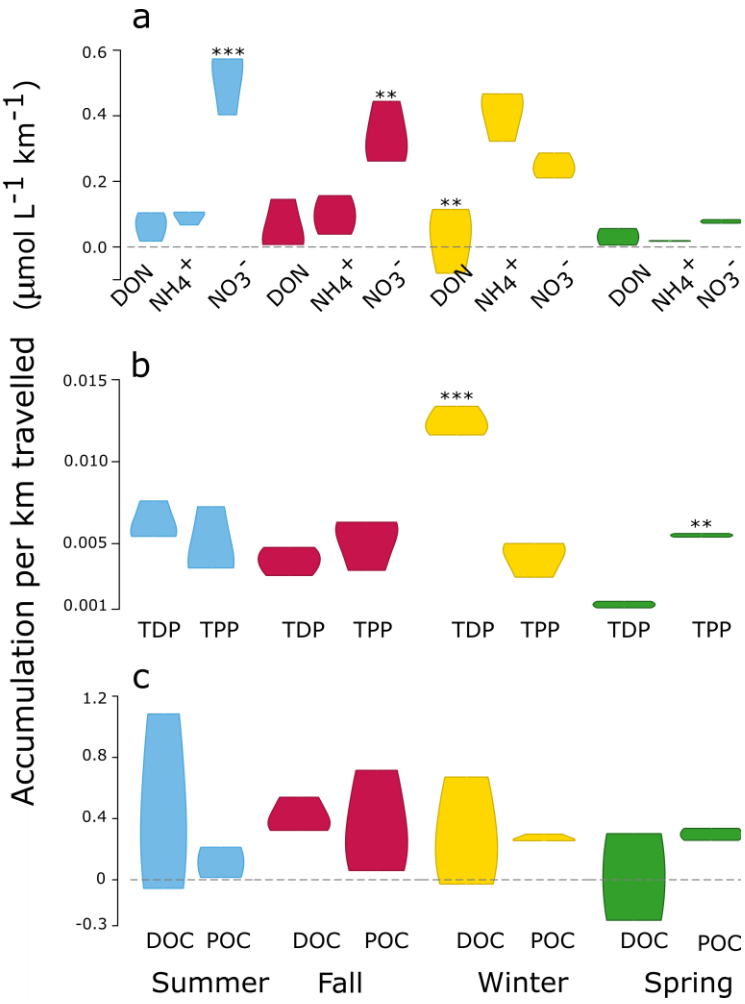

Figure 5 C, N, and P elemental form accumulation rates along the continuum, across seasons. Rates per form were calculated as the slope of change in concentrations per km travelled using linear regression. All rates are in µmol·L^{-1}·km^{-1}. Panel a shows rates for dissolved organic nitrogen (DON), ammonium (NH_4^+), and nitrate (NO_3^-). Panel b shows rates for total dissolved phosphorus (TDP) and total particulate phosphorus (TPP). Panel c shows rates for dissolved organic carbon (DOC) and particulate organic carbon (POC). Posthoc Tukey tests show significant differences among the rates per season (asterisks).

Rivière du Nord stoichiometry in a seasonal and land to ocean continuum

The ecosystem stoichiometry of *Rivière du Nord* spans a vast range from upstream to downstream sites, with marked differences among seasons (Fig. 6). Overall, the river's upstream stoichiometric ratios were the most variable, and downstream ratios converged to those rich in N and P, driven by land use changes in the landscape. Across the seasons, C: N and C: P ratios differed: the C: N ratios exported

by the river in spring (11.5) were much higher than in any other season (6.3, 6.7, 6.7 for summer, fall, winter), due to low N concentrations diluted by an overriding hydrological signal. Exported winter C: P ratios (219) were much lower than in any other season (392, 470, 501), due to low C and high P concentrations in winter (Table 2). Together, the seasonal ratios in this river almost span the range of the land to ocean continuum constrained by senesced terrestrial litter and Redfield ratios. To these literature extremes are added the impacted agricultural and pristine forested endmembers measured from the *Rivière du Nord*'s smaller tributaries. The forested endmembers are highly variable, particularly with regards to P, but the agricultural endmembers are all richer in N than the Redfield ratio.

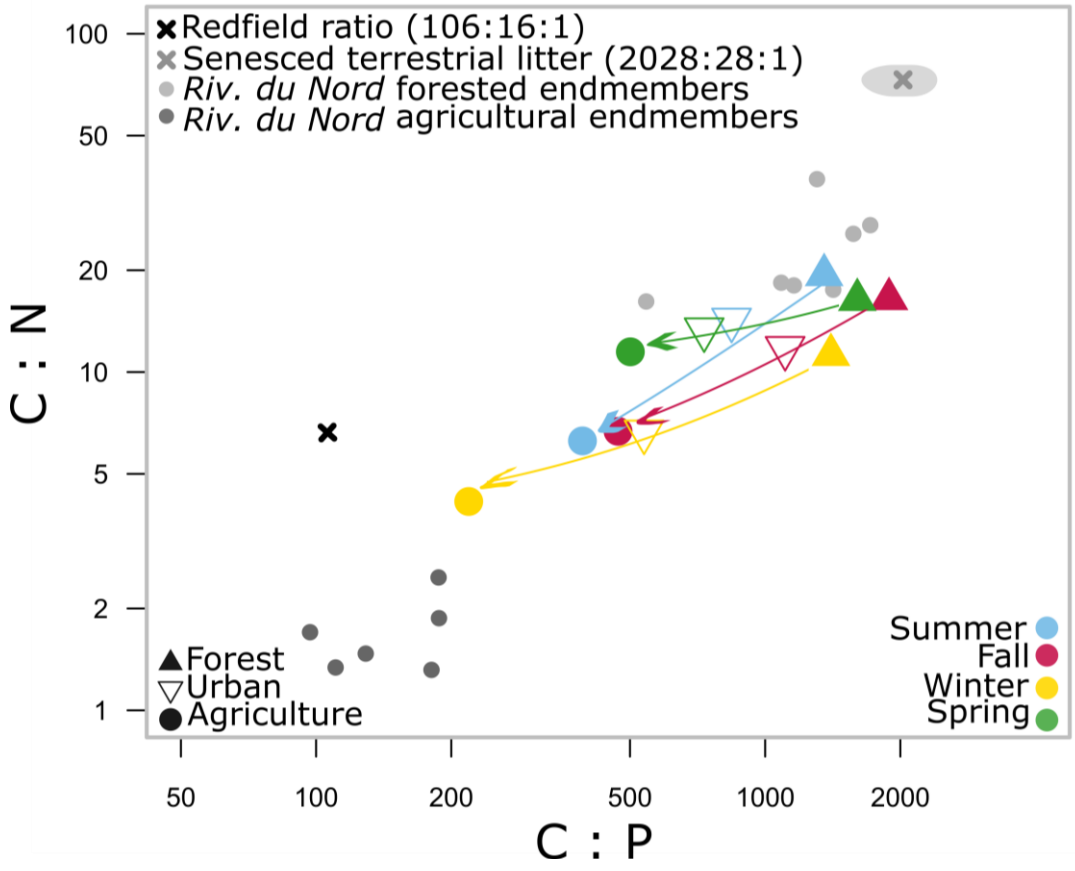

Figure 6 Distribution of C: N and C: P ratios of the *Rivière du Nord* with literature extremes, the black x is the Redfield ratio (Redfield et al., 1963) and the light grey x temperate senesced terrestrial litter (McGroddy et al., 2004). *Rivière du Nord* ratios are shown in blue, red, yellow, and green for summer, fall, winter, and spring ratios, respectively. Shapes (filled triangles, inverted triangles, and circles) represent differential land uses. Arrows show the direction of river flow. The light grey circles are the forested endmembers from the *Rivière du Nord* watershed and the darker grey ones are its agricultural endmembers. Axes are logged.

Discussion

In this study we showed that a sharp shift in land use and seasonal variation in hydrology led to major changes in C, N, and P elemental ratios in a seasonal ice covered north temperate river. All seasons combined, C, N, and P loadings increased with urbanisation and agriculture, albeit at different rates with nutrients accumulating particularly rapidly (Fig. 2a). Seasonal variation in different elemental forms further drove the overall ecosystem stoichiometry (Figs. 4 and 5). Summer and fall N were dominated by NO_3^-, winter N by NH_4^+, whereas in spring there was no obvious difference in accumulation among the N forms, but rates were generally lower due to dilution (Fig. 5a). Elemental P accumulation rates were similar in summer and fall, but dissolved P dominated in winter, and particulate P in spring (Fig. 5b). There were no obvious inter-seasonal patterns in DOC accumulation rates (Fig. 5c) although overall lower concentrations were observed during the winter. We suggest that a combination of seasonal and spatial changes in terrestrial loadings combined with differential within-system processing of elements led to widespread, but variable net accumulation of different forms of C, N, and P at the ecosystem level. As a consequence, the ecosystem stoichiometry of the *Rivière du Nord* shifted from C-enriched ratios in upstream sites to highly enriched nutrient ratios towards the river mouth (Fig. 6). This pattern was driven predominantly by human modification of the landscape, with seasonal difference in preferential accumulation of specific N and P forms as a function of changes in hydrology, temperature and light availability.

The resulting decrease in C to nutrient stoichiometries observed along the river's mainstem is comparable to what was reported along the aquatic continuum in a global synthesis (Maranger et al., 2018). This suggests a shift in stoichiometry from headwaters to lower reaches although both the initial stoichiometry and the causes for change along the axis of flow may vary. Looking across various regions, pairwise elemental ratios for unimpacted streams and rivers of different Strahler orders are reported to range from 444-2445 for C: P, 33-79 for C: N, and 11-41 for N: P (Kortelainen et al., 2006; Dittman et al., 2007; McGroddy et al., 2008; Weyhenmeyer & Conley, 2017). As for exports that also include more heavily impacted rivers located in the US, average C: N: P stoichiometry was estimated at 167: 25: 1, with paired ratios ranging from 83-35, 4-12, and 14-45 for C: P, for C: N, and N: P, respectively (Maranger et al., 2018). Interestingly in our spatial temporal evaluation of the *Rivière du Nord*, we span most of the range of the paired elements summarized here, from very high relative carbon content in the pristine shield area, regardless of stream order, to extremely low C: N and C: P

ratios particularly in the agricultural streams (1.66 and 141 respectively). The range in N: P ratios measured across sites and seasons in our system (32-166, mean = 77) is largely outside these reported literature values and reflects disproportionally higher N inputs to the *Rivière du Nord*. This can be explained by the increasing ratios of N: P in fertilizer use observed across the region (Goyette et al., 2016) due to relatively greater accessibility of synthetic N fertilizer including urea (Glibert et al., 2014), as well as a lack of legislative incentive to remove N from WWTPs in the province of Quebec (MTESS, 2020) as compared to the US (Yuan et al., 2014). The main driver of the patterns of more nutrient rich stoichiometries downstream as well as the idiosyncrasies in relatively higher N in the *Rivière du Nord* is a function of land use changes due to a sharp shift in geologies. Furthermore, seasonal differences in stoichiometries along the continuum were also observed and are likely a balance between differences in external sources and within system processing largely influenced by hydrology and ice cover.

In terms of seasons, winter stoichiometries were particularly distinct (Fig. 6), where lower C: N and C: P ratios were driven by relatively higher TP accumulation rates (Fig. 4), differences in N speciation (Fig. 5) and overall lower C concentrations throughout the river (Table 2). This resulted in a more dramatic range in C: P along the continuum largely driven by high accumulation rates of TDP. Rates for TN were also high, but similar to rates observed in summer and fall. What was unique for winter however was that NH_4^+ accumulation was as important as NO_3^-, whereas for the other seasons, no meaningful accumulation of NH_4^+ was observed. The distinct winter patterns for DOC and NO_3^- vs NH_4^+ could be explained by two, non-exclusive hypotheses. First, frozen winter conditions may constrain groundwater flows to deeper portions of the soils, away from the DOC-rich, near-surface organic sources. This deeper groundwater source, which has been shown to contribute up to 80% of water loads during winter flow (Peralta-Tapia et al., 2015; Tiwari et al., 2017), would tend to be lower in DOC (Tiwari et al., 2017). Second, high NH_4^+, high NO_3^-, and low DOC concentrations may be due to occurring, but reduced, internal processing, particularly in the upstream pristine sites, where high concentrations of NO_3^- may reflect NH_4^+ oxidation under the ice. Such winter processes have been observed before in lakes (Powers et al., 2017; Massé et al., 2019) and rivers (Ribot et al., 2012; Cruaud et al., 2020). Indeed, the accumulation of TDP and CO_2 observed under the ice, would suggest some level of ecosystem processing (Galantini et al., 2021) although the DOC lability is likely lower during winter. These processes likely occur throughout the river, but the discharge of the *Saint-Jérôme* WWTP, a secondary treatment of activated sludge, resulted in a disproportionate contribution of point

source nutrient inputs to total concentrations, compounded by winter low flow and ice cover. ln fact, the WWTP contributed 9.9% to the total river discharge at the moment of sampling, compared to 7.4, 4.0, 0.5% in summer, fall, and spring. This led to marked winter increases in both NH_4^+ and TP concentrations along the continuum that were either less dramatic or not observed during other seasonal sampling moments, and represented an input of 6.17 mg L^{-1} of NH_4^+ and 0.39 mg L^{-1} of TP from the wastewater. One probable explanation for the sustained NH_4^+ in winter is that the low light conditions under the ice limit its assimilation by primary producers (Hampton et al., 2017). However, it is unclear how much of the downstream NO_3^- buildup was due to nitrification or whether it originated from sustained groundwater inputs (Ator & Denver, 2012). Accumulation of N_2O under the ice (Galantini et al., 2021) suggests nitrification was potentially contributing to some of NO_3^- production, but the high sustained concentrations of NH_4^+ suggest that rates were either very low or saturated from continuous WWTP inputs. Yet there is a long history of agriculture in this region (Goyette et al., 2016), and as such winter nitrate inputs through legacy effects in groundwater is also likely occurring in the lower reaches of the river (Johnson & Stets, 2020). As a result of the potential differential inputs and processes given the unique combined conditions of winter, C: nutrient ratios were lowest during this season.

Despite lower overall accumulation of nutrients during the spring, we still observed decreasing C: nutrient patterns along the continuum, suggesting that land use derived inputs were above all the main drivers in the spatial heterogeneity of the ratios. However, the range in C: N ratios from upstream to downstream was more constrained during this high flow moment as compared to C: P, which was similar to the ranges observed in summer and fall (Fig. 6). There was weak accumulation for all forms of N and dissolved P due to high flow dilution in human-dominated landscapes (Gächter et al., 2004; Koenig et al., 2017). However, particulate P drove TP to accumulate relatively more than TN as a function of both a lack of dominant particulate N input (Goyette et al., 2019) and increased P load as a function of erosion in both urban and agricultural sections of the river (Meyer & Likens, 1979; Holtan et al., 1988). As for C, although POC concentrations and its relative proportion to TOC were both generally higher during spring, these differences were not significant as compared to other seasons. Although overall suspended matter concentrations were higher during spring (Table 2) they had the lowest %C (Fig. S1). As such these were likely largely composed of inorganic clays that transported P. Consequently, the exported N: P ratio was lower in spring compared to any other season. For the *Rivière du Nord*, changes in the composition of elements and their stoichiometry in

spring were the result of both increased watershed derived inputs of particulate P and a dilution of several dissolved nutrient forms during this high-flow moment.

Summer contrasts to spring in terms of flow and to winter in terms of temperature and ice cover. Thus, increases in water residence time, temperature and light availability should favour more internal processing along the continuum. Accumulation patterns in the summer were the most distinctive for N compared to other elements. Overall, concentrations shifted from DON-dominated forested reaches to NO_3^- in the agricultural region (Table 2). This was explained by a proportionally higher NO_3^- accumulation rate compared to other forms of N (Fig. 5). The surplus NO_3^- seen in summer could be due to a combination of internal processing and inputs from the watershed. The latter can be explained by high NO_3^- solubility in soils (Caraco & Cole, 1999), elevated fertilizer use (Goyette et al., 2016), combined with tile-drainage in our watershed (MRC d'Argenteuil, 2011). Decreases in NH_4^+ concentrations beyond the inputs from the WWTP are likely a combination of plant uptake due to light availability and summer nitrification both in the water column (Sebilo et al., 2006; Botrel et al., 2017) and the sediments (Strauss et al., 2004). Regardless, both increased inputs from watershed and internal nitrification would contribute to the relatively higher summer NO_3^- pool seen in the St-Lawrence Lowlands section of the *Rivière du Nord* (Fig. S2) although their relative importance remains unknown. Fall patterns were comparable to summer patterns for all elements, although concentrations of DON were on average the highest in the fall compared to other seasons (Table 2). This is a possible indication of algae and plants senescing in the river and surrounding landscape (Graça et al., 2015) that likely helps support under-ice processing in the winter. One noticeable difference between summer and fall, was that the N: P stoichiometry was relatively constant across the different land use sections in summer, whereas there was a decrease during the fall. A possible explanation was internal P loading during the summer from more reduced sediments that modified the ratios, particularly in the upper reaches. Higher CH_4 concentrations as a function of higher temperatures and lower flow during that period would support this hypothesis (Galantini et al., 2021). Despite this potential difference, C: N and C: P span similar ranges in both seasons suggesting some level of interplay with carbon processing that was not apparent in bulk estimates. Even though we did not observe decreasing C concentrations along the continuum, this does not mean that C was not qualitatively different either along the continuum or across seasons due to changes in sources and relative processing.

The spatial and seasonal patterns in the ecosystem stoichiometry in the mainstem of our single system covered ratios reported across the land to ocean continuum (Fig. 6). Headwater streams draining

pristine sub-catchments of the watershed have C: N: P ratios that are close to senesced litter, meanwhile downstream tributaries in the more agricultural sites have ratios that even surpass the Redfield ratio in terms of N and P enrichment. Thus in our system, increased nutrient loadings as a function of land use changes toward the river mouth drove the spatial patterns in ecosystem stoichiometry. Direct and indirect anthropogenic activities modulating the flow of elements across different regions will alter baseline stoichiometries, but a systematic account of how these are changing as a function of different drivers and within different contexts has yet to be fully explored. For example, freshwater browning in boreal regions (Clark et al., 2010) could counterbalance N and P enrichment, which may result in either maintaining or increasing C to nutrient ratios along a continuum. High atmospheric N deposition in pristine forested regions will lead to higher relative N export from watersheds (Mitchell et al., 1996; Fenn et al., 1998), thus changing ratios with C and P altering downstream productivity. Seasonal reduction in ice cover because of a warming climate will influence the production and accumulation of bioreactive N and P forms under ice as well as lead to an earlier flushing of all three elements, altering the phenology of food webs (Hampton et al., 2017). Such impacts at the within-river scale will thus not only depend on the total C, N, and P stoichiometry, but also on the biological reactivity of the dominant forms. At broader spatial scales, however, the terrestrial loadings and processing to and in the water are cumulative, and forms may shift along the land-ocean continuum. Therefore, the stoichiometry of total C, N, and P exported from a river delimits a broad range of potential ecosystem impacts for receiving ecosystems, and the expression of this potential will depend on how this stoichiometry is conserved and on how the main forms vary as water moves downstream. Overall, the studied temperate river had a wide range of variation in C: N: P despite its relatively narrow spatial extent compared to numerous possible combinations of climates, land cover, and land use found in different regions around the globe (Seekell et al., 2018). Our work suggests that even moderate human impacts can have profound effects on riverine ecosystem stoichiometry. Future inquiries in different regions or those undergoing rapid and more intensive environmental change will likely reveal unexpected C: N: P stoichiometric ratios that cannot be explained by natural biogeochemical processes alone. This will result in dramatic changes in ecosystem function within the receiving waters and those beyond.

Acknowledgements

We wholeheartedly thank L. Galantini for her continuous involvement in fieldwork preparation and execution, as well as help in laboratory analyses. We also thank A. Dupont, P. Maisonneuve, A. Proulx, R. LaBrie and other members passing through the Lapierre and Maranger laboratories for field and analyses assistance, with a special nod to M. Botrel for help with figure conceptualization, M. Talluto for exhaustive help with watershed analyses, A. Prince for delineating the subwatersheds, D. Bélanger for endless analytical help, and the staff at the *Station de biologie des Laurentides* for ceaseless logistical support. This work was funded by Natural Sciences and Engineering Research Council of Canada (NSERC) Discovery grants to JFL and RM with partial student support from an NSERC Collaborative Research and Training Experience Program (CREATE) EcoLac scholarship to S. Shousha. This work is a contribution to the *Groupe de Recherche Interuniversitaire en Limnologie* (GRIL), a strategic research group funded by *Fonds de Recherche du Québec: Nature et Technologie* (FRQNT). This work was carried out on the traditional lands of the Kanien'kehà:ka (Mohawk), Omàmiwinini (Algonquin) and Anishinabewaki. We are grateful to learn on and learn from these lands.

Supporting Information

Different forms of carbon, nitrogen, and phosphorus influence ecosystem stoichiometry in a north temperate river across seasons and land uses

Stéphanie Shousha[1], Roxane Maranger[1], Jean-François Lapierre[1]

[1]Université de Montréal, Département de Sciences Biologiques, Montréal, QC, Canada. Groupe de Recherche Interuniversitaire en Limnologie (GRIL).

*Corresponding author : stephanie.shousha@umontreal.ca

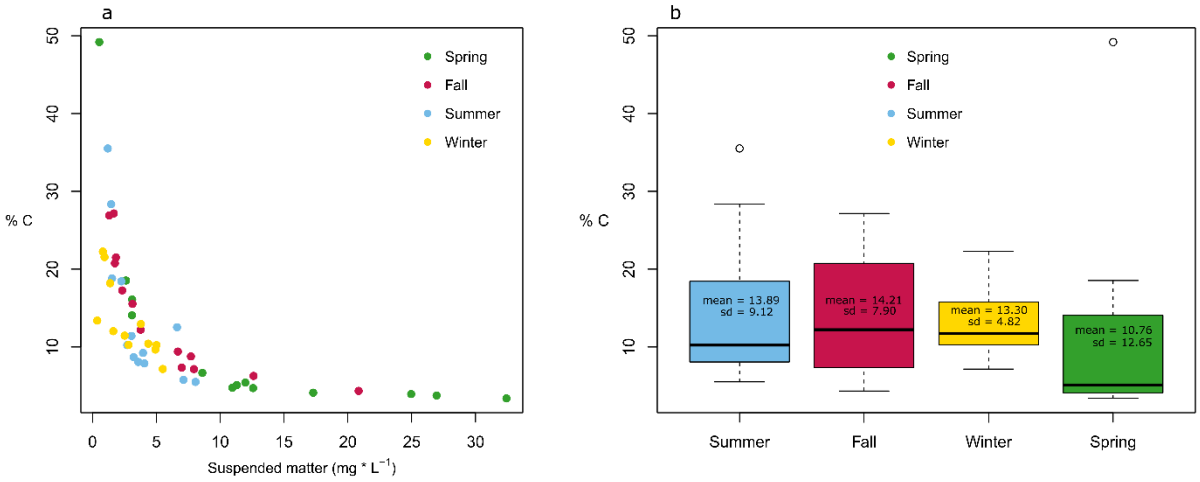

Supplementary Figure S1 Panel A shows the percent in carbon for suspended matter measured on filters. As the suspended matter was more concentrated on the filters (such as in spring), the proportion of C in that suspended matter was less important. Panel B shows the distribution in % C in each season. On average, spring had the lowest %C.

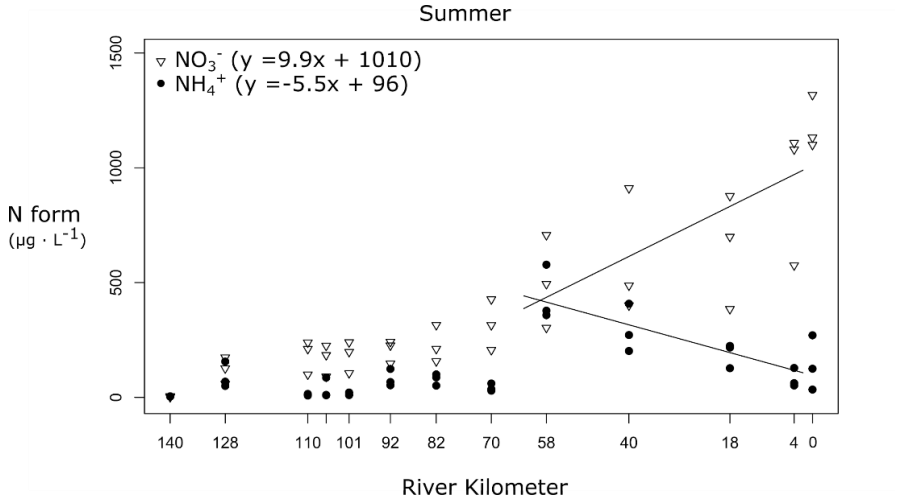

Supplementary Figure S2 Nitrate (NO_3^-) and ammonium (NH_4^+) concentrations (µg · L^{-1}) along the continuum for all three summer campaigns. Slopes for both variables starting at RKm 58 to 0 are significantly different from 0 (p-value < 0.005). The WWTP is situated between RKm 70 and 58.

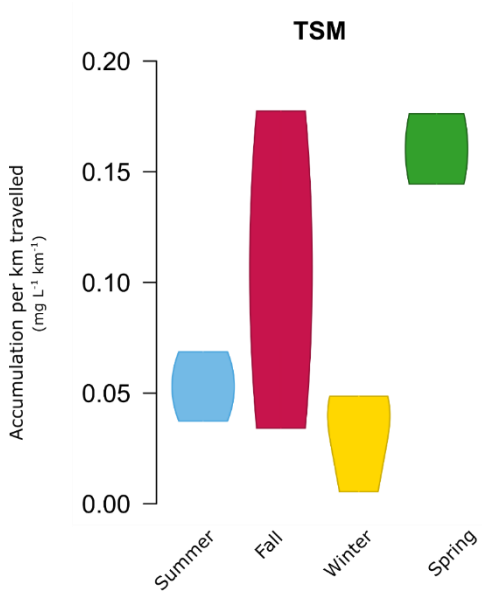

Supplementary Figure S3 Accumulation plot for total suspended matter (TSM, mg · L^{-1} · km^{-1}). Seasonal average rates were 0.05, 0.11, 0.03, and 0.16 for summer, fall, winter, spring, respectively. Post-hoc Tukey tests showed significant differences between summer and spring, and winter and spring accumulation rates (confidence intervals = 0.90).

Chapitre 2

Les saisons et l'utilisation du territoire contrastés altèrent la composition de la matière organique dissoute riveraine

Contrasting seasons and land uses alter riverine dissolved organic matter composition

Stéphanie Shousha[1], Roxane Maranger[1], Jean-François Lapierre[1]

[1] Département de Sciences Biologiques, Université de Montréal, Pavillon MIL, Montréal, 4 Québec H3C 3J7 Canada. Groupe de Recherche Interuniversitaire en Limnologie (GRIL)

Accepted for publication at *Biogeochemistry*.

Abstract

Different sources and fates control riverine dissolved organic matter (DOM) composition in catchments of contrasting land use and climate. However, assessing the changes in DOM composition together with nutrient forms along rivers exposed to these gradients remains rare. Here we quantified the spatial and temporal patterns in DOM components and nutrient forms along the mainstem of a 5th order river through sequential forested, urban, and agricultural reaches during low flow moments in summer and winter, and two contrasting springs, one with a historically rare flooding event. There were widespread abrupt shifts in the composition of DOM in low flow seasons that coincided with changes in land use whose sources could be inferred by endmember samples and nutrient changes. DOM pools considered bio- (microbial-like) and photo-labile (Peak C), along with reactive nutrient forms (ammonium, dissolved phosphorus) tended to accumulate during the winter compared to summer. This implied higher processing during summer as microbial-humic-like DOM and nitrate dominated. DOM composition remained relatively stable under typical spring high flow conditions with reduced retention time and processing, but major shifts were observed during an extreme flood year, pointing to unusual loadings of highly labile DOM. Overall, we found that despite relatively small changes in the quantity of DOM along the axis of flow in this north temperate river, there were major spatial and temporal shifts in its composition, associated with different nutrient forms. These changes inferred contrasting loading and processing potential depending on land use and seasonal patterns in temperature and hydrology.

Keywords: dissolved organic matter, nutrients, composition, rivers, seasons, land use

Introduction

Rivers are dynamic ecosystems that receive, transform, and export dissolved organic matter (DOM), inorganic nutrients, and other materials from their watersheds, with impacts on ecosystem processes and communities within the river and beyond. Riverine DOM contributes to the global carbon budget (Cole et al., 2007), is a source of energy to food webs (Fisher & Likens, 1973; Wetzel, 1995), and protects aquatic organisms by reducing exposure to UV radiation (Morris & Hargreaves, 1997). Depending on its origin, hence concentration and composition, however, DOM modulates these functions differently. For example, while humic substances may protect organisms from UV radiation (Morris & Hargreaves, 1997), smaller, protein-like molecules are preferred energy sources for heterotrophic bacteria (Massicotte & Frenette, 2011). DOM sampled in urban streams tended to reduce metal toxicity through greater binding affinity (Baken et al., 2011), but decreased microbial functional diversity in agricultural streams (Fasching et al., 2020). As changes in DOM composition result in shifts in bacterial community structure (Findlay et al., 2003) and functions (Judd et al., 2006), evaluating the sources and fate of different riverine DOM components may help better determine how rivers are responding to environmental change.

The amount and nature of DOM loaded from land to rivers depend, in part, on the land use and land cover (LULC) of the surrounding catchment. Increasing human populations have extensively converted pristine forested watersheds into more urbanised and agricultural ones (Pielke Sr. et al., 2011), altering soil organic matter properties and its connectivity with land (Lambert et al., 2017 and references therein). Anthropogenic land uses alter DOM concentration and composition in varying magnitude and direction, and these changes are often context dependent (Xenopoulos et al., 2021). Overall, most studies that consider DOM composition have found that smaller, microbial, protein-like components are more abundant in human-dominated catchments (Wilson & Xenopoulos, 2009; Hosen et al., 2014; Lambert et al., 2017; Chai et al., 2019, including others). By comparison, larger, more aromatic molecules appear to dominate in streams draining forested ones (Lu et al., 2015). Along the same line, in the Yangtze River, a catchment home to 430 million people, both DOC and low molecular weight, protein-like DOM concentrations increased along the mainstem, proportional to human population increases (Zhou et al., 2021). While recent studies suggest an effect of LULC on DOM composition, the direction and size of this effect in the context of other environmental changes remain poorly understood.

Once in the water, DOM transformation and removal depend largely on photochemical and microbial reactions, which selectively target specific DOM components. Aromatic and highly unsaturated polyphenols (Riedel et al., 2016) tend to be photodegraded through the cleaving of larger molecular weight molecules into smaller ones (Moran & Zepp, 1997) or oxidised into CO_2 (Cory et al., 2014). By comparison, algal-derived DOM is more easily consumed by heterotrophic bacteria (Benner, 2003). The presence of high inorganic nutrient concentrations can stimulate the degradation of DOM, either because autochthonously produced DOM is more labile or recalcitrant forms are more easily accessed (Farjalla et al., 2009; Wickland et al., 2012; Bengtsson et al., 2018). As different degradation processes vary over time and favour the removal of different DOM pools, their rates are not only influenced by LULC (Lu et al., 2013) but also by seasonal patterns in temperature, irradiation, and hydrology. In temperate streams and rivers, summer baseflow represents a period of high water residence time, temperature, and sunlight, which result in conditions of high processing potential. But winter also represents another low flow season, albeit with colder temperatures and reduced light availability, particularly in regions with ice and snow cover. The dominance of different nutrient forms among seasons is suggestive of differential processing potential (Shousha et al., 2021), but how this could alter DOM composition remains underexplored. In higher flow conditions, which occur in spring in temperate regions, DOC concentrations may be proportionally (Zarnetske et al., 2018), inversely, or even un-correlated with flow, presumably due to greater dilution (Winterdahl et al., 2014). In all cases, higher flows that reduce water retention times within the river will likely lower DOM transformation along the continuum, reducing compositional changes (Weyhenmeyer et al., 2012; Lambert et al., 2016; Raymond et al., 2016). Seasonal sampling of riverine DOM thus offers an opportunity to assess how moments of contrasting loading and processing potential may drive riverine DOM composition.

Nutrient concentrations and composition are known to vary along gradients of land uses (Merseburger et al., 2005; Shousha et al., 2021). Seasons of contrasting temperature, hydrology, and light availability can lead to a disproportionate accumulation of certain nitrogen (N) and phosphorus (P) forms along a river's axis of flow (Shousha et al., 2021). The presence of such forms can inform on the loadings and transformation processes responsible for potential changes in DOM composition. For example, if photo- or bio-labile DOM is associated with high concentrations of inorganic nutrients such as nitrate (NO_3^-), which are predominantly loaded from agricultural watersheds, this could point to either reduced mineralisation within the ecosystem or high flow conditions (Wiegner et al., 2009; Wu et al., 2019). In contrast, when relatively higher algal-derived DOM is observed with lower concentrations

of inorganic nutrients and photo-resistant DOM, a river is likely an active reactor (Casas-Ruiz et al., 2017). As such, a river mainstem of consistent Strahler Order that drains a gradient of land uses and undergoes seasonal extremes may offer a unique opportunity to study DOM composition and its association to certain nutrient forms. Assessing how DOM components, along with N and P forms, change with these conditions may provide greater insight as to when, where, and how a river receives, transforms, and exports different DOM types to downstream ecosystems, but such studies remain rare. Here we aim to determine how seasonal and land use gradients influence how a temperate river acts as a receiver, processor, and exporter of different DOM components. This study builds on the findings of Shousha et al. (2021) who found relatively constant DOC concentrations, i.e. DOM quantity, along the mainstem of a temperate river across seasons despite strong land use changes. Here we further quantify where and how DOM composition, i.e. quality, changed along the same river with its gradient of LULC during moments of seasonal extremes for three consecutive years. By considering the association of DOM composition with changing nutrient pools along a river mainstem across contrasting conditions of low, high, and extreme flows as well as high versus low temperatures and light availability, we determined which DOM pools were associated with differential loading and processing potentials.

Methods

Site description

Work was conducted in the *Rivière du Nord* watershed located ~100 kilometers north-west of Montreal, QC, Canada, in the Laurentians region. The watershed mainstem (146.6 km-long Strahler order 5) consecutively drains forested, urban, and agricultural regions (Fig. 1). Sites along the mainstem are numbered by River Kilometer (RKm), as the distance estimated from the river mouth. The forested (RKm 140 to 92) and urban (RKm 92 to 70) portions of the watershed are found in the Canadian Shield, a geographical province with strong topography, abundant lakes, temperate forest, and little topsoil. The forested subwatersheds are covered by < 5% impervious area and < 5% agriculture. The urban reach of the mainstem is characterized by impervious areas covering up to 37%. Agriculture (RKm 70 to outlet) in the lower half of the watershed is supported by rich fertile soils, covers 74% of the area, and is located in the rather flat geographical province of the St. Lawrence Lowlands. The river is situated in temperate climate and undergoes marked differences in hydrology, with high flows occurring in spring (April) and low flows occurring in summer (August) and ice/snow covered winter

(January). The *Rivière du Nord* watershed has been described in more detail in Shousha et al. (2021) and Galantini et al. (2021).

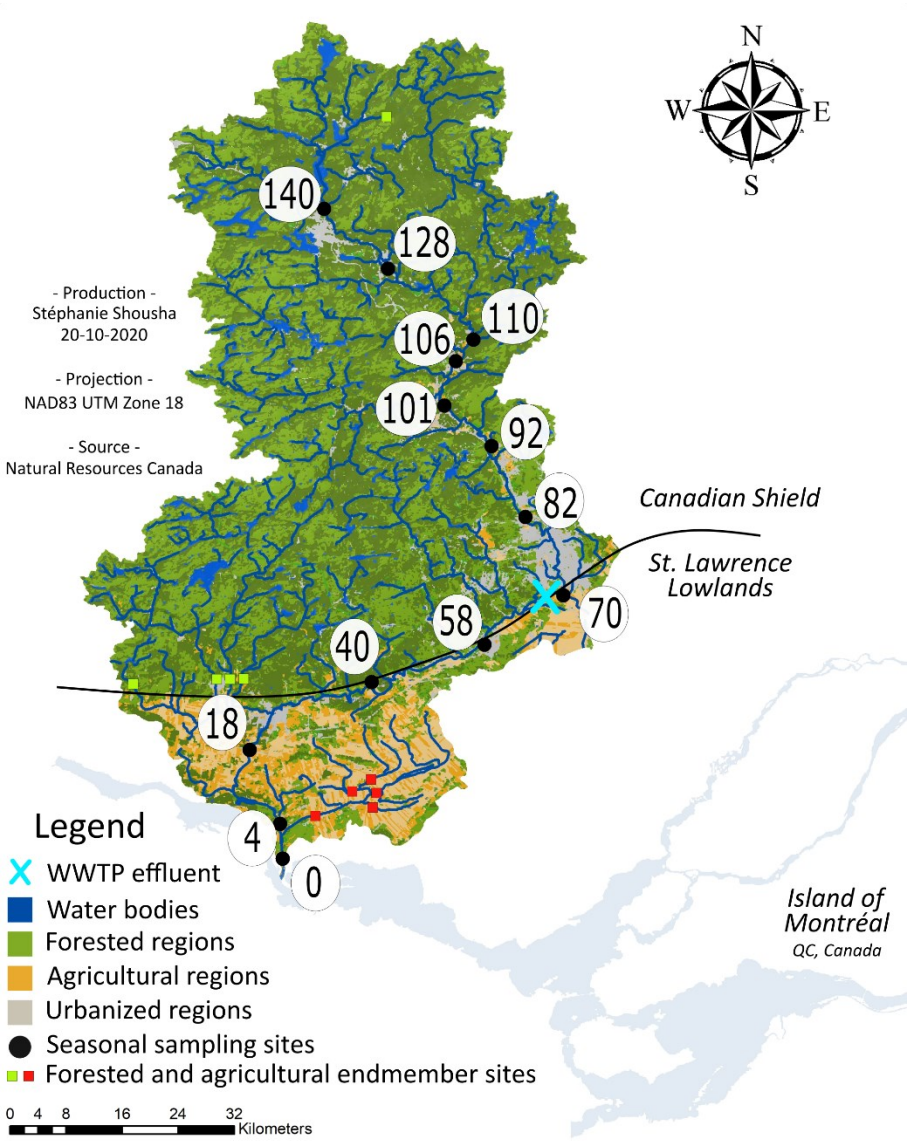

Figure 1 The *Rivière du Nord* watershed overlays two geological provinces, the Canadian Shield and the St. Lawrence Lowlands. Its mainstem drains a gradient of landscapes starting from mostly forested regions, to urban, then to agricultural reaches. The sites sampled during the snapshot campaigns are circled in white, while the forested and agricultural tributary endmembers sampled once in summer 2018 are represented by green and red squares, respectively. The largest wastewater treatment plant in the watershed is represented by a light blue X.

Geographical and hydrological analyses

We delineated the *Rivière du Nord* watershed and its subwatersheds using 1x1 meter digital LiDAR elevation data (Gouvernement du Québec, 2016a) in the ArcHydro Toolbox of the ESRI ArcGIS version 10.5.1 193 (ESRI, 2017). Land use and land cover data (Natural Resources Canada, 2009) were intersected with the subwatershed layer to estimate %forest, %urban and %agriculture. Daily discharge data was downloaded from the *Saint-Jérôme*'s gauging station just above RKm 70 (MDDELCC, 2018a). Discharge at every site was estimated using the relationship between discharge at the gauging station and proportion of subwatershed surface area. Spring flood recurrences were calculated following $recurrence = (N + 1) / r$, where N is the number of full years with available discharge data (here, 1930 to 2021) and r is the rank of the maximum annual value of mean daily flows. For spring 2018, the maximum annual value at the *Saint-Jérôme* gauging station (218 $m^3 s^{-1}$) ranked the year 27th with a recurrence of 3.41 years. Spring 2019 ranked 3rd with a maximum annual value of 303 $m^3 s^{-1}$ and a recurrence of 30.7 years, indicating this magnitude of flood has a ~3% chance of occurring every year. As such, we refer to 2019 as a historically rare flood year.

Sampling design

We sampled 13 sites along the mainstem of *Rivière du Nord* once every season from summer 2017 to winter 2020, resulting in 11 campaigns. Sampling was conducted over a two-day window to reduce hydraulic variability, but targeted hydraulic extremes within each year to capture contrasting moments of flow, light availability and temperature. Summer and winter both represented seasons of low flow but had contrasting temperatures and light availability (winter season being ice and snow-covered). Spring sampling was conducted during yearly maximal flow, which was on average up to 11-fold summer baseflow. To characterise forest and agriculture endmember signatures of DOM components and nutrient pools, we also targeted contrasting headwater tributary sites, five draining > 90% forest cover and five draining > 90% agriculture in summer 2018. As such, when we refer to endmember sites, we refer to the sites in the tributaries draining mostly forested land cover or agriculture land use. In summer 2021, we sampled the effluent of the wastewater treatment plant (WWTP) serving the largest town in the urban region, *Saint-Jérôme* (population of just over 77 000) as an additional urban endmember. This WWTP discharges just downstream of RKm 70 (Fig. 1; effluent discharge coordinates 45.53, -74.33). Human and industrial activities as well as the types of wastewater treatments are assumed to have remained similar throughout the study period, suggesting that DOM composition in the WWTP affluent and effluent at the measured time point represents characteristic

loadings. However, it is possible that this composition is more variable and certain interpretations related to this topic should be made with caution.

Field measurements

For the 13 mainstem sites, we collected water samples in the middle of the river, just below the surface. This was done by lowering a Van Dorn sampler from a bridge or from a boat, or when neither option was feasible, walking out as far as possible without disturbing sediments and collected water facing the current. In winter, holes in the ice were drilled with an ice-auger. Prior to sampling, bottles for nutrient sampling were soaked in a 10% HCl solution for 24h and rinsed with Milli-Q water multiple times. During sampling, we conditioned the bottles with river water three times before filling them and stored them in coolers. Water temperature and conductivity were measured with a hand-held meter (Yellow Springs Instrument, Ohio, United States).

Sample preparation

We stored unfiltered water collected in opaque 0.5L bottles in the dark at -20°C for total N (TN) and total P (TP) analyses. The remaining water was filtered through 0.45 µm Filtropur S 155 polycarbonate filters using a syringe (Sarstedt, Nümbrecht, Germany). Filtrate was collected in 125mL HDPE bottles for ammonium (NH_4^+) and nitrate (NO_3^-), in 250mL bottles for total dissolved N (TDN) and P (TDP), and in 40mL pre-combusted amber vials for dissolved organic matter (DOM) absorbance and fluorescence measurements. Nitrogen and P samples were stored in the dark at -20°C and DOM, in the dark at 4°C.

Nutrient analyses

Detailed methods for the measurement of N and P forms have been described in Shousha et al. (2021). Briefly, N forms (NO_3^-, NH_4^+, TDN, TN) were measured using a Latchat QuickChem 8000 flow injection analyser (Latchat Instruments, Loveland, United States; USEPA-350.1, 1993; USEPA-352.3, 1993). Dissolved inorganic N (DIN) was calculated as the sum of NO_3^- and NH_4^+. Dissolved organic N (DON) was calculated as the subtraction of DIN from TDN. Particulate N, as the difference between TN and TDN, accounted for less than 3% of TN and was henceforth disregarded. Phosphorus forms (TP, TDP) were analysed with a segmented flow analyser (Astoria-Pacific, Clackamas, United States; USEPA-365.1, 1993). Total particulate P (TPP) was estimated as the subtraction of TDP from TP.

DOM optical properties

The coloured fraction of DOM (CDOM) absorbance was measured with a Shimadzu UV-1800 spectrophotometer (Agilent Technologies) using a 1cm optical path length in a quartz cuvette from 190 to 900nm (1nm increments). Concentrations of CDOM are reported as the pathlength-corrected absorbance at 440nm. The DOM aromaticity proxy, $SUVA_{254}$, was calculated as the pathlength-corrected absorbance at 254nm divided by DOC concentration (Weishaar et al., 2003). We measured the fluorescent fraction of CDOM, FDOM, with a Cary Eclipse Fluorescence spectrophotometer (Agilent Technologies) in 1cm quartz cuvettes across excitation and emission wavelengths of 230 to 450 (5nm increments) and 240 to 600 (2nm increments), respectively. FDOM emission and excitation matrices (EEMs) were corrected using the paRafac.correction R library (LaBrie et al., 2017; R Core Team, 2019). This package corrected all the EEMs simultaneously for the inner filter effect and for minor deviations in the light path of the lamp, removed the Raman and Raleigh scattering, and transformed the intensity of the fluorescence which is measured at the peak of the component in Raman units (RU), and referred to as F_{max}. EEMs were then analysed using the parallel factor analysis (PARAFAC) model (Stedmon et al., 2003) in MATLAB 8.2 (MathWorks, Natick, MA, USA) with the DOMFluor toolbox (Stedmon & Bro, 2008). The model was based on 1078 samples originating from various Québec aquatic ecosystems from temperate and boreal climates. The model validated 5 distinct components (De Bonville et al., 2020; Supplementary Fig. 1), described in Table 1 as the excitation and emission fluorescence peaks. The change in DOM reported here refers only to the coloured fraction of organic matter that fluoresces (Stubbins et al., 2014), and can be compared with the rich literature using the OpenFluor website interface (Murphy et al., 2014). C1 has been associated with terrestrially derived DOM, thought to be photo-resistant (Ishii & Boyer, 2012; Kothawala et al., 2014; Zhou et al., 2019). C2 has also been associated with terrestrial humic-like components, but is considered more photo-labile and has been found in a number of ecosystems, such as saline lakes (Osburn et al., 2011), thermokarst ponds (Wauthy et al., 2018), and large rivers (Wünsch et al., 2017). C3, often characterized as "microbial humic-like", has been found in particulate organic matter of summer storms in two South Korean rivers (Derrien et al., 2020), in oligotrophic shallow lakes where it was more photo-resistant than other components (Soto Cárdenas et al., 2017), and in a medium-high impacted Italian river, where it correlated strongly with a protein-like component in summer (Retelletti Brogi et al., 2020). Its M-peak has also been found in stream water, soil leachates, and leaf leachates (Garcia et al., 2018). C4 matched with a large number of OpenFluor studies, ranging from large rivers with often high land-use to shallow or saline lakes, and peatlands. In large rivers, such as

the Meuse and Congo Rivers, authors characterized the equivalent component as widespread, terrestrial, humic-like, and susceptible to photodegradation, where its contribution decreased in urban and agricultural subcatchments (Lambert et al., 2017) or under conditions of lower flow (Lambert et al., 2016). C5 matched with the widely reported protein-like component thought to be freshly produced or imported in a variety of riverine ecosystems (Lapierre & del Giorgio, 2014; Gonçalves-Araujo et al., 2015; Osburn et al., 2016; Chen et al., 2017), and has been found in water extracted organic matter from soils and litter in temperate forests (Wu et al., 2021).

Using the FDOMIndices function from the paRafac.correction R library (LaBrie et al., 2017), we calculated the fluorescence index (FI), the freshness index (β:α), and the humification index (HIX). FI is used to differentiate between microbial and terrestrial sources of DOM (McKnight et al., 2001), β:α indicates the contribution of freshly released DOM (Wilson & Xenopoulos, 2009), and HIX increases with greater humicity (Ohno, 2002).

Table 1 Description of the 5 DOM PARAFAC components with associated literature. λEx/λEm refers to the maximum fluorescence in excitation and emission for every component.

	λEx/λEm	Description	OpenFluor TCC >0.95 references*	References other than OpenFluor, with associated Ex/λEm	
C1	245 / 490	Terrestrial humic, rivers draining peatlands	Zhou et al. (2019)		
		Peak A, humic-like fluorophores	Kothawala et al. (2014)		
		Ubiquitously terrestrial, UVC-humic, photoresistant, smaller molecular size		Ishii & Boyer (2012)	< 230-260 / 400-500
C2	285 / 512	Reoccurring humic-like FDOM	Wünsch et al. (2017)		
		Ubiquitous humic-like, photolabile	Murphy et al. (2018)		
C3	< 245 (310) / 414	Humic-like, found in leaf and soil leachates	Derrien et al. (2020)		
		Microbial humic-like	Retelletti Brogi et al. (2020)		
		Peak M found in leaf litter of deciduous forests (M_L)		Garcia et al. (2018)	240 (305) / 404 310 / 436
		Peak A+M, unrelated to environmental variables, microbial activity or DOM optical indices		Williams et al. (2010)	< 250 (310) / 416
C4	345 / 452	Widespread terrestrial, humic-like, susceptible to photodegradation	Lambert et al. (2017) Lambert et al. (2016)		
		Traditional Peak C	Søndergaard et al. (2003) Chen et al. (2018)		
		Peak C, probable autochthonous origin	Osburn et al. (2011)		
		Peak C, photolabile	Zhou et al. (2019)		
		Peak W, detergents and whitening agents		Mostofa et al. (2010) Niloy et al. (2021)	≈ 340 / 445

C5	270 / 300	Protein-like, soil and litter from temperate mixed forest	Wu et al. (2021)		
		Protein-like	Gonçalves-Araujo et al. (2015)		
		Amino acid-like	Osburn et al. (2016)		
		Free protein-like, in riverine sediment pore water		Chen et al. (2017)	270 / 302

* There were only two OpenFluor references for C1, and they matched with a Tucker congruence coefficient (TCC) of > 0.90.

All analyses were carried out at the *Université de Montréal*'s GRIL (*Groupe de recherche interuniversitaire en limnologie*) analytical lab. The composition of the C, N, and P pools was estimated as the percent that each elemental form contributed to total C, N, or P concentrations. For example, $\%NH_4^+ = [\,NH_4^+\,]/[\,Total\,N\,]$.

Statistical analyses

Potential shifts in composition were determined with linear and piecewise regressions using the relative contribution of C1-C5 to total fluorescence (expressed as %C1-%C5) as a function of river kilometer. A significant linear relationship would represent a gradual shift in composition, while a significant breakpoint relationship would represent an abrupt shift in composition. For the breakpoint model, the potential breakpoint as well as the intercepts and slopes of each regression line (before and after the breakpoint) were free parameters in the model. We fit both linear and piecewise models in a Bayesian framework using Stan and rstan (Stan Development Team, 2019a, 2019b). Minimally informative regularising priors on the intercepts, slopes, and residual standard deviation parameters, as well as a boundary avoiding prior on the breakpoint were used to avoid the trivial cases where the breakpoint snaps to the outlet or headwater of the river network. In the case of an abrupt shift (piecewise model), the most probable river kilometer where the shift occurs was noted. These river kilometers (RKm) were then compared among components and seasons.

From these analyses, numerous breakpoints were identified with regards to chemical composition around the heavily urbanised areas of *Saint-Jérôme*, between the geological provinces suggesting chemically distinctive reaches upstream and downstream from that area. As such, we quantified the differences between forms of C, N, and P (in %) as the arithmetic difference between the two reach segments, after having centered and scaled the values. Using $\%NH_4^+$ as an example, the formula was the following:

Difference in abundance between mainstem reaches	=	*% NH_4^+ average in downstream sites*	–	*%NH_4^+ average in upstream sites*

A positive resulting value would suggest a greater contribution of NH_4^+ to the total N pool in the downstream reach. These differences are the values plotted in Fig. 4 (x-axis), Fig. 5b (y-axis) and Fig. 5c (x-axis), and labeled *"Difference in abundance between mainstem reaches"*. The same calculation was performed to quantify the difference between seasons (winter averages minus summer averages, Fig. 4 y-axis labeled *"Difference in abundance between seasons"*), and between endmembers (agricultural endmembers minus forested endmembers, Fig. 5a y-axis *"Difference in abundance between endmembers"*). To elucidate whether mainstem C, N, and P pools could be explained by forested or agricultural inputs (as represented by the sampled endmembers), we calculated:

Contrast between endmember and mainstem (Fig. 5c y-axis)	=	*Difference in abundance between endmembers (Fig. 5a y-axis)*	–	*Difference in abundance between mainstem reaches (Fig. 5b y-axis)*

A positive resulting value would suggest that the endmembers (whether agricultural or forested) are richer in a certain variable than the mainstem (whether upstream or downstream). This would infer that the endmember is an important source of that variable. A negative value would suggest that the source of the variable to the mainstem is other than agricultural or forested (ex: groundwater, in situ production, urban).

Results

Climatic conditions

There were large differences in environmental and climatic conditions among seasons (Table 2), except for fall which was similar to summer in terms of discharge, although typically colder. Fall was excluded from further analyses to focus on the most contrasting conditions to assess DOM component and nutrient loading and processing potentials. To do that, we considered average summer and winter conditions as well as the two different springs, the more typical high flow of 2018 and the historical flood of 2019, which had the third highest ever recorded flow since 1931. During the 2-day campaigns, air and water temperatures were highest in summer (mean of 23.5°C and 21.5°C respectively) and lowest in winter (mean of -0.5°C and -0.6°C respectively). Discharge during those campaigns at the *Saint-Jérôme* gauging station (between RKms 70 and 82) was lowest for winter (11.1

$m^3 s^{-1}$) and highest during spring, reaching 143.6 $m^3 s^{-1}$ (2018, normal spring thaw) and 246.3 $m^3 s^{-1}$ (2019, major flood). For both spring flows, we sampled within one day of peak flow.

Table 2 Climatic conditions are shown by season. These include air and water temperatures, discharge averages of the 2-day snapshot campaigns recorded at the *Saint-Jérôme* gauging station, three-month seasonal discharge averages recorded at the *Saint-Jérôme* gauging station, yearly peak flow for both spring campaigns, and some river description. Data represent the average of the variable ± standard deviation.

Variables	Summer (average of 3 campaigns)	Winter (average of 3 campaigns)	Springs 2018	Springs 2019
Air temperature (°C)	23.5 ± 3.4	-0.5 ± 5.2	15.9 ± 4.2	6.5 ± 1.5
Water temperature (°C)	21.5 ± 2.3	-0.6 ± 1.0	4.0 ± 2.1	2.0 ± 0.7
Snapshot discharge ($m^3 s^{-1}$)	17.8 ± 7.1	11.1 ± 1.1	143.6 ± 23.8	246.3 ± 18.3
Campaign dates			(May 6 and 7)	(April 25 and 26)
Three-month seasonal average ($m^3 s^{-1}$)	11.2 ± 8.3 (July – September)	18.1 ±12.1 (January – March)	49.26 ± 51.0 (April – June)	81.65 ± 73.9 (April – June)
River properties	Low-flow, high light availability, warm	Ice and snow cover in 10 out of 13 sites	Typical high flow year	Historical rare flood year

Non-linear changes in DOM composition

The composition of the fluorescent DOM pool, expressed as the percent contribution of each PARAFAC component to the total fluorescence, shifted non-linearly from upstream to downstream for a little more than half the cases. In particular, for most relationships of %C1-5 versus river kilometer, the piecewise relationship with one breakpoint better explained the shift in composition than the no-breakpoint linear model (Fig. 2; example of model output in Supplementary Fig. S2). For summer and winter, 6 out of 10 relationships resulted in significant breakpoints between RKm 74 and 76 with a mean at RKm 75. This suggests a shift in DOM composition, that changed in terms of strength or direction almost immediately following the urban reach, which also coincided with the transition to the more anthropogenically impacted region of the St. Lawrence Lowlands. For either summer or winter, %C5 had no abrupt shift in composition, but there was a slight linear increase from upstream to downstream during winter (from 2.2% to 5.9%, $R^2 = 0.33$, p-value < 0.001). In the typical high-flow spring of 2018, there was no abrupt shift in composition for any component: %C1, %C3, %C4, and %C5 had no relationship with RKm, and both linear and breakpoint models performed equally well to quantify the change in %C2 which appeared to decrease gradually along the continuum along with %C4 (Fig. 2). Contrary to spring 2018, the piecewise model best represented the abrupt change in composition for all components in spring 2019. On average, the breakpoints were estimated at RKm 85, which is situated at the end of the forested region and the beginning of the major urban one. Based on the widespread shift in DOM composition following the transition from the Canadian

Shield to the St. Lawrence Lowlands, we then treated the river as two different functional units: the pristine upstream reach (sites at RKm 140 to 82), and the anthropogenic reach altered by urban and agricultural land use changes (sites at RKm 70 to the outlet). Following a slightly different breakpoint for spring 2019, the pristine reach in this season included sites from RKm 140 to 92, and the downstream impacted reach included sites from RKm 82 to the outlet.

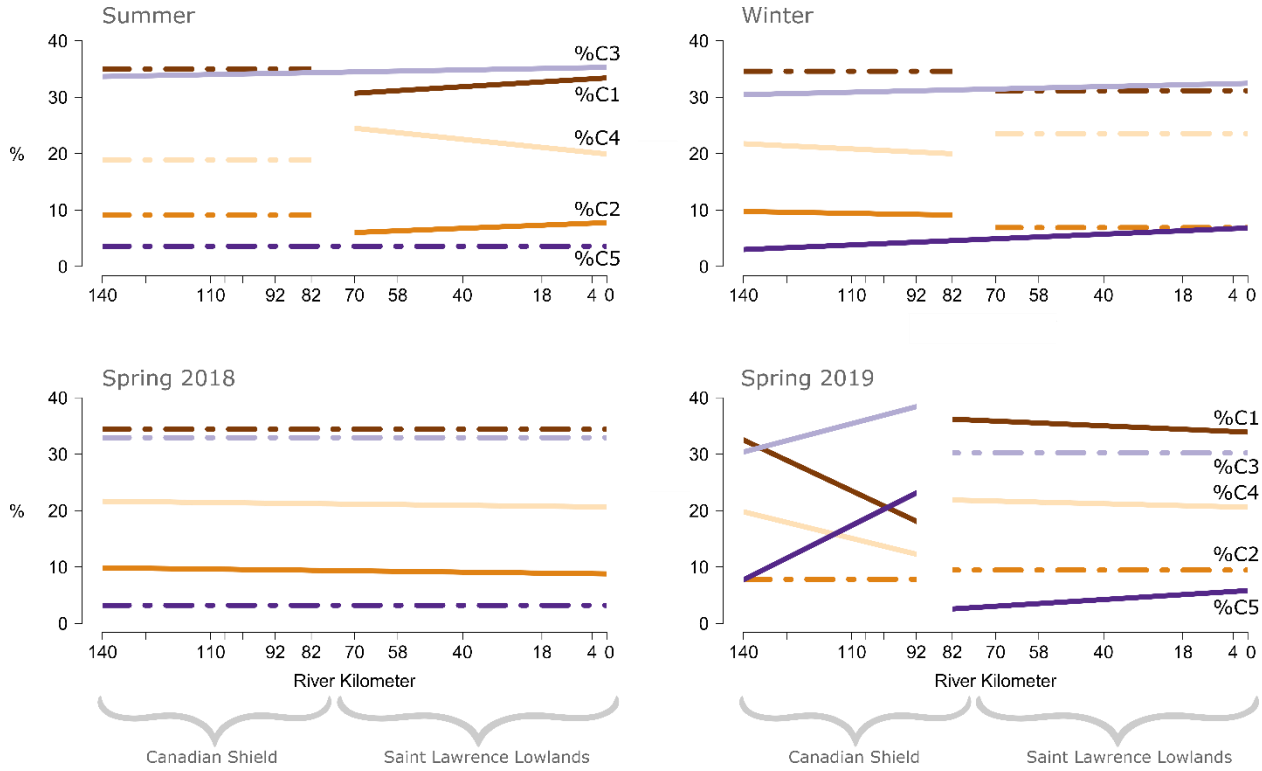

Figure 2 Upstream-downstream changes in DOM components for summer, winter, typical spring of 2018, and extreme flood spring of 2019. The summer and winter slopes include all three years of sampling. Y-axes are proportion of variable from 0 to 40 (%). X-axes are River Kilometer (RKm). The linear relationships significantly different from 0 (p-value < 0.1) are represented by solid lines, and the horizontal slopes that represent no change by dashed lines. The raw data and associated slopes are shown in Supplementary Figs. S3 and S4.

Compositional changes in high flow seasons

DOM composition (%C1-5) appeared virtually unchanged during the typical high flow season of spring 2018 as most upstream-downstream variations were small (Fig. 2). However, there were pronounced changes in composition in spring 2019 and we wanted to determine if these changes were related to shifts in concentrations. Indeed, shifts were mostly driven by the unusually high C5 concentration found upstream (mean = 0.47 Raman Units (RU), sd = 0.31, with a wide range of 0.17

to 1.07 RU; Fig. 3), which were on average 5-fold higher than those downstream (mean = 0.09 RU, sd = 0.04). Spring 2019 upstream C5 concentrations were also on average 8-fold higher than those of spring 2018 (mean = 0.059 RU). The spring 2019 C3 concentrations followed a similar trend (Fig. 3). These sharp shifts in DOM components in 2019 were coherent with the patterns in HIX and β:α (Supplementary Figs. S5-S8), which showed the lowest (least humified) and highest (freshest) values during the major flood year (Table 3).

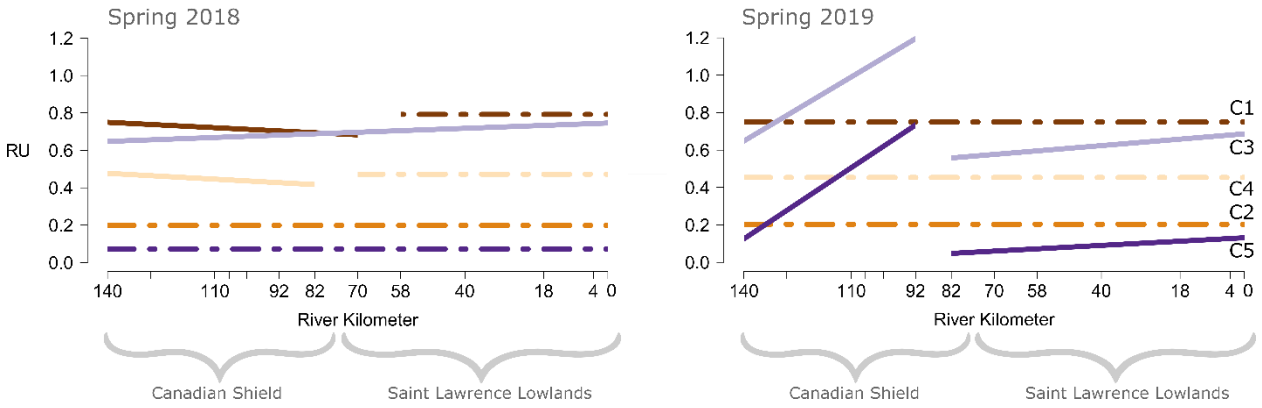

Figure 3 Upstream-downstream changes in DOM components for the typical high flow spring of 2018 and the extreme high flow spring of 2019. Y-axes are fluorescent intensities reported in Raman Units (RU) from 0 to 1.2. X-axes are River Kilometer (RKm). The linear relationships significantly different from 0 (p-value < 0.1) are represented by solid lines, and the horizontal slopes that represent no change by dashed lines. The raw data and associated slopes are shown in Supplementary Fig. S4.

Compositional changes in low flow seasons

Winter vs summer

There were less pronounced, but consistent changes in the DOM components and associated nutrient forms in the two low flow seasons of summer and winter compared to spring, and these changes differed depending on LULC and season. The biggest spatial changes were for %C4 and %NH_4^+, which showed the highest relative increase from upstream to downstream, and conversely for %C1-2 and %DON, which showed the highest decrease (Fig. 4 x-axis). The biggest seasonal differences were for %NH_4^+, %TDP, and %C4, which were relatively more abundant in winter, and for %C3, %DON, and %TPP which were relatively more abundant in summer (Fig. 4 y-axis). Thus, %C1, %DON and %TPP found in the bottom-left quadrant (c) were more dominant in moments of high processing potential and areas of pristine sources of terrestrial material (summer, upstream), whereas %C4-5,

%TDP and %NH_4^+ found in the top-right quadrant (b) were more dominant in moments of low processing potential and areas of urban or agricultural sources (winter, downstream; Fig. 4).

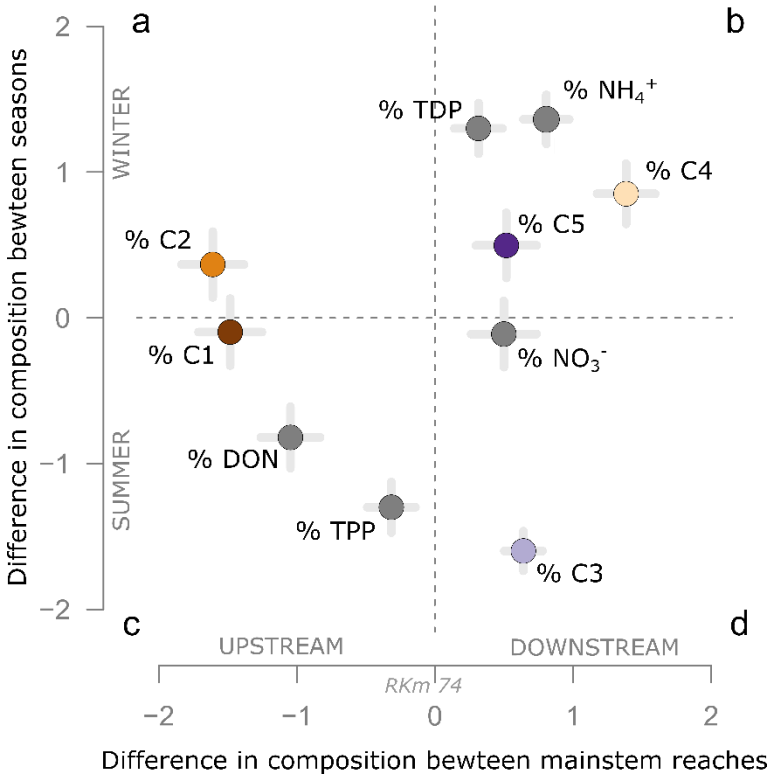

Figure 4 Changes in the composition of DOM components and nutrient forms from upstream to downstream (x-axis from left to right) and between winter and summer (y axis top or bottom). Values represent the arithmetic differences of % C, N, P between seasons (y-axis) versus arithmetic differences between reaches (x-axis). Colours match colours used in Figs. 2 and 3, and grey is used for N and P forms.

Forest, urban, and agricultural endmembers

Tributaries draining primarily forested or agricultural catchments (i.e., "endmembers"), as well as the effluent of a WWTP, had contrasting composition in DOM components and in nutrient forms (Table 3, Supplementary Figs. S9, S10 for significant differences). Percent DOM components 1, 2 and 4 were on average higher in the forested endmembers. Percent C3 was higher in the agricultural endmembers and highest in the WWTP effluent. C5 was found in almost identical, low proportions in both forested and agricultural endmembers (mean of 2.8 ± 0.9% of total fluorescence), but reached a high of 11.4% in the effluent. This DOM anthropogenic signature co-occurred with change in relative nutrient composition, with NO_3^- representing most (79.9 ± 7.0%) of the N pool in agricultural endmembers and NH_4^+ (93.2%) and TDP (88.0%) representing most of the N and P pools in the WWTP effluent.

Most (75.5 ± 7.7%) of the N in the forested endmembers consisted of DON. No P form significantly differed in forested or agricultural endmembers.

Upstream-downstream shifts in DOM as a function of endmember sources

We determined if the composition, and upstream to downstream shifts in DOM components and nutrient forms could be inferred from the different endmember sources during the summer. As the endmember sites were only sampled in summer, comparisons with the mainstem were only assessed for that season. DOM components C1 and C2 were relatively more abundant upstream (Fig. 5b) as well as in the forested endmembers (Fig. 5a), suggesting that a relative decrease in these components along the mainstem was coherent with a change in the inputs going downstream. There were no significant changes in protein-like C5 among endmembers nor along the mainstem, suggesting that it was not predominantly driven by changes in loadings. C3, TPP, and NO_3^- were relatively more abundant in the agricultural endmembers (Fig. 5a) compared to the mainstem reaches (Fig. 5c). This suggests that agricultural loadings are important sources of these DOM and nutrient forms for downstream sites. In contrast, DON, NH_4^+, TDP and C4 were relatively more abundant in the mainstem, independent of river reach, than in the endmembers (Fig. 5c). This suggests that sources other than forested loadings support concentrations of DON in upstream sites, and that sources other than agricultural loadings support concentrations of NH_4^+, TDP and C4 in downstream sites. WWTP effluent could plausibly account for NH_4^+ and TDP (Supplementary Figs. S11, S12), but apparently did not account for proportional increase in C4 (Table 3).

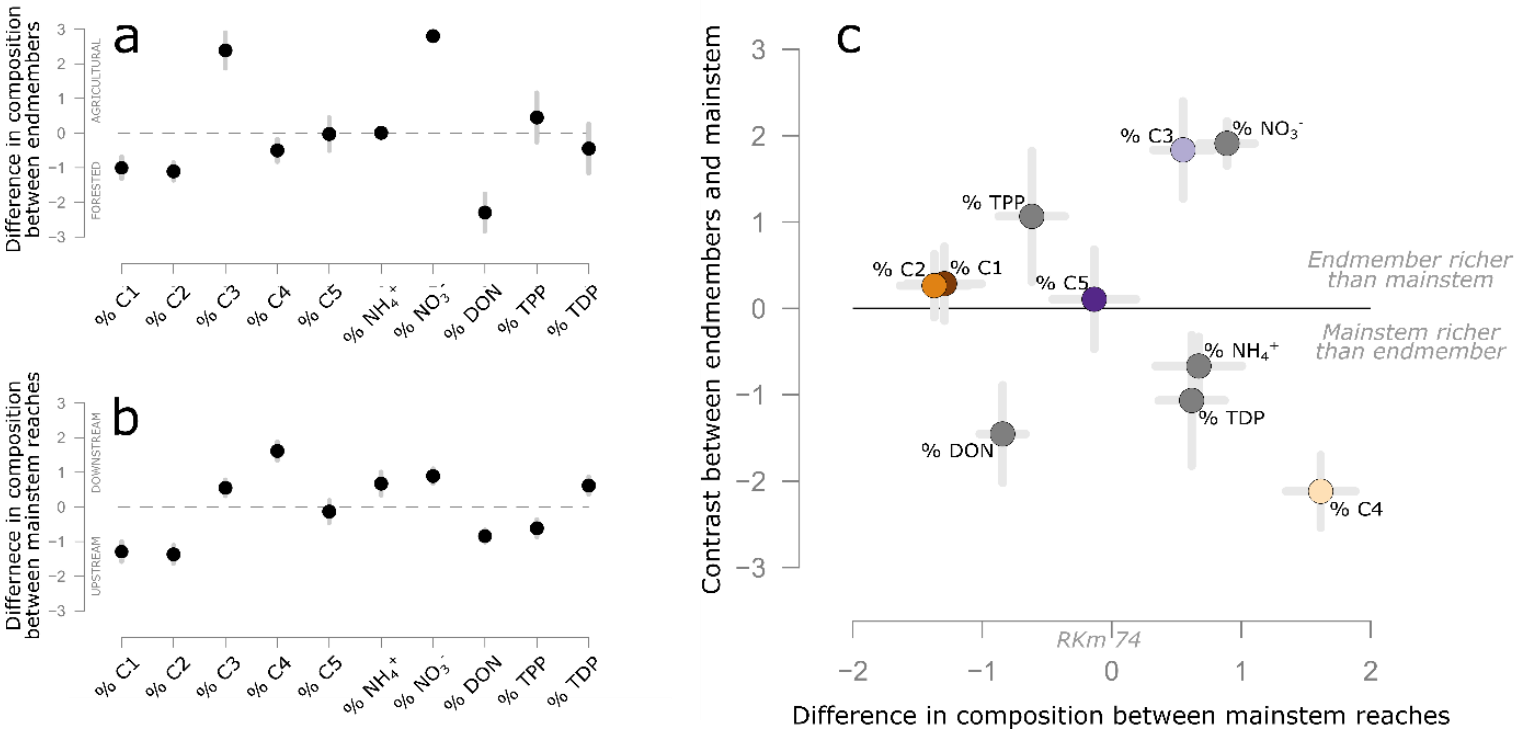

Figure 5 Arithmetic differences in % C, N, and P between forested and agricultural endmembers (panel a), and mainstem reaches (panel b). Panel c (y-axis) shows the difference between panels a and b, and helps explain difference in composition between endmembers and mainstem. Variables plotting above the horizontal 0 represent a higher proportion of the C, N, and P pools in the forested or agricultural endmembers compared to the mainstem pools; variables plotting below the horizontal 0 represent a higher proportion of the C, N, and P pools in the mainstem. Values were taken from the summer seasons only.

Table 3 Averages ± standard deviations of % C1-C5, % elemental nutrient form, and certain proxies for summer, winter, and springs in both upstream pristine and downstream impacted regions, extreme forested and agricultural endmembers sampled in summer 2018, and the *Saint-Jérôme* WWTP intake and effluent sampled in summer 2021.

	Canadian Shield (Upstream)				Saint-Lawrence Lowlands (Downstream)				Endmembers		WWTP [c]	
Variable	Summer	Winter	Spring 2018	Spring 2019	Summer	Winter	Spring 2018	Spring 2019	Forest	Agric.	Intake	Effluent
	(n=21)	(n=21)	(n=6)	(n=6)	(n=18)	(n=18)	(n=7)	(n=7)	(n=5) [a]	(n=5) [b]	(n=1)	(n=1)
% C1	34.7 ± 1.1	35.2 ± 1.0	34.6 ± 1.1	24.4 ± 6.8	32.2 ± 2.1	31.2 ± 1.4	34.2 ± 1.4	35.0 ± 1.2	35.1 ± 0.5	33.9 ± 0.9	9.4	25.2
% C2	8.6 ± 0.3	9.4 ± 0.4	9.7 ± 0.1	8.7 ± 0.9	7.0 ± 1.2	7.0 ± 0.5	9.0 ± 0.3	9.6 ± 0.2	9.2 ± 0.6	8.2 ± 0.3	4.2	5.5
% C3	34.0 ± 0.9	30.8 ± 0.7	31.7 ± 0.7	34.9 ± 3.9	35.0 ± 1.5	32.2 ± 0.5	32.7 ± 1.3	29.9 ± 0.5	32.5 ± 2.1	35.7 ± 0.8	50.1	42.0
% C4	18.6 ± 0.9	20.7 ± 0.8	21.4 ± 0.6	15.5 ± 3.6	22.0 ± 2.1	23.5 ± 1.0	21.0 ± 0.5	21.2 ± 0.7	20.0 ± 1.5	19.8 ± 0.1	9.8	15.8
% C5	4.1 ± 1.6	3.8 ± 1.4	2.6 ± 1.2	16.4 ± 7.6	3.9 ± 1.4	6.1 ± 2.3	3.1 ± 0.6	4.3 ± 1.8	3.8 ± 1.0	2.3 ± 0.6	26.4	11.4
% NH_4^+	8.9 ± 7.9	25.2 ± 9.3	6.5 ± 1.4	7.1 ± 0.8	15.8 ± 11.3	44.5 ± 9.3	10.0 ± 4.0	9.0 ± 1.1	1.2 ± 1.1	1.7 ± 0.8	-	93.2
% NO_3^-	32.9 ± 18.8	43.9 ± 5.6	46.0 ± 2.5	62.6 ± 3.3	53.8 ± 13.6	37.4 ± 7.2	50.2 ± 3.9	57.9 ± 3.6	11.9 ± 5.2	79.9 ± 7.0	-	3.6
% DON	54.6 ± 24.4	31.3 ± 10.0	45.9 ± 6.2	28.0 ± 5.1	26.2 ± 11.3	15.0 ± 10.7	36.5 ± 4.8	29.8 ± 1.9	75.5 ± 7.7	15.8 ± 7.1	-	3.2
% TDP	45.5 ± 12.1	70.0 ± 14.7	42.8 ± 16.7	30.4 ± 8.2	54.9 ± 10.3	70.7 ± 7.7	24.4 ± 3.3	22.2 ± 5.3	51.6 ± 17.3	51.9 ± 13.7	-	88.0
% TPP	54.5 ± 12.1	30.0 ± 14.7	57.2 ± 16.7	69.6 ± 8.2	45.1 ± 10.3	29.3 ± 7.7	75.6 ± 3.3	77.8 ± 5.3	48.4 ± 17.3	48.1 ± 13.7	-	12.0
$SUVA_{254}$	4.6 ± 0.6	4.7 ± 0.7	5.7 ± 0.5	5.0 ± 0.5	4.4 ± 0.8	4.2 ± 0.8	5.0 ± 0.4	5.0 ± 0.4	5.0 ± 0.5	3.2 ± 0.2	0.99	2.0
CDOM	4.4 ± 2.0	3.4 ± 1.5	6.0 ± 0.5	3.9 ± 0.8	4.6 ± 2.6	3.4 ± 1.7	5.49 ± 0.5	3.9 ± 0.7	6.5 ± 1.3	5.7 ± 0.3	1.8	1.4
FI	1.20 ± 0.06	1.24 ± 0.06	1.21 ± 0.04	1.22 ± 0.08	1.45 ± 0.2	1.52 ± 0.1	1.21 ± 0.07	1.19 ± 0.05	1.23 ± 0.05	1.38 ± 0.04	1.66	1.62
β:α	0.51 ± 0.03	0.50 ± 0.02	0.46 ± 0.02	0.90 ± 0.31	0.50 ± 0.04	0.51 ± 0.02	0.48 ± 0.03	0.47 ± 0.02	0.50 ± 0.04	0.62 ± 0.01	0.89	0.81
HIX	0.92 ± 0.02	0.93 ± 0.01	0.94 ± 0.01	0.79 ± 0.08	0.92 ± 0.02	0.91 ± 0.02	0.93 ± 0.01	0.92 ± 0.02	0.93 ± 0.01	0.95 ± 0.01	0.65	0.84

[a] These are the forested endmembers sampled in summer 2018, represented as green squares in Fig. 1.
[b] These are the agricultural endmembers sampled in summer 2018, represented as red squares in Fig. 1.
[c] These refer to the wastewater treatment plant intake and effluent sampled in summer 2021, represented as a light blue X in Fig. 1.

Discussion

To empirically assess the origin and fate of DOM in a north temperate river, we targeted river reaches and seasons of contrasting potential in terms of loadings and processing. We found that despite relatively low quantitative changes in the concentrations of dissolved organic carbon (Shousha et al., 2021), there were consistent changes in the fluorescent DOM composition that were modulated by seasons and land use, and that were informed by patterns observed for nutrient composition. This suggests that loading and processing mechanisms of different types of DOM are compensative rather than cumulative in this river. In moments or areas of low processing, the observed shifts in DOM composition would be predominantly due to compositional differences in the inputs from varying land use and land cover. Conversely, in a scenario where all inputs are qualitatively equal, changes in DOM composition would be due to the preferential removal of certain pools via photochemical or microbial degradation, flocculation, or sedimentation. Realistically, both loading and processing mechanisms interact to control DOM composition, and considering joint patterns with N and P forms allowed us to determine how the *Rivière du Nord* receives, transforms and exports different pools of DOM across land uses and seasons.

DOM composition under contrasting loading potentials: low flow conditions

During low flow seasons we observed widespread, sharp breakpoints in the upstream-downstream patterns of DOM and nutrient concentrations and composition, suggesting qualitative changes in the loadings from land. These were typically found at the boundary of the Canadian Shield and the St. Lawrence Lowlands geological provinces (Fig. 2). Across this boundary, the upstream DOM and nutrient pools shifted from a higher %C1-2 and %DON, to being enriched in %C3-4-5, $\%NH_4^+$, and $\%NO_3^-$ (Fig. 4 x-axis); P forms varied the least. Mechanisms that may explain this shift include groundwater or subsurface inputs from forested or agricultural landscapes, urban inputs, and autochthonous production, but not all mechanisms affect all forms or river reaches equally. For example, C1 and C2 are widely recognized as DOM pools of terrestrial, forested origins (Ishii & Boyer, 2012; Wünsch et al., 2017), and DON has been found to contribute ~80% of total N in streams draining unimpacted forested watersheds (Hedin, 1995; McGroddy et al., 2008). This supports the higher relative abundance of C1-2 and DON in the upstream mainstem reach which is dominated by forest cover. Interestingly, C1 percent contribution revealed a stepwise decrease across the breakpoint,

when other components became more abundant, followed by a linear increase post-breakpoint. This suggests relatively important punctual inputs of other components around the breakpoint, as opposed to a more continuous input of ubiquitous C1. As a result, the accumulation of C1 along the downstream portion of the mainstem was faster than other components.

Moving downstream, C3 and C4 became dominant relative to the total FDOM pool, consistent with presumed agricultural and urban sources. The increasing dominance in C4 concurred with higher proportions of NH_4^+ in the downstream mainstem reach, coherent with an urban source for both pools that may originate from WWTP inputs (Gücker et al., 2006; Waiser et al., 2011; Shousha et al., 2021). In particular, we measured high concentrations and proportions of NH_4^+ and TDP in the *Saint-Jérôme* WWTP effluent (22.7 mg L^{-1} and 0.28 mg L^{-1}, respectively), which accounted for 9.9 and 7.4% of the total river discharge in winter and summer, respectively (Shousha et al., 2021). C4, NH_4^+ and TDP were all relatively more abundant in the mainstem than in the agricultural endmembers (Fig. 5c), suggesting that the sharp increase of these forms downstream is explained by a non-agricultural, urban source. A component similar to our C4 (λEx/λEm = 345/452), Peak W, has previously been identified in detergents and whitening agents (Mostofa et al., 2010; Niloy et al., 2021), which is coherent with an urban point source. However, C4 was not particularly dominant in the WWTP effluent (15.8% or 0.778 RU in effluent vs 21.9% or 0.721 RU in the downstream mainstem). To solely account for the stepwise increase in C4, the WWTP effluent concentration should have been ~3 RU. This suggests that C4 in our study may originate from an urban source other than from the WWTP, but our data do not allow us to identify it.

Both urban and agricultural inputs appeared as important sources of C3. Up to 90% of the stepwise increase at RKm 74 can be explained by the WWTP effluent ($[C3]_{upstream}$ = 0.81, $[C3]_{downstream}$ = 1.006, $[C3]_{effluent}$ = 2.072; assuming a 7.4% contribution of effluent to mainstem discharge). Downstream, agricultural inputs could have sustained C3 concentrations in the rest of the downstream reach, as C3 was relatively higher in the agricultural tributary endmembers than in the downstream mainstem reach (1.9 vs 1.05 RU, Fig. 5), but these inputs are likely largely diluted when they reach the mainstem, as the mainstem's discharge was over 30x that of the main agricultural tributary. A similar pattern was observed for NO_3^- (downstream mainstem: 713 ug L^{-1} or 55%, agricultural endmembers: 5861 ug L^{-1} or 82%), which we have attributed to an agricultural source (Shousha et al., 2021), consistent with the wide use of tile drainage in the region (MRC d'Argenteuil, 2011) and the high mobility of NO_3^- in the soil matrix (Caraco & Cole, 1999). A recent study conducted in a river of similar size, land use, and

geology found a DOM component similar to our microbial humic-like C3, and associated it to autochthonously produced DOM (Retelletti Brogi et al., 2020). Other studies conducted in a variety of aquatic ecosystems support that this component may have some non-terrestrial origins (Asmala et al., 2014; Retelletti Brogi et al., 2021). In the *Rivière du Nord* watershed, the higher C3 concentrations found in the agricultural tributaries could be due to direct in situ autochthonous production supported by the higher N and P concentrations or recent production of this component in agricultural soils and its subsequent leaching to the mainstem.

Finally, protein-like C5 was generally the least variable from upstream to downstream during low-flow moments (Fig. 2, Supplementary Fig. S4), suggesting an ubiquitous behaviour that may be explained by a tight balance between input or production and processing in the river of this labile component (Lapierre & del Giorgio, 2014). C5 was dominant in the WWTP effluent (sampled during the summer; Supplementary Fig. S11), yet we did not measure a significant breakpoint going downstream in low flow conditions (Fig. 2, Supplementary Fig. S3), suggesting rapid uptake. Under very urbanised land use, a similar DOM component has been shown to increase with human population in the 6 000km long Yangtze River (Zhou et al., 2021), but in the *Rivière du Nord,* land use appeared insufficient to break the balance between input and removal. In contrast to land use, the extreme flow conditions of spring 2019 however, led to unusually high concentrations and proportions of C5 (Figs. 2, 3), suggesting different loadings are possible under different hydrological settings.

DOM composition under contrasting loading potentials: extreme flow conditions

The observed behaviour of DOM and its coupling with nutrients provide evidence of distinct loading scenarios occurring as a function of land use and hydrological events. High flows would typically lead to low transformation of DOM (Weyhenmeyer et al., 2012; Lambert et al., 2016; Raymond et al., 2016), and this was indeed the pattern observed for spring 2018 in the *Rivière du Nord* (Figs. 2, 3). In this context, however, the major shifts observed during the historical flood of 2019 were surprising, with very high concentrations and proportions of the protein-like C5 and microbial humic-like C3 in the upstream portion of the river (Fig. 3). Two lines of evidence may explain this pattern. As the upper forested region of the watershed is mainly covered with deciduous trees (Abrinord, 2015), fresh litter decomposition that accumulated in top soils, rich in protein-like (Wu et al., 2021) or microbial humic-like (Garcia et al., 2018) organic matter, may have been temporarily transported to the mainstem during the flood. These inputs would coincide with the most forested RKms along the mainstem (RKms 140

to 92), while the RKms more downstream that are surrounded by less forest would not have received such inputs, thus shifting the breakpoint from ~75 to 84 in spring 2019. Another possible source could be sewage overflows from several small sewered villages upstream of *Saint-Jérôme* during the flood in 2019 (4 villages in sequence, total population ~30 200). The WWTP intake sampled in summer 2021 was enriched in C3 and C5 (Table 3, Supplementary Fig. S11) and should largely represent other sewer intakes in the region. DOM indices may also help support this provenance. Although $SUVA_{254}$ and FI stayed relatively constant at 4.65 ± 0.73 L mg^{-1} m^{-1} and 1.3 ± 0.16, respectively throughout the mainstem and among seasons, suggesting a strong overall aromatic content of the DOM pool flowing in *Rivière du Nord*, other indices varied between periods of low and high flow, and LULC changes (Supplementary Figs. S5-S8). The freshness index (β:α) was highest (0.90) in the spring 2019 upstream mainstem reach compared to any other moment or place, forested (0.49) and agricultural (0.62) endmembers included, but very close to the WWTP intake (0.89) and effluent (0.81; Table 3). β:α values close to 1 are indicative of strong microbial activity and have been measured in several other WWTPs (Li et al., 2020). The humification index (HIX) in the spring upstream mainstem reach (0.79) resembled the WWTP intake HIX (0.65), which could also point towards potential, somewhat diluted, sewage overflow sources. Similarly, low HIX values were indeed found in other WWTP intakes or effluents (Li et al., 2020). Another study with a strong urban gradient found a positive relationship between tyrosine and tryptophan components and discharge at their most downstream gauging site (Zhou et al., 2021), which they hypothesised came from treated and untreated sewage flushing over impervious areas. However, in the *Rivière du Nord*, there were no obvious signs of higher overflow frequency or magnitude in 2019 vs 2018 (MDDELC, 2021). Furthermore, in terms of a nutrient response, the NO_3^- concentration was almost 1.5 times higher in the upstream mainstem reach during the extreme flood year (368 ug L^{-1}) compared to the more normal 2018 year (287 ug L^{-1}), whereas NH_4^+ remained the same (2018 = 50 ug L^{-1}, 2019 = 57 ug L^{-1}). This suggests that overflows were likely not the main source of DOM during the extreme flood, as we would have captured a strong NH_4^+ signal. Higher NO_3^- combined with the C3 and C5 however may be a function of a stronger leaching from septic beds, along with higher inputs from subsurface flow after winter N processing (Creed & Band, 1998). Approximately 70% of the population in the northern reaches of the river's wastewater is treated through septics and even modest urbanisation in the area can impact the NO_3^- signal in surface waters (Charrier Tremblay et al., 2020). While it is not possible to assess whether decomposed leaf litter, overflows, septic leaching or subsurface inputs contributed more to the changes in C3 and C5, these changes combined with higher NO_3^- suggests that these likely co-occurred, and it was clear that

extreme flow events led to unusually high loadings toward the end of the pristine reach of the river (Figs. 2, 3) resulting in major breakpoints in the DOM composition of certain components along the river at high flow.

DOM composition under contrasting processing potentials

Differences between summer and winter DOM composition hinted at variations in the preferential removal of certain forms as a function of light and temperature availability. Both seasons were dominated by %C1 and %C3 (Fig. 2), but the DOM pool in the downstream reach was richer in %C4-5, $\%NH_4^+$ and %TDP in winter (Fig. 4, quadrant b), and in %C3 and $\%NO_3^-$ in summer (quadrant d). This illustrates how the DOM and nutrient pools differ in same systems under similar flow conditions in two seasons with contrasting processing potential. The largest change in DOM components between both seasons was for %C3, which we propose originated from recent production either in the agricultural soil or, more probably, in the water through phototrophic processes during the summer. In winter, lower light and temperature would reduce autochthonous production, thus explaining the lower C3 concentrations (Supplementary Fig. S4) and proportions (Fig. 4) compared to summer. The second largest change was for %C4. Relative abundances for the whole river were almost the same (20.1% vs 19.9% in summer and winter, respectively), but concentrations of other components in winter were smaller, leading to a higher dominance of %C4, especially downstream. Following the breakpoint at RKm 74, winter C4 concentrations also increased from upstream to downstream, but decreased during summer (Supplementary Fig. S3). As C4 is thought to be photolabile (Dainard et al., 2015; Zhou et al., 2019), ice and snow cover may have protected it from irradiation during the winter. C5 was also more dominant in winter than in summer (Fig. 4), potentially due to lower uptake. While there was no stepwise increase in concentrations in either season, the slow and steady increase in winter C5 (Supplementary Fig. S3) may be explained by reduced uptake under the ice and groundwater inputs rich in microbial-like DOM (O'Donnell et al., 2010; Hobara et al., 2014; Peralta-Tapia et al., 2015; Shen et al., 2015). Thus, the most abundant forms in winter (C4, C5, NH4+, TDP) highlight not only the inputs of highly reactive or bio-labile forms of C, N, and P from predominantly urban or groundwater sources, but also the lower processing potential during the cold and dark winter season that allow these pools to persist in the water. The pool of DOM and nutrients measured downstream during summer highlights how the most bio-reactive forms measured during winter have been removed between the urban reach and the river mouth. The summer downstream

pool reflects within stream production (dominated by C3) and likely groundwater inputs for NO_3^- from the fertile plains of the St. Lawrence Lowlands.

Through the seasons, the Rivière du Nord exports alternating pools of DOM and nutrients that differ in their reactivity and persistence as a function of land use, land cover, and climate. These findings likely transpose well to most temperate rivers, which like Rivière du Nord tend to be exposed to large gradients of land uses across their continuum and experience seasonal variations in hydrology, temperature, and light availability. In temperate regions where snow accumulates, both spring precipitation and snowmelt constitute major drivers of riverine peak flow (Berghuijs et al., 2016). Snowmelt may contribute less to spring flows as winter temperatures increase (Ouranos, 2015; Pulliainen et al., 2020) and vernal window lengthens (Grogan et al., 2020), but precipitation is predicted to increase in winter and spring in certain regions of North America such as in Québec, Canada (Mailhot et al., 2008, 2012) with more extreme events likely to occur in the future (Trenberth et al., 2003), reducing snow mass, a trend already seen in the last decades in North America. Extreme spring flows may become more frequent and mobilise unusually large amounts of microbial and protein-like sources of DOM from land to water, while summer droughts may be more common and lead to preferential removal of specific pools of DOM and nutrients. Combined with urban expansion and agricultural intensification, the predicted changes in seasonal hydrology and ice/snow cover thus have the potential to greatly affect how temperate rivers receive, process and export DOM and nutrients of various sources and fates in the aquatic environments, with impacts on ecosystem processes of the rivers themselves and the downstream receiving environments.

Acknowledgements

We wish to thank L. Galantini for continued fieldwork and analysis support, R. LaBrie for help with PARAFAC modelling, and M. Talluto for help with the Bayesian model. We also thank M. Botrel for her curiosity and expertise in data visualisation and D. Bélanger for laboratory analyses support. Natural Sciences and Engineering Research Council of Canada (NSERC) Discovery grants to J.-F.L. and R.M. funded this work, as well as partial student support to S.S. via her NSERC collaborative Research and Training Experience Program (CREATE) EcoLac scholarship. We carried out the work for this article on the traditional lands of the Kanien'kehà:ka (Mohawk), Omàmiwinini (Algonquin) and Anishinabewaki.

Supporting Information

CONTRASTING SEASONS AND LAND USES ALTER RIVERINE DISSOLVED ORGANIC MATTER COMPOSITION

Stéphanie Shousha[1,2], Roxane Maranger[1,2], Jean-François Lapierre[1,2]

[1]Université de Montréal, Département de Sciences Biologiques, Montréal, QC, Canada.

[2]Groupe de Recherche Interuniversitaire en Limnologie (GRIL).

*Corresponding author : stephanie.shousha@umontreal.ca

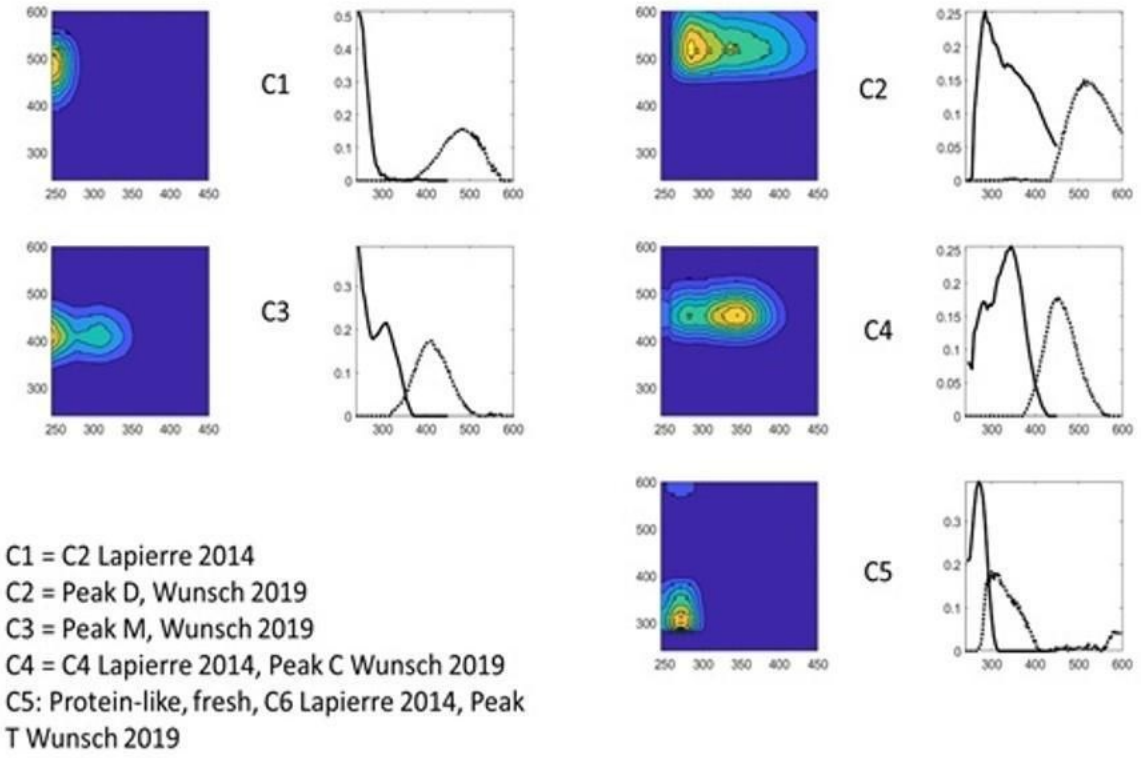

Supplementary Figure S1 Five DOM components identified using Parallel Factor Analysis (PARAFAC).

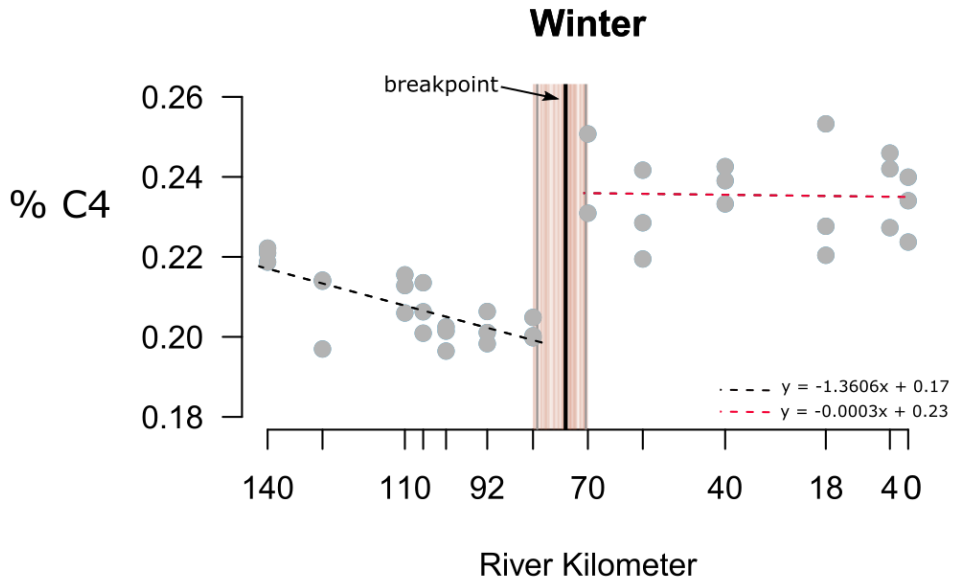

Supplementary Figure S2 Bayesian model output showing where the estimated breakpoint would fall along the river. The thick black vertical line represents the breakpoint median of 3000 estimation outputs (RKm 75.2) for the variable "winter %C4". The thin grey vertical lines represent the 95% credible intervals. The thin dust-coloured vertical lines show an example of 100 of those 3000 estimation outputs. Estimated rates of change in %C4 are also shown with the black dotted line (pristine reach) and the red dotted line (impacted reach). These linear regressions were modelled via the Bayesian breakpoint model and estimated slopes and intercepts are -1.3606 and 0.17, and -0.0003 and 0.23, for the pristine and impacted reaches, respectively.

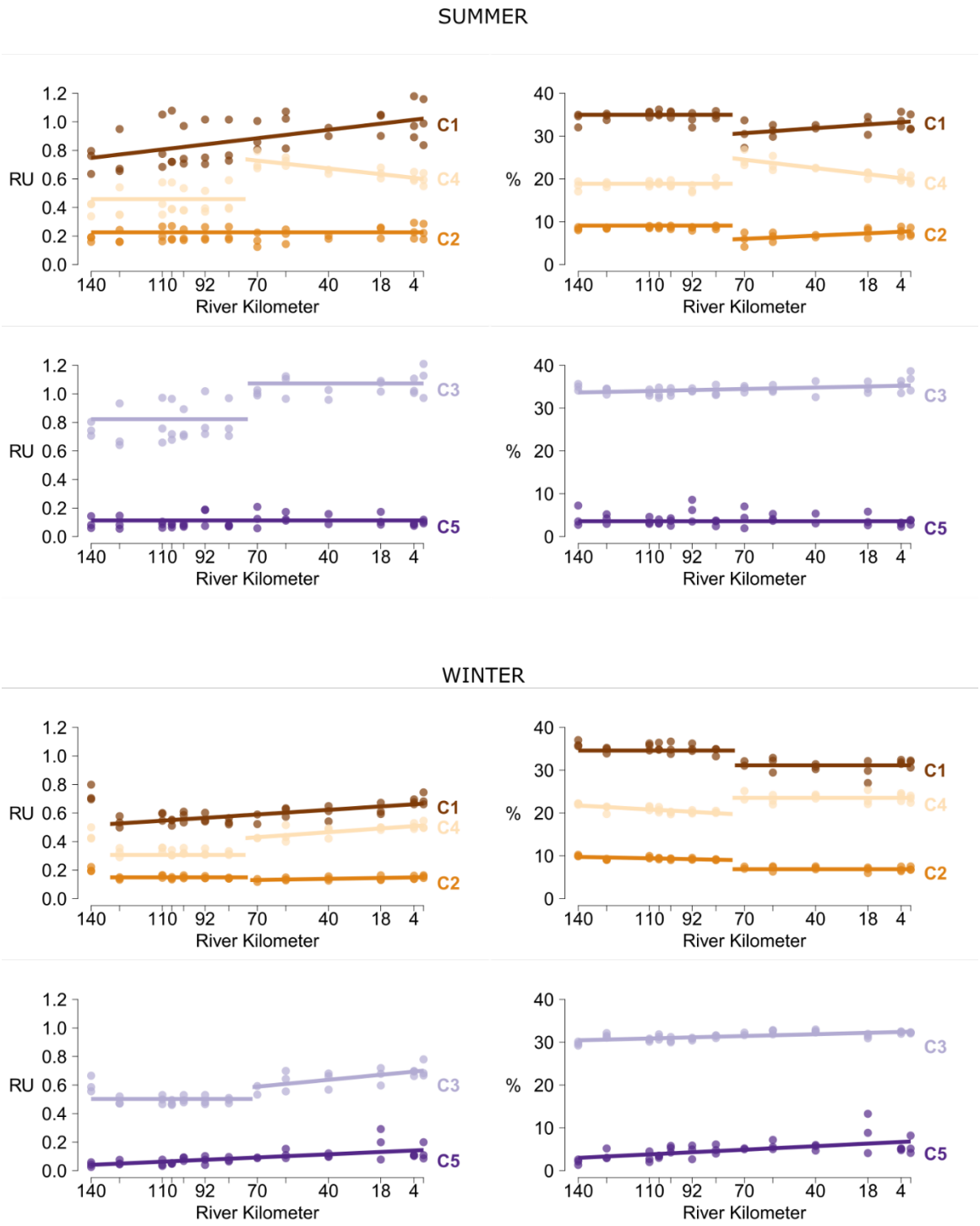

Supplementary Figure S3 Model outputs for C1-5 RU (left) and % (right) for summer and winter, showing all data points collected during the three years of sampling. A break in the slopes shows a breakpoint. Slopes not significantly different from 0 were plotted horizontally.

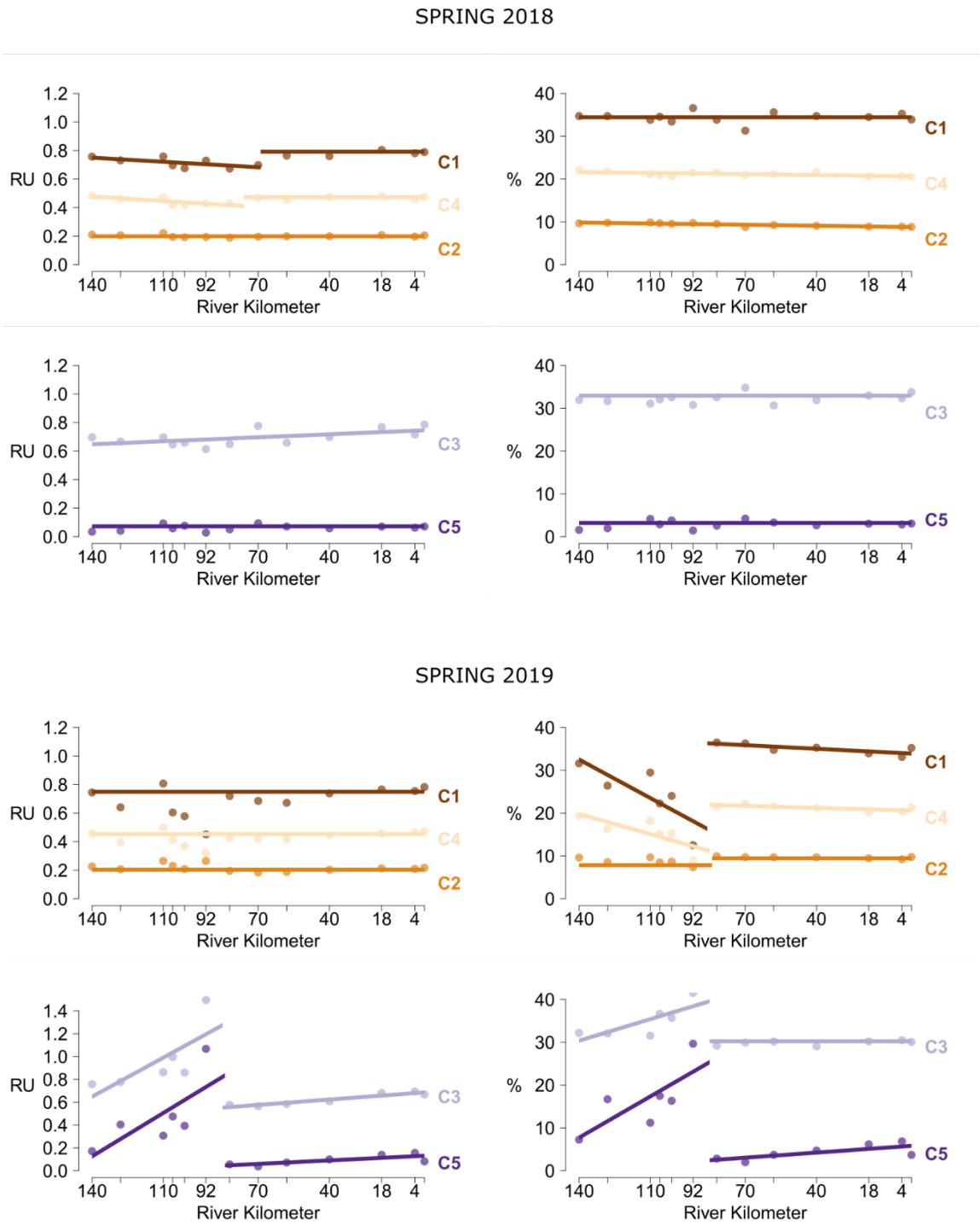

Supplementary Figure S4 Model outputs for C1-5 RU (left) and % (right) for spring 2018 and spring 2019 showing all data points collected during the two years of sampling. A break in the slopes shows a breakpoint. Slopes not significantly different from 0 were plotted horizontally.

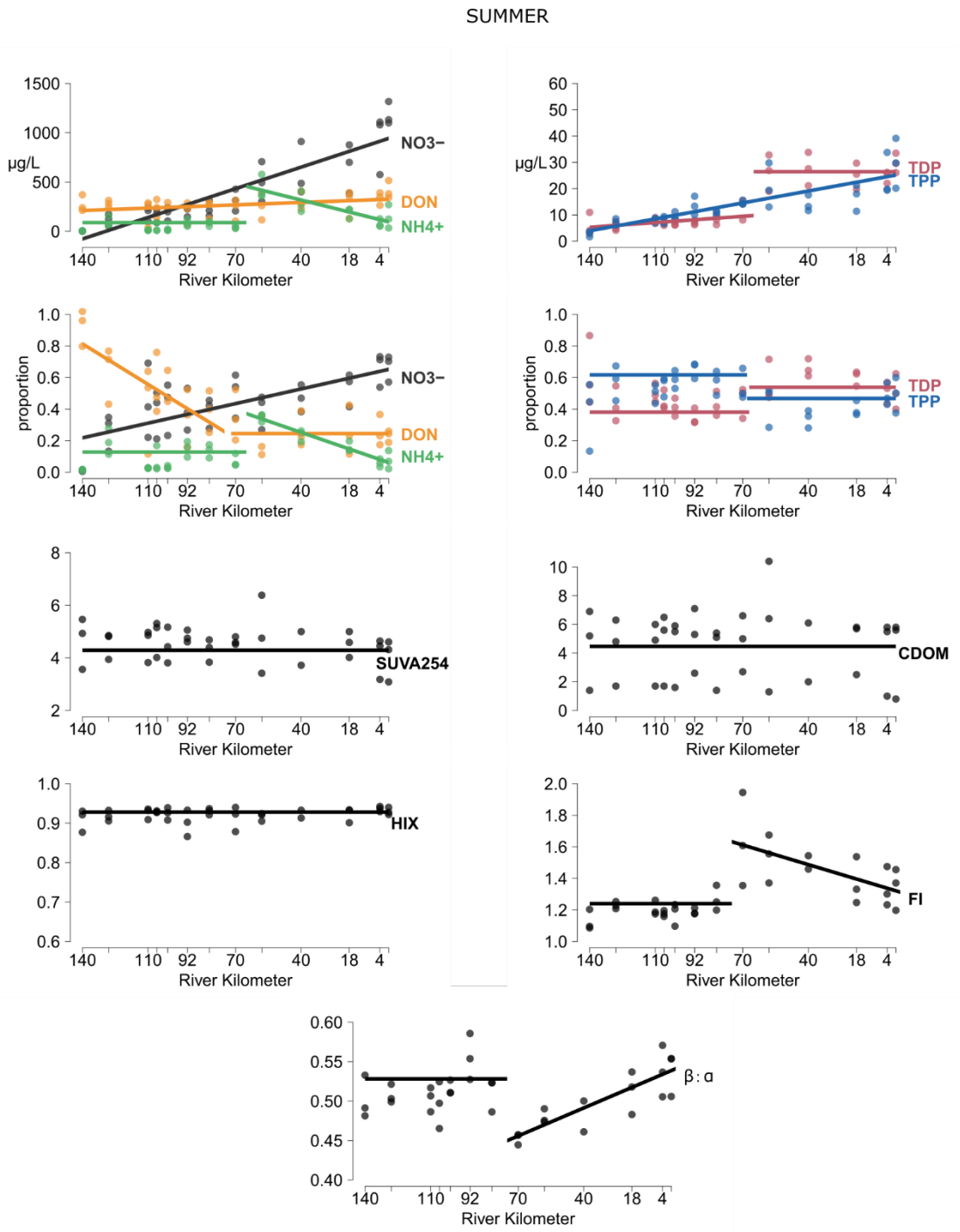

Supplementary Figure S5 Model outputs for nutrient forms (NO_3^-, NH_4^+, DON, TDP, TPP) in concentration and proportion and DOM indices ($SUVA_{254}$, CDOM, HIX, FI, β:α) for summer showing all data points collected during the three years of sampling. A break in the slopes shows a breakpoint. Slopes not significantly different from 0 were plotted horizontally.

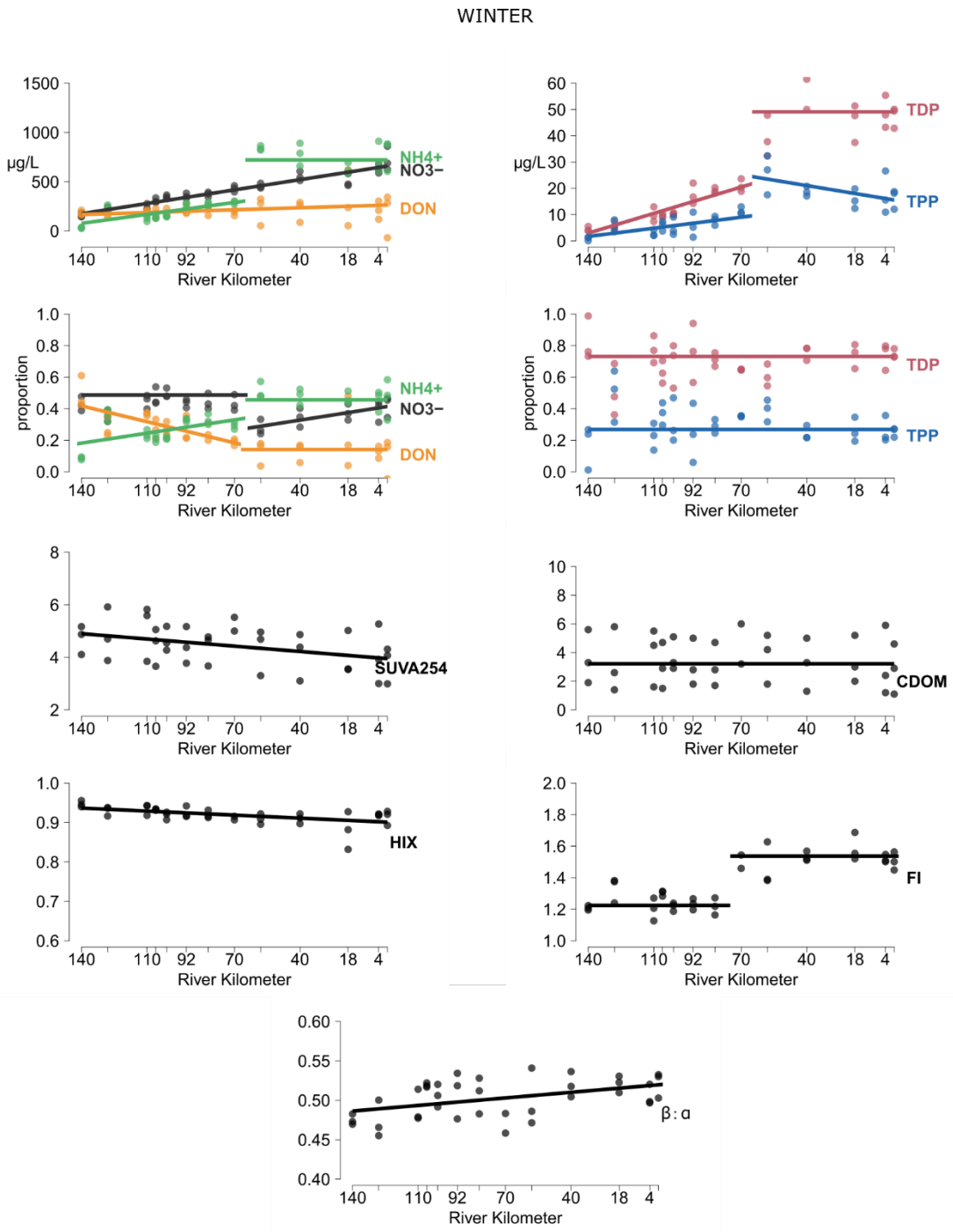

Supplementary Figure S6 Model outputs for nutrient forms (NO_3^-, NH_4^+, DON, TDP, TPP) in concentration and proportion and DOM indices ($SUVA_{254}$, CDOM, HIX, FI, β:α) for winter showing all data points collected during the three years of sampling. A break in the slopes shows a breakpoint. Slopes not significantly different from 0 were plotted horizontally.

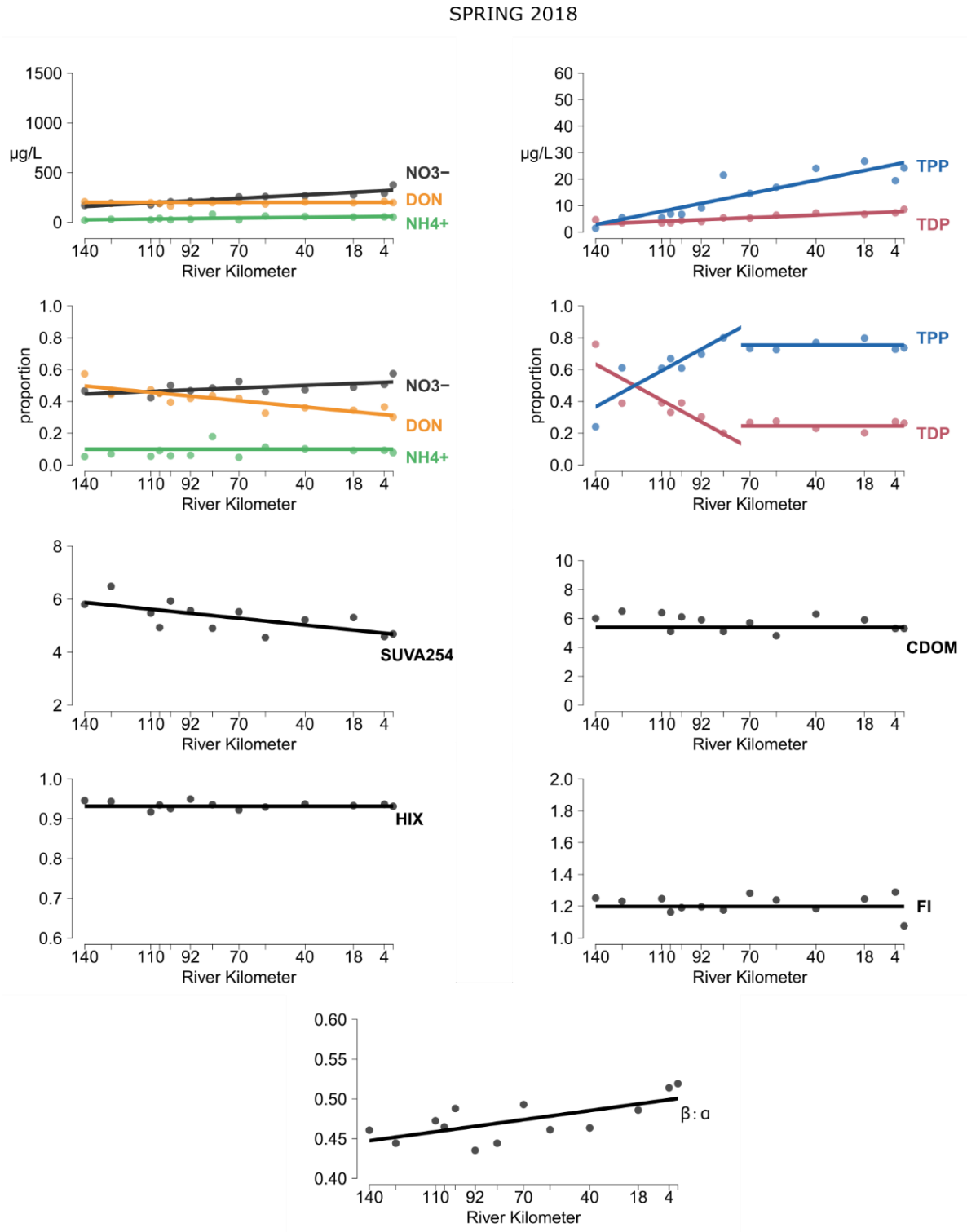

Supplementary Figure S7 Model outputs for nutrient forms (NO_3^-, NH_4^+, DON, TDP, TPP) in concentration and proportion and DOM indices ($SUVA_{254}$, CDOM, HIX, FI, β:α) for spring 2018 showing all data points collected during the sampling campaign. A break in the slopes shows a breakpoint. Slopes not significantly different from 0 were plotted horizontally.

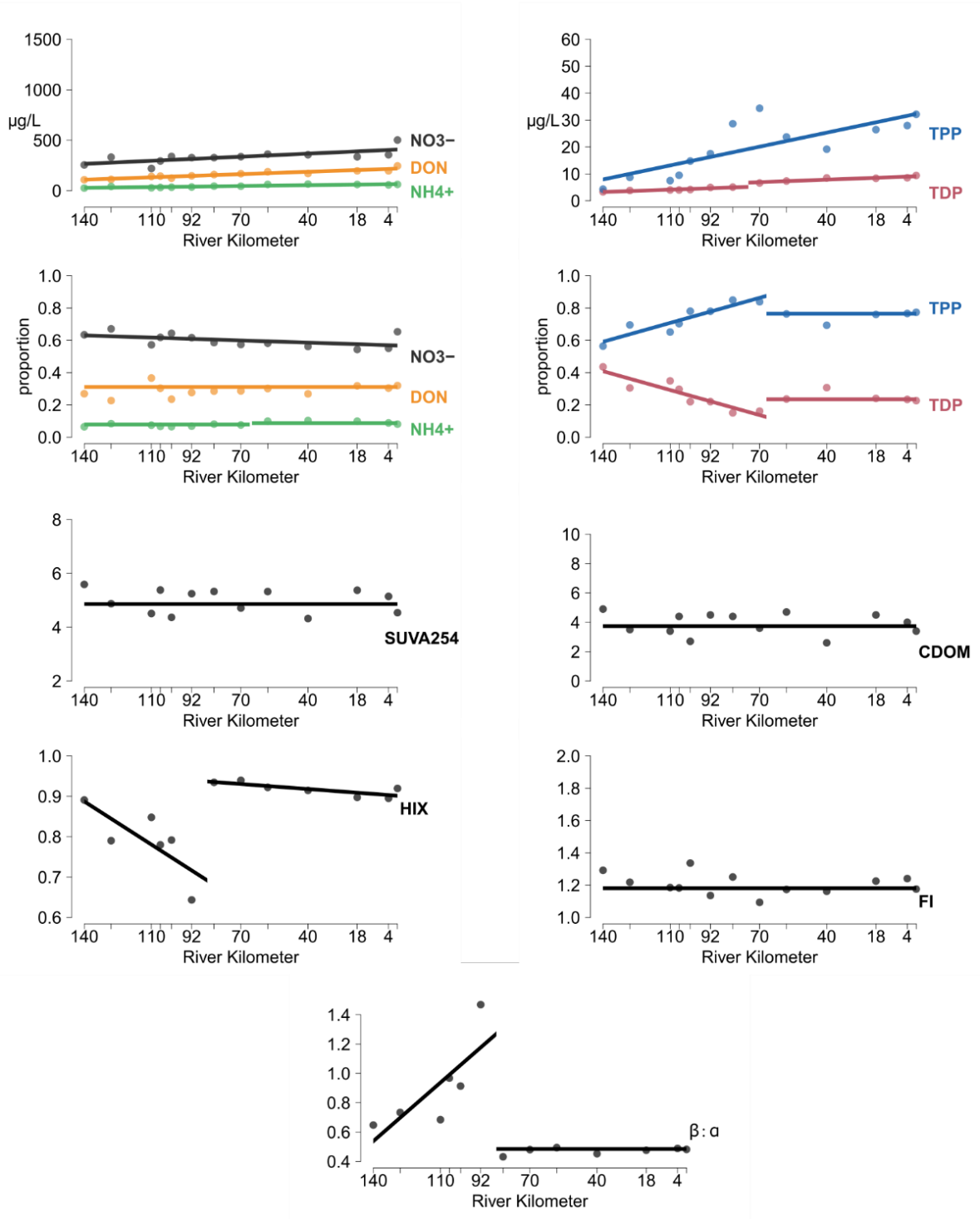

Supplementary Figure S8 Model outputs for nutrient forms (NO_3^-, NH_4^+, DON, TDP, TPP) in concentration and proportion and DOM indices ($SUVA_{254}$, CDOM, HIX, FI, β:α) for spring 2019 showing all data points collected during the sampling campaign. A break in the slopes shows a breakpoint. Slopes not significantly different from 0 were plotted horizontally. Notice the different y-axis scale for β:α (0.4 – 1.4) instead of 0.4 – 0.6 like in the other seasons.

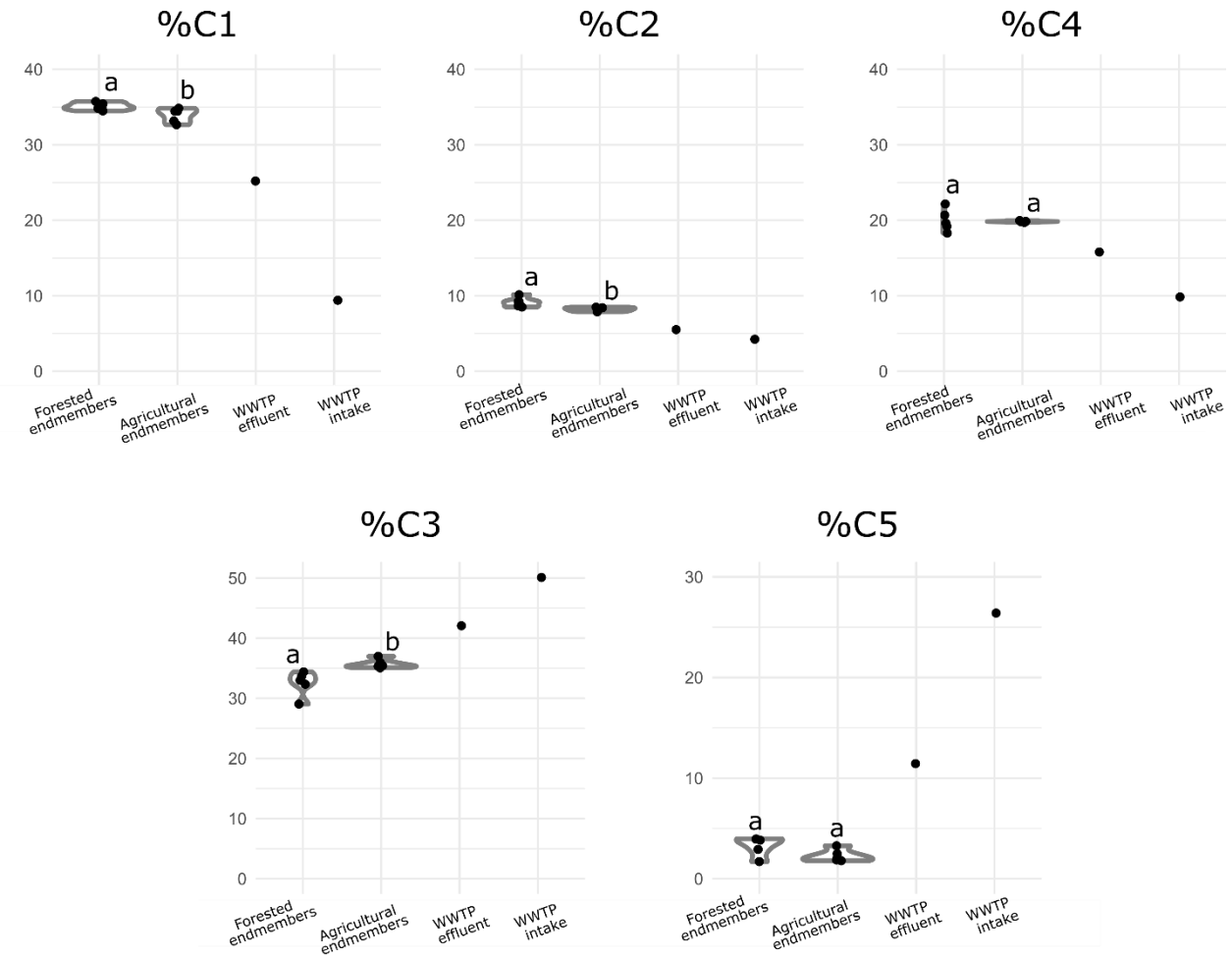

Supplementary Figure S9 Violin plots (grey) with raw data (black) plotted for each DOM component (%C1-5) across the endmembers (forested, agricultural, WWTP). Letters show significant differences by unpaired t-test (%C1-2-3-5) or non-parametric wilcoxon test (%C4) between forested and agricultural endmembers. WWTP values could not be tested due to inexistent variance.

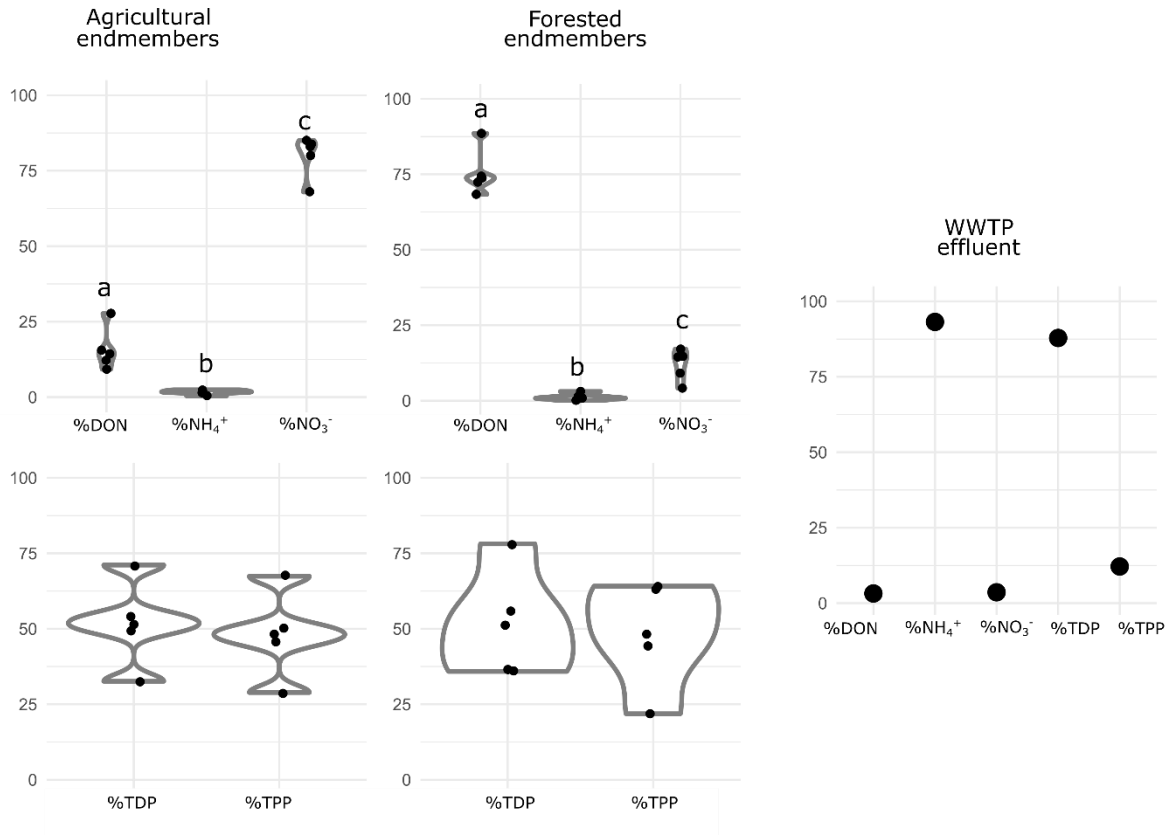

Supplementary Figure S10 Violin plots (grey) with raw data (black) plotted for N and P forms across each endmember (forested, agricultural, WWTP). Letters show significant differences by one-way anovas followed by Tukey tests (%DON-NH_4^+-NO_3^-) or unpaired t-test (%TDP-TPP) among N forms and between P forms. WWTP values could not be tested due to inexistent variance.

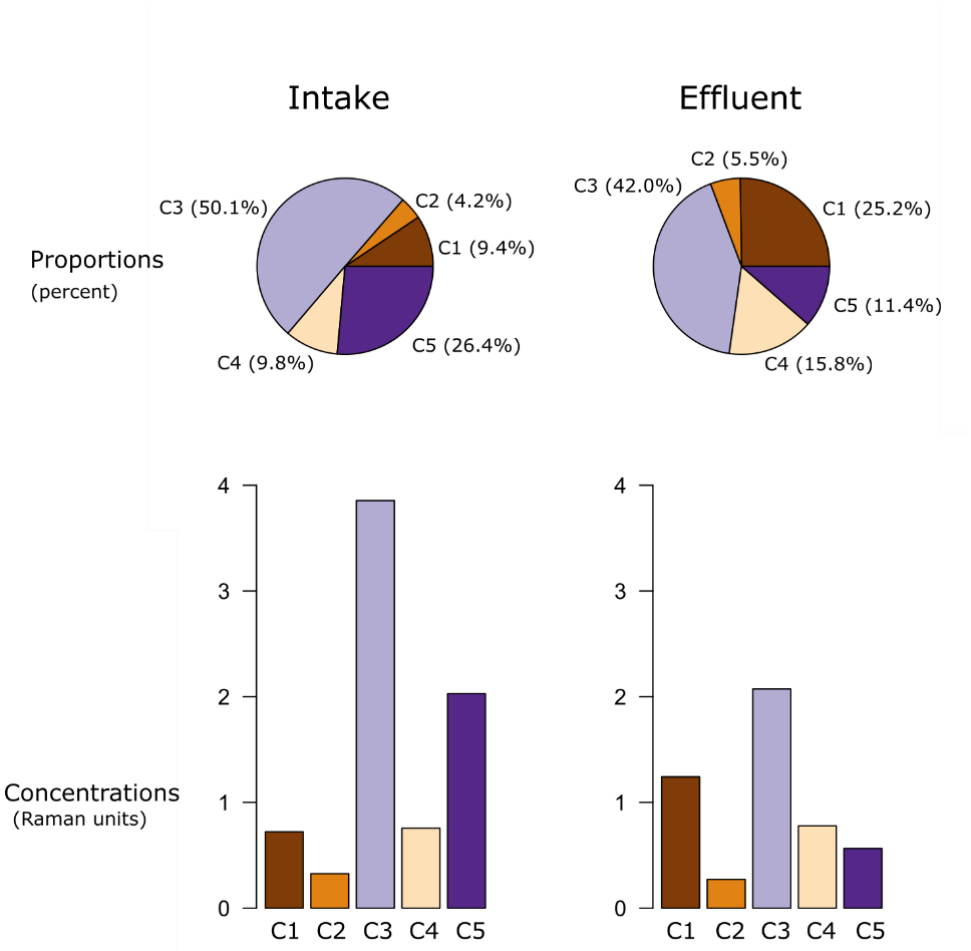

Supplementary Figure S11 DOM components measured in the intake and effluent of the *Saint-Jérôme* wastewater treatment plant in August 2021. Proportions are represented as pie charts (percentage) and concentrations as bar plots (Raman units).

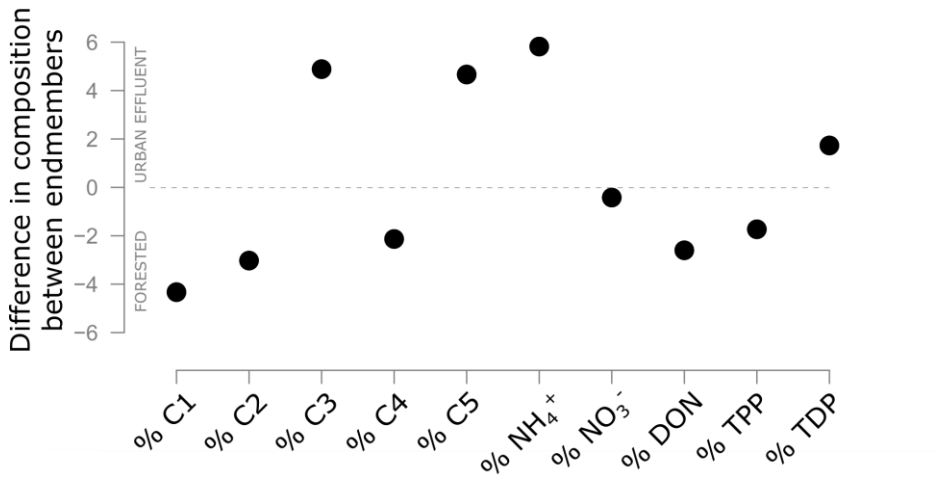

Supplementary Figure S12 Difference between the urban and forested endmembers for dissolved organic matter components (%C1-5) as identified by PARAFAC, and %nutrient forms (ammonium (NH_4^+), nitrate (NO_3^-), dissolved organic nitrogen (DON), total particulate phosphorus (TPP), and total dissolved phosphorus (TDP)). Values were calculated as the difference in the z-scores of the urban effluent (August 2021 sampling) and forested tributary endmember average (summer 2018 sampling).

Chapitre 3

La précipitation et les apports anthropiques contrôlent les changements décennaux de carbone, d'azote, et de phosphore riverains dans une rivière tempérée

Precipitation and anthropogenic inputs drive decadal changes in carbon, nitrogen, and phosphorus riverine loads in a north temperate river

Authors : Stéphanie Shousha[1], Roxane Maranger[1], Jean-François Lapierre[1]

[1]Université de Montréal, Département de Sciences Biologiques, Montréal, QC, Canada. Groupe de Recherche Interuniversitaire en Limnologie (GRIL).

In preparation

Abstract

Changes in precipitation and land use have affected the loads of carbon (C), nitrogen (N) and phosphorus (P) in receiving waters. However, how these drivers differentially affect riverine C, N, and P remain poorly understood. We quantified long-term (1980-2020) trends in riverine C, N, and P loads at three sites along the mainstem of a north temperate river in Québec, Canada, that successively drain forested, urban, and mixed land-use areas. Riverine N and to a lesser degree C loads tended to increase over time, with major inter-annual variation largely resolved by variation in precipitation. While increases in riverine N were consistent with historical increases in net anthropogenic N inputs (NANI), P loads tended to decrease over time despite increases in net anthropogenic P inputs (NAPI) to the landscape. Although anthropogenic N and P inputs on land both increased, P was preferentially removed over time, through targeted municipal wastewater treatment. This retention of P was reflected in the inter-annual patterns of riverine C: N: P ecosystem stoichiometry at the river mouth, which was stable until 2000 then became enriched, particularly with N over P in recent decades. Our work shows the discrepancy of C, N, and P watershed exports to a river from decadal changes in precipitation, management of point source P pollution, and urban expansion and synthetic N fertiliser use through agricultural intensification, with consequences on the magnitude and stoichiometry of the riverine C, N, and P in a north temperate watershed.

Keywords: rivers, stoichiometry, carbon, nitrogen, phosphorus, decadal trends

Introduction

Carbon (C), nitrogen (N), and phosphorus (P) are at the base of aquatic ecosystem metabolism (von Schiller et al., 2017), but excess loadings of these elements can adversely impact ecosystem functioning (Stutter et al., 2018). There have been widespread increases in the loads of C, N, and P from land to water in response to changing climate and human modifications to the landscape (Howarth et al., 1996; Ballard et al., 2019; Kritzberg et al., 2020), with consequences like decreased nutrient retention, eutrophication, and lower drinking water quality (Carpenter et al., 1998; Graeber et al., 2021). However, terrestrial loading of individual elements to a river may differ across or within a watershed as a function of different land use practices or physical watershed features (Goyette et al., 2019). As such, riverine ecosystem stoichiometry can be a useful framework to understand the integration of gain and loss patterns of different elements at the watershed scale (Maranger et al., 2018). The approach has been successfully applied along the mainstem of a river, where stark differences were measured as a function of seasonal climate and upstream-downstream land use gradients (Shousha et al., 2021). It remains to be seen, however, how long-term changes in climate and land use may differentially influence the input and retention of C, N, and P on land and in the water, consequently influencing riverine loads and their resulting stoichiometries.

It is well known that C, N, and P loadings have been influenced by land use and/or climate changes (Carpenter et al., 1998; Zarnetske et al., 2018). Anthropogenic N and P inputs to land have increased mostly because of intensive agriculture and urban population growth (Howarth et al., 1996; Carpenter et al., 1998), and from an agricultural fertiliser use point of view, N inputs appear to have outpaced P inputs more generally (Glibert et al., 2014). In terms of transfers from land to water, N, as nitrate, is more mobile in the soil matrix (Caraco & Cole, 1999), and precipitation or runoff has been shown to increase the anthropogenic N fraction exported to rivers (Howarth et al., 2006; Han et al., 2009; Howarth et al., 2012). P on the other hand is highly reactive and tends to bind to the soil matrix (Sharpley et al., 2013). As such, P often enters rivers in a particulate form (Holtan et al., 1988; Paytan & McLaughlin, 2011) and increased riverine P loads tend to be influenced by flashier discharge patterns rather than annual precipitation (Goyette et al., 2019). In managed watersheds, delivery pathways are also a function of landscape modifications that promote runoff. For example, tile drainage has been shown to accelerate N transport accounting for > 80% of inputs loaded to waters (McIsaac & Hu, 2004), whereas stormwater runoff from even moderately urbanised regions have higher P loads than less managed regions (Yang & Toor, 2018). The main land use drivers of N and P have been shown

to influence dissolved riverine C concentrations and composition, but these vary in direction and magnitude (Xenopoulos et al., 2021). Other environmental changes, directly or indirectly related to human impacts such as precipitation (Vidon et al., 2008; Zarnetske et al., 2018), long-term changes in acidification recovery (Clark et al., 2010; Kritzberg et al., 2020), and reforestation practices (Kritzberg, 2017), have been shown to increase dissolved C in rivers because of C release from soil under less acidic conditions and increasing flow paths through organic matter rich soil. Disentangling whether C, N, and P move from land to water because of natural or anthropogenic drivers over decadal timescales in the same watershed can help us understand when, where, and how these different elements enter rivers.

A large proportion of anthropogenic N and P inputs is removed or stored in different watershed compartments, with only 15-30% of N and 5-15% of P added to landscapes being exported to receiving waters on average (Howarth et al., 1996; Han et al., 2013; Goyette et al., 2016; Hong et al., 2017). In the case of diffuse agricultural inputs, removal can be either through plant harvest, or for N, through permanent denitrification losses (Van Breemen et al., 2002). However, N and P from fertiliser inputs are increasingly stored in catchment soils or groundwaters, potentially leading to legacy effects (Haygarth et al., 2014; Van Meter et al., 2016; Goyette et al., 2018). The high mobility of nitrate through the soil matrix may explain the higher fraction exported compared to P, but its storage as organic N in the soil is also important, and accumulations in groundwater are particularly significant (Van Meter et al., 2016). Soils are known to accumulate the majority of diffuse P inputs (Sharpley et al., 2013; Haygarth et al., 2014), with only a small fraction reaching groundwater, reservoirs, or landfills (Van Meter et al., 2021). Dammed reservoirs are also known to generally retain N and P in the landscape (Harrison et al., 2009; Maavara et al., 2015), and have even been used as management strategies to retain P over time (Hu et al., 2020). However, excess loads over time can turn reservoirs from sinks to sources, at least in the case of N (Teodoru & Wehrli, 2005). Diffuse sources can also come from an increase in rural population growth affiliated with septic inputs (Kaushal et al., 2011). However, recent population expansion mostly occurs in urban centers where human sewage is concentrated and treated in different manners (Carey & Migliaccio, 2009), which then enters rivers as point sources. In terms of sewage treatment, the emphasis has been on P removal in most developed countries, with limited treatment in low- and middle-income countries with a growing emphasis on the need to retain N (Pagilla et al., 2006). As such, long-term time series of N and P fractional exports would uncover changes in riverine nutrient loads over time and space in response to development choices.

In this study, we aim to understand how loads of C, N, and P have varied over the last four decades in a north temperate river that consecutively drains a forested region, one that has experienced increased urban development, and an area with a long history of agriculture. Specifically, over a 40-year period, we quantified C, N, and P riverine loads as well as their stoichiometry as a function of changes in climate and net anthropogenic inputs of N and P to land at three sub-watersheds along a river's mainstem with an increasing gradient of human pressure.

Methods

Description of study site

The *Rivière du Nord* watershed is situated north-west of Montréal, in the Laurentians region of Québec, Canada. The mainstem, a 140 km-long river of Strahler order 5, initially drains a largely forested landscape, then an urban, and finally an agricultural one (Fig. 1a). Agricultural land use is constrained to fertile plains of the St. Lawrence Lowlands located in the southern-most third of the watershed. North of the St. Lawrence Lowlands is the Canadian Shield, a geological province covered with very little topsoil, a mix of conifer and deciduous trees, lakes and rivers. Most urban development occurred along the river banks.

Three sites along the *Rivière du Nord* mainstem have been sampled periodically by the *Ministère de l'Environnement et de la Lutte contre les changements climatiques* (MELCC, 2022a) since ~1980, with measurements available for dissolved organic carbon (DOC), total nitrogen (TN) and total phosphorus (TP) in the *Banque de données sur la qualité du milieu aquatique* (BQMA). For our study, we named those sites based on their location along the mainstem, using the outlet as river kilometer 0 (Fig. 1a). These sites coincided with major changes in land cover and land use (Natural Resources Canada, 2009). Forest and water covered 87% and 6% of the landscape drained by the most upstream site, RKm 101, and agriculture and urban land uses 1.5% and 0.4%. The watershed area between RKms 101 and 58 was covered by more impervious areas (11%), and agriculture (12%). RKm 58 also captured the wastewater treatment plant effluent of three towns discharging in the river, including the largest town in the watershed at RKm 70, *Saint-Jérôme*, for which the effluent discharge was estimated to be ~10% of total river discharge in low flow seasons (winter and summer). Finally, the watershed area from

RKms 58 to 4 was more covered by agricultural land uses (16%) with little impervious areas (2%), the rest being forest cover (70%). Wetlands represent less than 0.2% of total watershed area.

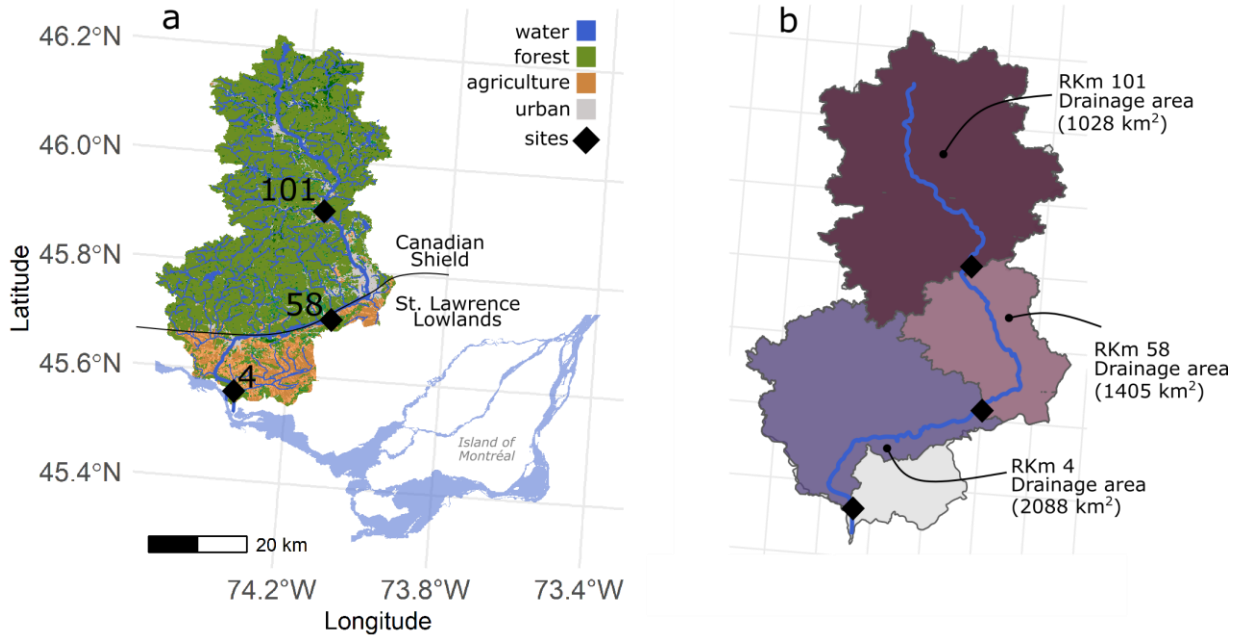

Figure 1 Land use and land cover map of the *Rivière du Nord* watershed, positioned with regards to the Island of Montréal (panel a). The thick blue line in the watershed shows the river's mainstem. The three water quality sites are River Kilometers 4, 58, and 101. Panel b shows cumulative drainage areas for the three sites. The grey area is not drained by RKm 4.

Quantification of changes in anthropogenic nutrient inputs on land

To quantify human activities on the landscape historically, we used the Net Anthropogenic Nitrogen/Phosphorus Input (NANI, NAPI) mass balance models following Goyette et al. (2016). The N and P budgets were calculated for a 5-year interval from 1981 to 2016 using municipal-level data which was the finest scale available. There are 39 municipalities within the *Rivière du Nord* watershed, 27 of which have more than 30% of their surface area in the watershed. Municipality surface area ranged from 16 to 485 km^2 (median = 97 km^2, mean = 134 km^2, sd = 114 km^2). The models are the sum of the following categories:

NANI = food + feed + fertiliser + biological N fixation + atmospheric N deposition (eq. 1)

NAPI = food + feed + fertiliser + laundry and dishwasher detergent (eq. 2)

Overall, to quantify each category, we multiplied agricultural or population data by coefficients (ex: percent N or P content), resulting in kilograms of N and P imports or exports to a municipality. To

obtain kg N or P km^{-2} yr^{-1}, each category and the overall budgets were then divided by the surface area of municipalities (MAMH, 2010), respecting the historical territorial reorganisations that influenced surface area (Supplementary Table 1). Data sources, coefficients and their descriptions can be found in Supplementary Table 2 and are detailed in Goyette et al. (2016). Two variables in the model are themselves the result of other equations:

Food

Food = human consumption – crop yield distributed to humans – animal product (eq. 3)

Food (eq. 3) refers to the amount of N and P imported by a municipality to sustain its human population. The model assumes that harvested crops ("crop yield distributed to humans") and livestock ("animal product") within a municipality first feed their own human populations and are hence subtracted from human consumption.

Feed

Feed = dynamic animal intake – crop yield distributed to animals (eq. 4)

Feed (eq. 4) refers to the amount of N and P imported by a municipality to sustain its livestock population. Again, the model assumes that harvested crops ("crop yield distributed to animals") first feed their own livestock population and are hence subtracted from animal intake. Insufficient crop yield production will result in net imports of Feed, while excess crop yield will be exported out of the municipality.

Historical changes in riverine C, N, and P

To estimate riverine loads (kg km^{-2} yr^{-1}), we used the loadest and loadflex models (Runkel et al., 2004; Appling et al., 2015). Briefly, the models predict daily solute concentrations based on both daily discharge data and observed solute concentrations. Daily discharge data was downloaded from the *Saint-Jérôme* gauging station (45.79, -74.01; Centre d'expertise hydrique du Québec; MDDELCC, 2018) from 1979 to 2020 and used with the proportion of subwatershed surface area to estimate discharge at all three sites. Historical solute data was downloaded from the BQMA for the three sites and spanned roughly 1979 to 2020 (with some variables starting in 1985), to which we added our own sampling data (Shousha et al., 2021; Supplementary Table 3). On average, for all variables, the frequency of sampling

was bi-monthly. Then, model outputs were divided by cumulative catchment area (Fig. 1b) to obtain areal weighted riverine loads.

Climate conditions over time

To explore whether climate or atmospheric deposition variables (precipitation, temperature, sulfur deposition) could explain the trends seen in C, N and P loads, monthly precipitation and temperature data (1980-2020) were downloaded for 19 stations on and around the *Rivière du Nord* watershed (Government of Canada, 2021a; Supplementary Fig. S1 a). We then interpolated annual precipitation, as the sum of rain and snow accumulated on land, and mean annual temperature for all years by making a template grid of 0.01-degree resolution (Supplementary Fig. S1 b).

We quantified annual runoff as the ratio between streamflow (mm yr^{-1}) to precipitation (mm yr^{-1}). Specifically, we used daily streamflow at the *Saint-Jérôme* gauging station, converted it to yearly discharge (m^3 yr^{-1}), divided it by the area it drains (1163 km^2), and converted it from meters to millimeters. We then downloaded daily total precipitation data from the *Saint-Jérôme* weather station from 1980-2020 and converted them to annual precipitation (mm yr^{-1}).

Statistical analyses

To facilitate interpretation of patterns among the 39 municipalities, we used hierarchical agglomerative clustering to identify groups that had similar patterns of change in the parameters of NANI and NAPI (equations 1 and 2) over time, where the Dindex (Charrad et al., 2014) determined the optimal number of clusters as three (dendrogram shown in Supplementary Fig. S2). Using these clusters, we averaged NANI and NAPI categories for every census year.

To compare the N and P inputs on land (5-year interval census data) to riverine loads (annual data), we derived a 5-year average of river estimates around the focal census year (census year: 2001, riverine load average: 1999 – 2003). As 2016 was the last census year, we included riverine loads until the last full data year, 2020.

To determine whether and how exports of anthropogenic N and P influenced historical C: N: P ecosystem stoichiometry, we focused on the most downstream site of the river (RKm 4) as the

integration of terrestrial loadings from different land cover and land uses, and processes across seasons and years. Elemental ratios were calculated as the molar ratios of riverine loads.

Results

Overall trends

There was little difference in the patterns of riverine C load across sites in the *Rivière du Nord* mainstem, but a slight increase can be observed for all sites over time (Fig. 2). Overall, DOC loads for the three sites ranged from 1891 to 4890 kg km^{-2} yr^{-1} (mean = 3123, sd = 662). Riverine N and P loads were more variable. N loads in the two most downstream sites, RKm 58 (urban) and RKm 4 (mixed), ranged from 281 to 881 kg km^{-2} yr^{-1} (mean = 493, sd = 108) and increased steadily from ~1990. N loads in the forested site, RKm 101, ranged from 218 to 406 kg km^{-2} yr^{-1} (mean = 306, sd = 50). The trends in P for the two most downstream sites were similar to one another, remaining constant until ~1998 (mean = 49, sd = 10), after which they dropped by more than half and then tended to increase starting in 2010. As a result, mean P loads for both sites across years was 38 kg km^{-2} yr^{-1} whereas they were 18 kg km^{-2} yr^{-1} for forested RKm 101 on average, where they decreased continuously by more than half between 1980 and 2020.

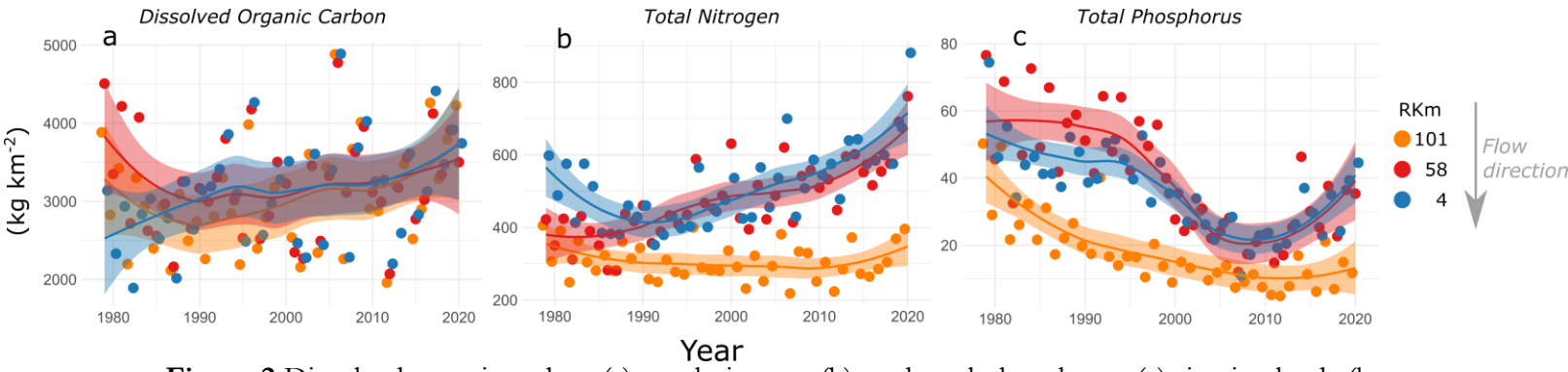

Figure 2 Dissolved organic carbon (a), total nitrogen (b), and total phosphorus (c) riverine loads (kg km^{-2}) per year for three sites along *Rivière du Nord* from 1980-2020. RKm 101 is the most upstream site, followed by RKm 58, and RKm 4 which is situated 4 kilometers upstream from river mouth (RKm 0). Nonparametric curve fittings (LOESS; locally weighted scatter-plot smoother) are shown to help follow the trends. The larger variations observed at the beginning of the timeframe (~1980-1985) may be an artifact of loadest and loadflex models lacking earlier data points.

Climate trends

Mean annual precipitation (1070 mm, sd = 100) ranged from 907 mm in 2001 to 1364 mm in 2006 and explained 51% of the variance in riverine DOC loads (p-value < 0.01; Fig. 3a). Temperature and

sulfur deposition did not explain meaningful additional variation. Precipitation explained 42% of variance in TN loads for RKms 4 and 58 (p-value < 0.01; Fig. 3b), and there were no differences in intercept or slope between these sites. Precipitation explained 48% of the variance for TN at RKm 101 (p-value <0.01), but loads were much lower for any given amount of precipitation. Precipitation did not explain significant amounts of variability in P at any site, but the two downstream sites were always significantly higher than the upstream site (Fig. 3c).

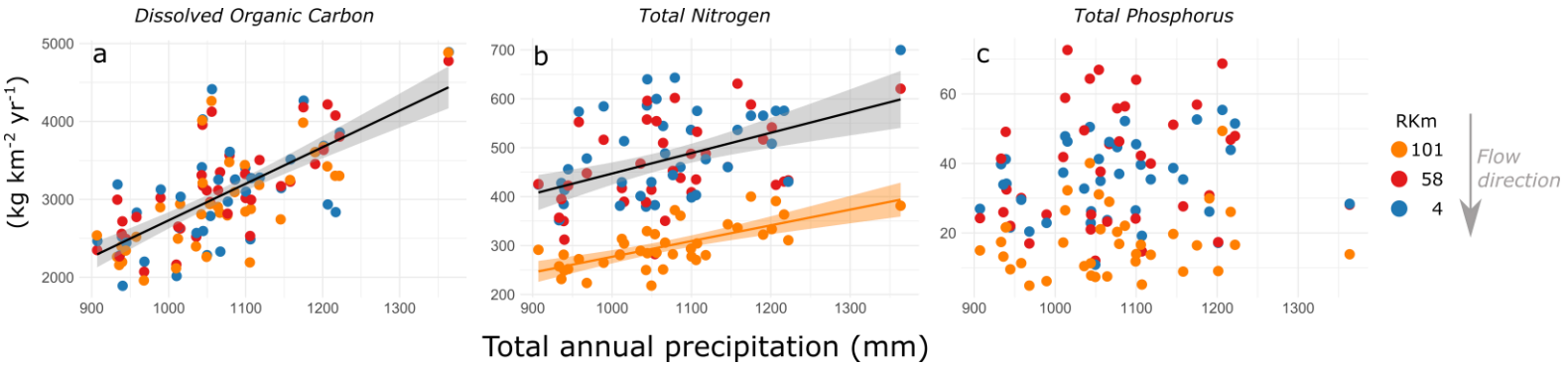

Figure 3 Dissolved organic carbon (a), total nitrogen (b), and total phosphorus (c) riverine loads (kg km^{-2} yr^{-1}) versus annual precipitation (mm) for three sites along the *Rivière du Nord* mainstem from 1980 to 2020. Annual precipitation includes rain and snow. Analyses of covariance determined that DOC linear regression slopes and intercepts were not significantly different among RKms. Equation of the slope was y = 4.69x – 1962 (R^2 = 0.51, p-value < 0.01). TN slopes were not different among RKms, but intercepts between RKms 4-58 and 101 were significantly different (p < 0.01). Equation of the RKms 4-58 was y = 0.42x + 30 (R^2 = 0.21, p-value < 0.01) and equation for RKm 101 was y = 0.32x – 44 (R^2 = 0.48, p-value < 0.01). TP loads were twice as high at sites RKm 4 and 58 than 101.

Changes in land inputs

Figure 4 shows the Net Anthropogenic Nitrogen and Phosphorus inputs (NANI and NAPI, respectively) for 1981, 2016, and the difference between both years to quantify the overall change in nutrient inputs. Across all years and municipalities, NANI averaged 1332 kg km^{-2} (sd = 1249) and ranged from ~ 500 kg N km^{-2} in Doncaster, a Mohawk First Nations Reserve (shown in Fig. 4a) to 7827 kg N km^{-2} in the most populated municipality in 2016, *Saint-Jérôme* (805 habitants km^{-2}, shown in Fig. 4b). Despite the lack of census information about population and agricultural activities in Doncaster, this municipality should be largely uninhabited as it serves as a hunting and fishing territory reserved for the Mohawk First Nation (Gouvernement du Québec, 2012). As such, NANI in this municipality was estimated as entirely due to atmospheric N deposition. Across all years and

municipalities, NAPI averaged 141 kg km^{-2} (sd = 354) and ranged from -47 kg P km^{-2} to 1394 kg P km^{-2}. Doncaster, again given limited available information, was estimated as having no NAPI.

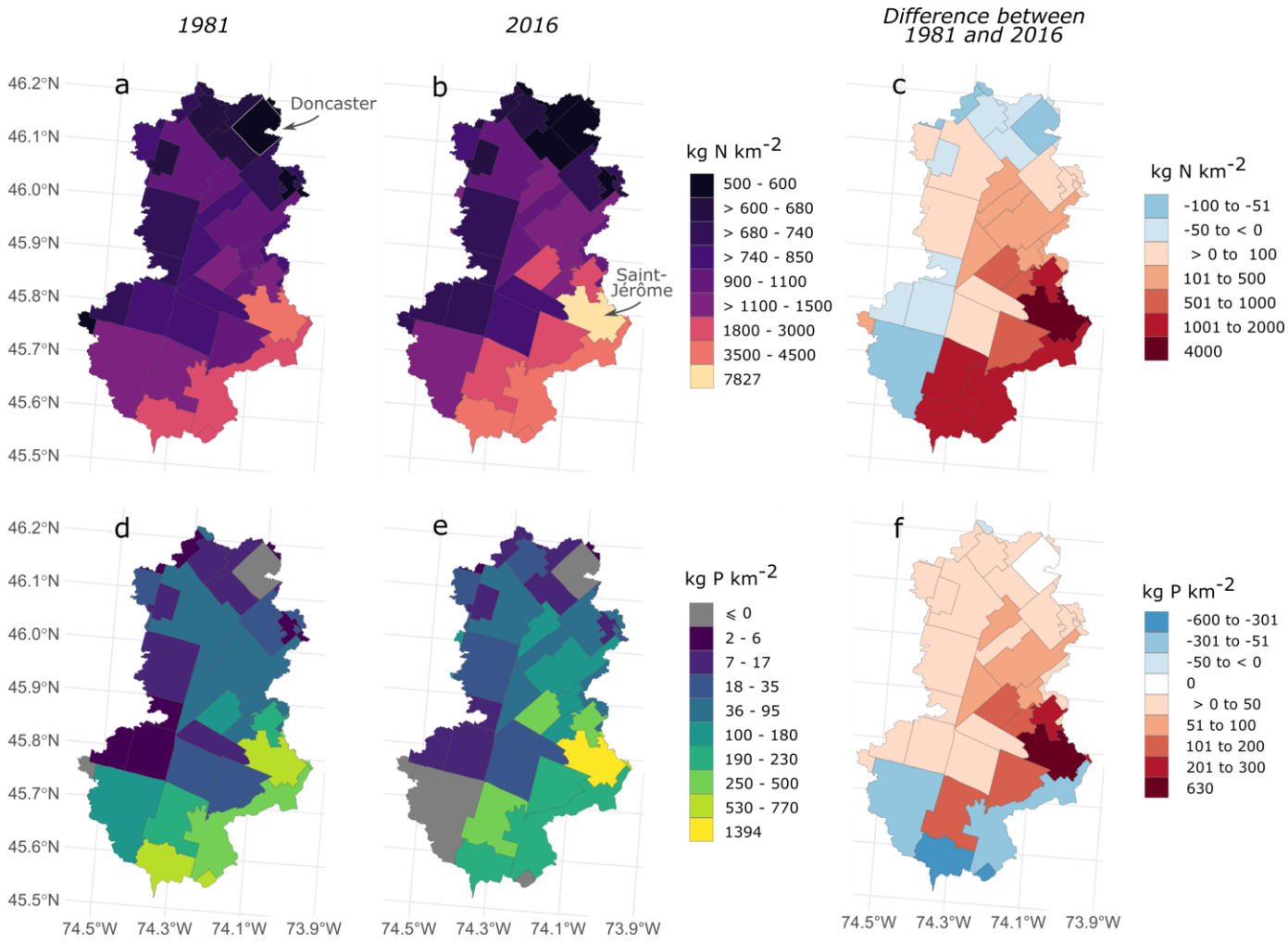

Figure 4 Six *Rivière du Nord* maps showing historical changes in Net Anthropogenic Nitrogen Inputs (top) and Net Anthropogenic Phosphorus Inputs (bottom). Panels a and b show the NANI for 1981 and 2016, respectively. The legend bar to the right of panel b is log-transformed. Panel c shows the difference between both years, where municipalities in red represent an increase from 1981 to 2016, and in blue represent a decrease. Panels d and e are the equivalent of a and b but for NAPI, where municipalities in grey represent a net export of P (negative values). Panel f shows the difference between both years, where municipalities in white represent no change from 1981 to 2016.

NANI & NAPI land use categories

The clustering analysis identified three groups of municipalities that had similar temporal changes in the different terms involved in the NANI and NAPI calculations (Supplemental Fig. S2), which

roughly correspond to those that were "forested", "urban", and "agricultural". In all clusters, NANI (kg-N km^{-2} yr^{-1}) increased at a higher rate than NAPI (kg-P km^{-2} yr^{-1}), urban and agricultural municipalities had a higher rate of N increase than forested municipalities, and NAPI tended to decrease over time in the cluster of agricultural municipalities (Table 1).

Table 1 Rate of change in total N and P inputs from 1981 to 2016 for clustered forested, urban, agricultural municipalities, and ratio of the change between those NANI and NAPI rates.

	Forested	Urban	Agricultural
NANI (kg km^{-2} yr^{-1})	0.41	24.5	29.9
NAPI (kg km^{-2} yr^{-1})	0.15	4.4	-4.7
NANI: NAPI	9.2	5.2	4.5

Total NANI and NAPI budgets were strongly influenced by the dominant human land use category that emerged from the clustering, and these were in turn influenced differentially by the specific input terms (Fig. 5). For forested municipalities, 92 ± 7.8% of the total N budget consisted of atmospheric N deposition, which remained constant through the decades (range = 586 to 782 kg km^{-2}) with a peak of 782 kg km^{-2} in 2001. For urban municipalities, human consumption (variable in eq. 3) surpassed atmospheric deposition after 2001 and dominated the total N budget with 54 ± 11.2% in 2016. Human consumption was also the most important category for the P budgets in the urban municipalities (77 ± 7.1% in 1981 to 94 ± 7.3% in 2016). Agricultural municipalities were dominated by crop yield and fertiliser inputs for both N and P budgets (Fig. 5), for which we observed large variability.

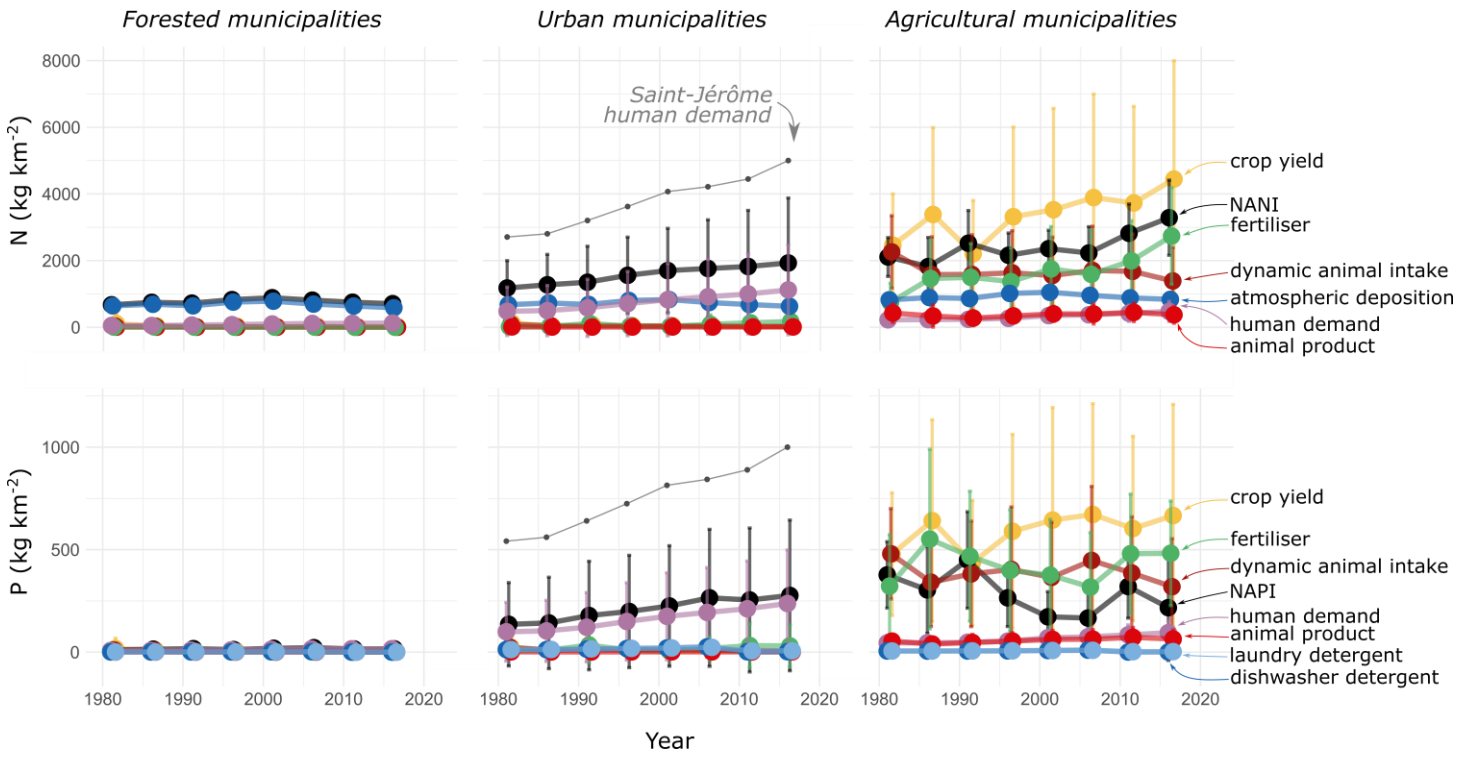

Figure 5 Categories of Net Anthropogenic Nitrogen (N) Inputs (top) and Net Anthropogenic Phosphorus (P) Inputs (bottom) per census year from 1981 to 2016 in kg N or P km^{-2}. NANI categories include overall NANI (black), crop yield (yellow), animal product (red), fertiliser (green), dynamic animal intake (crimson), atmospheric N deposition (dark blue) and human consumption (purple). NAPI categories include overall NAPI (black), detergents for laundry (light blue) and dishwashers (dark blue). Values represent mean and standard deviations for grouped municipalities according to the cluster analysis (Supplementary Fig. S2). Panels are named following the municipalities' broad LULC geographic locations (Fig. 1). The grey dots in the urban (middle) panels show the human consumption specifically for the municipality of *Saint-Jérôme* (but are also included in the average of human consumption (purple)) to emphasize the importance of this specific NANI and NAPI category in more densely populated urban areas.

Relationship between landscape inputs and riverine loads

There were large differences between N and P trends, both in terms of anthropogenic landscape inputs and riverine loads (Fig. 6). For the most upstream site draining mostly forested landscape, RKm 101, neither NANI (mean = 896, sd = 65 kg km^{-2}) nor NAPI (mean = 57, sd = 7 kg km^{-2}) increased significantly through the years, and TN riverine loads remained rather constant (mean = 305, sd = 20 kg km^{-2}) whereas TP loads dropped by more than half, from 35 ± 14 kg P km^{-2} in 1981 to 13 ± 5 kg P km^{-2} in 2016.

For the two downstream sites, RKms 58 and 4, there was a strong linear relationship between NANI and TN riverine loads ($p < 0.001$, $R^2 = 0.59$). In contrast, while NAPI increased (from 117 to 178 kg km^{-2} at RKm 58, and 122 to 145 kg km^{-2} at RKm 4), riverine TP loads decreased by almost half in both sites (52 to 33 kg P km^{-2}).

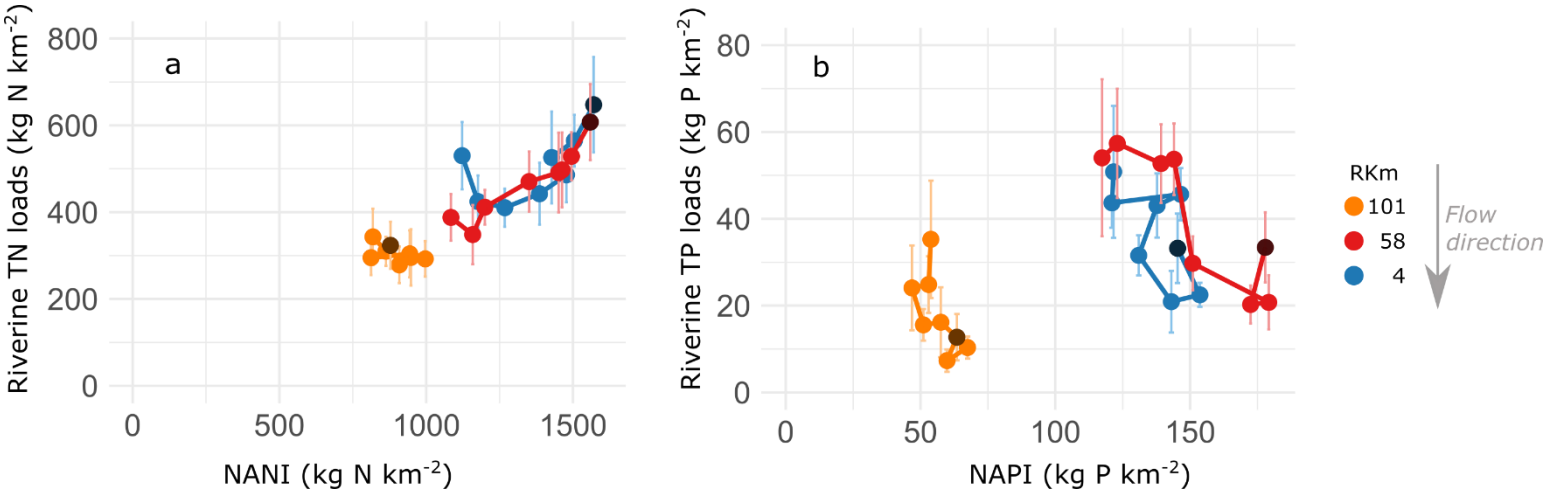

Figure 6 Riverine loads of TN (a) and TP (b) versus Net Anthropogenic Nitrogen and Phosphorus Inputs (NANI and NAPI). Yellow, red and blue colours represent sites at RKm 101, 58, and 4. The eight census years appear linked in chronological order, the darker circles representing the last census year, 2016. Riverine loads represent a 5 year mean around the focal census year, with vertical bars as the standard deviation.

Fractional export and historical stoichiometry

On average, for the last 40 years, the fractional export of NANI to riverine TN loads has been relatively stable (37 ± 5%, Fig. 7a), suggesting that just over a third of the yearly net human inputs on land were exported towards the river. P, however, was more variable. The fractional export of NAPI decreased from 31% in 1996 to 15% in both 2006 and 2011, then increased again in 2016 (23%), resulting in an overall average and standard deviation of 27 ± 10%.

To quantify how, once in the water, N and P varied with respect to C and to each other, we plotted C: P, C: N, and N: P molar ratios of loads across years (Fig. 7b). C: N had the least variation (7.2 ± 1.4) and ranged from 10.6 (in 1991) to 4.7 (in 2013), supporting N-enrichment over time. C: P varied more (251 ± 112), ranging from a low of 109 (in 1979) to a high of 554 (in 2008), largely as a function of P removal, whereas N: P (36 ± 17) ranged from 17 (in 1992) to 87 (in 2007) both as a function of decreased P and increased N. From 1980 to 2020, C: N: P exports shifted from 130: 23: 1 to 217: 44: 1, with a C and N peak in 2007-2008 of 554: 87: 1. The decline in N: P and C: P ratios after 2008 appears to largely be driven by an increase in P entering the river over the last 15 years (Fig. 2c), that was not fully explained by changes in NAPI.

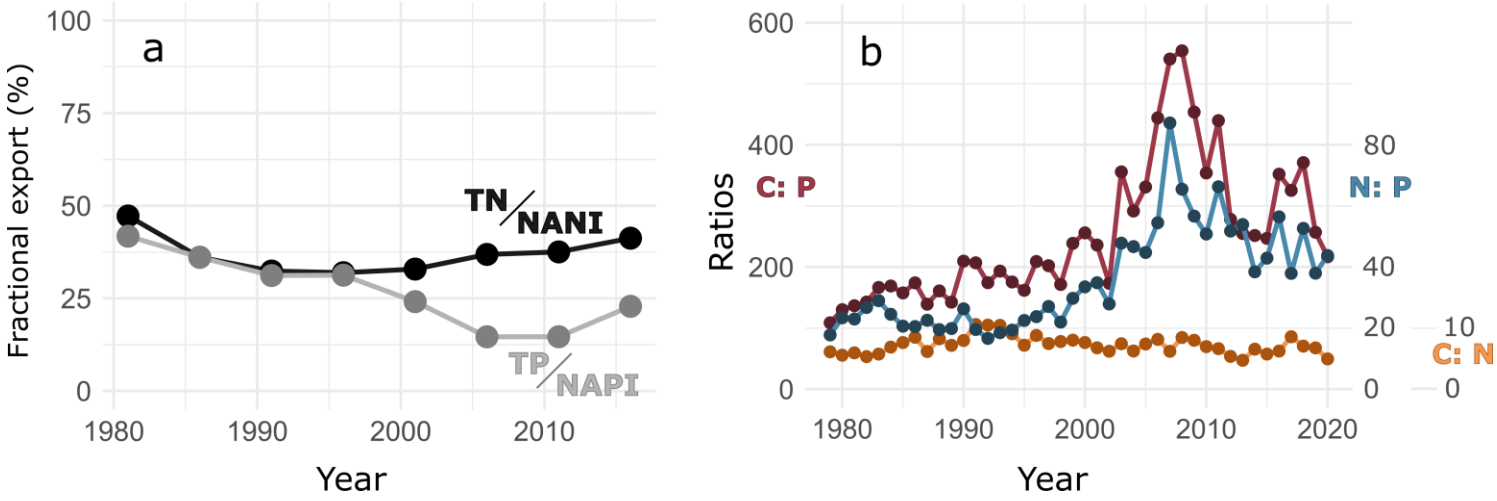

Figure 7 Panel a shows the fractional export (%) of NANI and NAPI observed in TN and TP riverine loads, respectively (kg N or P km^{-2}), across years for the most downstream site. Panel b shows molar C: P, N: P, and C: N ratios for riverine loads across years at the same site, RKm 4. All ratios have their own scale, with the left y-axis showing the scale for C: P (0 – 600), and the two right ones showing the scales for N: P (0 – 80) and C: N (0 – 10).

Discussion

In this study, we found that changes in annual precipitation and in anthropogenic nutrient inputs to land differentially affected the long-term trends in riverine loads of C, N and P of a north temperate river, with cascading effects on their stoichiometry at the ecosystem level. Among the three elements in this study, C was the most strongly influenced by climate induced precipitation patterns, with more than half of the inter-decadal variation in riverine loads being explained by mean annual precipitation

(Fig. 3). The long-term trends in C loads might reflect some level of hydrologically driven browning (de Wit et al., 2016), as atmospheric deposition of sulfur had a non-significant effect on the observed DOC increases ($p = 0.34$), but there was no obvious increasing precipitation trend (Supplementary Fig. S4a), only inter-annual variability. The increasing DOC concentrations observed in the last fifteen years could be the result of higher runoff (Supplementary Fig. S4e) likely caused by more impervious surfaces as a result of urban expansion, or by increased autochthonous production due to higher nutrient inputs. Precipitation (as well as runoff) also explained almost half the variation in riverine N loads. This was expected at the most upstream site (forested RKm 101), as hydrology is a strong driver of N losses in more forested catchments (Mitchell et al., 1996; Inamdar et al., 2015). The weaker correlation with precipitation and N loads in the two most downstream sites (urban RKm 58 and mixed-land use RKm 4), however, suggests an influence of sources other than natural soil exports. Lastly, P loads were not explained by precipitation at any site, implying that other factors were driving the patterns seen here.

Historical changes in N loads within a single watershed were strongly and positively correlated with anthropogenic N inputs to the watershed (Fig. 6; for both urban RKm 58 and mixed-land use RKm 4, Supplementary Table 4). The linear relationship between inputs to land and riverine loads implies that the fractional export of anthropogenic N sources exported to the river has varied little over time (Fig. 7a). As such, any change in watershed NANI will be reflected in the water, and to reduce this transfer, the source of the inputs should be identified – which this approach permits – and subsequently regulated. Notwithstanding the 54 kilometers that separate the two downstream sites (Fig. 1), the similarity in their loads could suggest that the N exported from RKm 58 was largely reflected in the patterns observed at RKm 4 with no meaningful inputs in between, diffuse or point. Across years, N loads at both sites (493 ± 108 kg km^{-2} yr^{-1}) resembled those in urbanised catchments (lowest from literature ~ 650 kg km^{-2} yr^{-1}; Groffman et al., 2004; Kaushal et al., 2006, 2011; Han et al., 2009) rather than agricultural and highly developed ones (> ~ 3000 kg km^{-2} yr^{-1}; McIsaac & Hu, 2004; Hong et al., 2013; Chen et al., 2016). Dissolved inorganic N loads and NANI were also correlated historically in the Yangtze River in China, where population density largely explained the relationship (Chen et al., 2016). Similarly, the *Rivière du Nord* TN-NANI relationship could be more related to municipalities that fall into the urban categories, which have increased over the course of our evaluation period, and for which highly populated towns have surpassed the NANI of municipalities classed as agricultural (Fig. 5). Furthermore, given the topography of the river, that section actually receives limited inputs from the surrounding agricultural lands as the mainstem flows along the divide

of the geological provinces. A tributary with some agricultural activities enters at RKm 19 that may have somewhat replenished what may have been consumed between the wastewater inputs from the urbanised area of *Saint-Jérôme*. Regardless, we suggest that wastewater dominated the N inputs in that river reach as the most significant agricultural tributary only entered at RKm 2 (Fig. 1) and was not captured in this monitoring program.

While the pattern in N loads at the upstream site (forested RKm 101) could be resolved in part by precipitation (Fig. 3), our measured loads were higher than reports from other undisturbed catchments (Howarth et al., 1996; Lewis, 2002). Atmospheric N deposition, known to influence the amount of N found in streams of forested catchments (Aber et al., 2003), was the dominant NANI input in the more forested municipalities, where our estimated inputs were higher than in other undisturbed sites (280 kg km^{-2}; Lewis, 2002). Furthermore, many of our more forested catchments had some level of urbanisation, either as small towns or through cottage development. Even low levels of urbanisation has been shown to influence aquatic N concentrations (Charrier Tremblay et al., 2020), and proximity of N sources (towns, septic tanks) to the mainstem may influence our overall N loads (Alexander et al., 2000; Kaushal et al., 2011). As roughly two-thirds of the population in the studied river catchment are served by septic tanks and most of the small towns were historically established along the mainstem (Allard & Painchaud-Francoeur, 2017), these N sources, along with high atmospheric deposition, may explain the higher loads observed at forested site RKm 101.

Unlike N, riverine TP and NAPI were negatively correlated at all three sites, suggesting a decoupling in the inputs and loads at the watershed scale. A recent study in the Yangtze showed that an increase in the number of dams led to a decrease in TP loads because of higher sediment interception (Hu et al., 2020). As such, management choices result in the creation of nutrient retention control points that influence riverine loads. Following government-subsidised construction of WWTPs in the 1990s and legislation of septic tank (MTESS, 2021a; MELCC, 2022b), TP loads have decreased by half from 2000 to 2010, from 76 533 ± 16 445 kg yr^{-1} to 32 795 ± 7 390 kg yr^{-1} at RKm 58, and the *Saint-Jérôme* WWTP alone (location on Supplementary Fig. S3 map) could account for up to 24 276 ± 5 230 kg yr^{-1} of this phosphorus (72% of the total reaching its intake; 2017 – 2020 average).

Despite the precipitous drop in riverine TP at the turn of the century, a recent increase in loads has been observed. This is apparently not due to an increase in anthropogenic inputs as NAPI did not significantly increase at either downstream site since 2006 (Fig. 6b), nor should it be legacy effects (Goyette et al., 2018) as the only major agricultural tributary merged downstream of RKm 4. But as

the NAPI fractional export increased in recent years (Fig. 7b), other factors likely explain this increase. Flashiness of precipitation has been shown to favour P transport across multiple watersheds in the broader region (Goyette et al., 2019), but flashiness was not observed in this particular system (Supplementary Fig. S4d, f). Rather, an increase in runoff quantified as the ratio between annual discharge to annual precipitation at *Saint-Jérôme*, increased 1.5-fold from a 1980 – 2000 average to 2010 – 2020 (Supplementary Fig. S4e) and could explain this recently observed increase in riverine TP. Impervious surfaces are known to increase delivery of P to surface waters (Hobbie et al., 2017; Müller et al., 2020), and stormwater runoff often leads to higher P concentrations (Yang & Toor, 2018). Although there is no clear linear trend between TP loads and runoff (Supplementary Fig. S4g), as both increased in the last 10 years, we suggest changes in delivery pathways through human modification have led to the recent increases observed in riverine TP, in our downstream more urbanised sites.

Overall, the large variability captured in ecosystem stoichiometry of a single river was a function of the interannual variability of forty years of precipitation, land use intensification, and management strategies. Human activities on land largely dominated the effects of natural drivers, leading to differential loading rates to the *Rivière du Nord*, with varying consequences on ecosystem stoichiometry over time. Other studies of ecosystem stoichiometry also recorded variability, albeit for different reasons. A global synthesis of U.S. rivers found a spatial stoichiometric range of 374: 24: 1 (terrestrial exports) to 238: 24: 1 (freshwater loads) with differential rates of losses of all elements along the freshwater continuum, which the authors linked to differential retention (Maranger et al., 2018). Another synthesis of comparative land use types reported ranges of 2123: 59: 1 (forested waters) to 267: 53: 1 (agricultural waters), where differences in ratios were linked to nutrient inputs (Stutter et al., 2018). Here, C: N: P ranged from 130: 23: 1 in 1980 to 217: 44: 1 in 2020, with a peak of 554: 87: 1 in 2007-08 (Fig. 7b). The relatively stable C: N (7.2) ratio that we measured over time is coherent with the common effect of precipitation on both elements (Fig. 3), where the slight decrease in the ratio over time was primarily explained by an overall increase in NANI (Fig. 4). As a result, both C: P and N: P ratios followed an inverse U shape (Fig. 7b), whose peak matched the construction of the WWTP in *Saint-Jérôme*, but this is currently changing as a function of an increased runoff ratio, altering the delivery of P and C most notably, possibly as a function of urban expansion.

The watershed (spatial) and decadal (temporal) scales studied here showed that the balance between inputs, retention, and delivery for C, N, and P could be depicted though changes in historical ecosystem stoichiometry. Our results support that overall C riverine inputs from this temperate watershed are

largely a function of hydrologic variation in precipitation and runoff patterns, with limited influence from changes in land use over the past 40 years. Although hydrology also influenced riverine N, we argue that the strong link between riverine N loads and increasing anthropogenic inputs to land supports that human activities play a more significant role in these transfers. In the case of the impacted reach assessed in our ecosystem, increasing urbanisation and wastewater non-treated for N entering as point sources appear to be the most significant sources of NANI. As such, a decrease in riverine TN could be attained with specific N treatments in WWTP for this watershed (Rahimi et al., 2020), as was shown for P. NANI and NAPI has been a successful and simple tool used to help understand change in riverine loads at different scales for several decades (Howarth et al., 1996; Howarth et al., 2012), however NAPI was never as strong of a predictor as NANI. Our study shows that this may be a function of human interception of point source P pollution in watersheds where urban inputs dominate. Legislation and changes in wastewater treatment shown here dramatically decreased P and resulted in significantly higher N: P and C: P ratios. One of the challenges of not reducing N and maintaining high N: P ratios is that when nutrient concentrations are high, toxic cyanobacteria and other harmful algal blooms are favoured (Scott et al., 2013; Glibert et al., 2014). Furthermore, it creates conditions where excess N accrues along the aquatic continuum and is delivered to the coasts resulting in coastal degradation (Howarth, 2008; Paerl & Scott, 2010). As such, where possible, a dual nutrient removal strategy should be supported in systems where WWTPs are the main sources of N inputs (Paerl et al., 2004; Conley et al., 2009). However, the situation is much more complicated when sources of NAPI and NANI are diffuse. There, reduction in fertiliser use and landscape level restoration efforts including the construction of wetlands (Cheng et al., 2020) may be the most effective practices. Regardless, reducing inputs should always be the main strategy, as although ratios matter (Elser et al. 2022 PNAS), and provide valuable information on sources and transformations at the ecosystem scale (Maranger et al., 2018; Shousha et al., 2021), ratios need to be placed in the context of being in high or low nutrient systems.

Acknowledgements

We thank J.-O. Goyette for having passed on the knowledge of the Net Anthropogenic Nitrogen/Phosphorus Input models. Funding was supported by Natural Sciences and Engineering Research Council of Canada (NSERC) Discovery grants to J.-F.L. and R.M., and via a partial student

NSERC collaborative Research and Training Experience Program (CREATE) EcoLac scholarship to S.S.

Supporting Information

Precipitation and anthropogenic inputs drive decadal changes in carbon, nitrogen, and phosphorus riverine loads in a north temperate river

Stéphanie Shousha[1], Roxane Maranger[1], Jean-François Lapierre[1]

[1]Université de Montréal, Département de Sciences Biologiques, Montréal, QC, Canada. Groupe de Recherche Interuniversitaire en Limnologie (GRIL).

*Corresponding author : stephanie.shousha@umontreal.ca

Municipalities in Québec have merged an unmerged over the years. These changes in administrative borders needed to be taken into account when compiling NANI and NAPI. For example, in the *Rivière du Nord* watershed, today's *Saint-Jérôme* municipality is the result of a 2002 fusion between four municipalities: *Saint-Antoine, Bellefeuille, Lafontaine* and a smaller municipality also named *Saint-Jérôme*. If we were to compare the NANI or NAPI of the municipality named *Saint-Jérôme* in 2001 to the *Saint-Jérôme* NANI or NAPI in 2006, we would see an incommensurable step-wise increase in N and P budgets, because the 2006 *Saint-Jérôme* included three other municipalities not included in the 2001 *Saint-Jérôme*. To compare budgets prior to municipal merges to those of current municipalities, we summed the budgets of municipalities fated to merge. Of the 39 municipalities covering the *Rivière du Nord* watershed, 15 merged or unmerged during the 1981-2016 census years of interest. Supplementary Table 1 thus reports the complete historical description of municipalities that underwent territorial reorganisation in the watershed.

Supplementary Table 1 List of municipalities in the *Rivière du Nord* watershed that underwent a territorial reorganisation.

Mirabel	**Local Municipality**	**Year in which a reorganisation took place**	**Municipalities merged, and details when the reorganisation was not a merge (name change, municipality creation, surface area change, etc.)**
	Ville de Sainte-Scholastique	1971	A section of *Sainte-Thérèse-Ouest, Paroisse de Saint-Augustin, Village de Saint-Augustin, Paroisse de Saint-Benoît, Village de Saint-Benoît, Paroisse de Saint-Canut, Paroisse de Saint-Antoine-des-Laurentides, Paroisse de Saint-Hermas, Paroisse de Saint-Janvier-de-Blainville, Municipalité de Saint-Janvier-de-la-Croix, Paroisse de Saint-Jérusalem-d'Argenteuil, Paroisse de Sainte-Monique, Paroisse de Sainte-Scholastique,* and *Village de Sainte-Scholastique*
Deux-Montagnes	*Mirabel*	1973	Name change from *Ville de Sainte-Scholastique.*
Argenteuil	*Saint-Placide*	1994	*Village de Saint-Placide, Paroisse de Saint-Placide*
	Lachute	1966	*Lachute, Auersville*
	Brownsburg-Chatham	1999	*Brownsburg, Chatham*
Rivière du Nord	*Grenville*	2002	*Calumet, Canton de Grenville*

	Prévost	1973	*Lesage, Prévost, Shawbridge*
	Sainte-Sophie	2000	*Sainte-Sophie, Village de New Glasgow*
Matawinie	*Saint-Jérôme*	2002	*Lafontaine, Saint-Antoine, Bellefeuille, Saint-Jérôme*
	Entrelacs	1967	Name change from *Wexford*
	Chertsey	Nov. 1991	*Paroisse du Lac-Paré, Canton de Chertsey*
Laurentides		1994	*Saint-Calixte's Beaulac* sector (7 km²) is annexed to *Chertsey*
	Doncaster	1851	930 km²
		1853	64 km² given to Mohawk community
		1971	Revised to 79 km²
	Val-Morin	1922	Separates from *Sainte-Adèle*
	Saint-Faustin—Lac-Carré	1944	Name change from *Canton de Wolfe*
		1957	Separation: north part becomes *Lac Supérieur*, south part becomes *Saint-Faustin-Sud*
		1960	Name change from *Saint-Faustin-Sud* to *Saint-Faustin*
		Early 1996	*Saint-Faustin, Lac Carré*
	Lantier	1948	Separates from *Canton de Doncaster*
	Lac Supérieur	1957	Separates from *Saint-Faustin*
	Sainte-Lucie-des-Laurentides	1961	Name change from *Canton de Doncaster*
	Sainte-Agathe	1999	*Sainte-Agathe des Monts, Sainte-Agathe Sud*
		2002	*Sainte-Agathe, Saint-Agathe Nord*
Pays d'en Haut	*Ivry-sur-le-Lac*	From 27 Feb. 2002 to 1 Jan. 2006	Merged with *Saint-Agathe*
	Sainte-Anne-des-Lacs	1946	Separates from *Paroisse Saint-Sauveur*
	Wentworth-Nord	1958	Separates from *Wentworth*
	Sainte-Adèle	21 Nov. 1981	*Mont-Rolland, Mont-Gabriel*
		1997	*Mont-Rolland, Sainte-Adèle*
	Sainte-Marguerite	17 Oct. 2001 to 1 Jan. 2006	Merged with *Estérel*
	Estérel	17 Oct. 2001 to 1 Jan. 2006	Merged with *Sainte-Marguerite*
	Saint-Sauveur	2002	*Saint-Sauveur, Saint-Sauveur des Monts*

Supplementary Table 2 List of sources for coefficients used to calculate all categories in the NANI and NAPI models at the municipal level in Québec, Canada. Data from Population and Agricultural censuses also need to be downloaded to calculate the N and P budgets.

Model category	Source	Details
AGRICULTURAL CENSUS		
	Statistics Canada, 1982a, 1987a, 1992a, 1997a, 2002a, 2007a, 2012a, 2017a	
POPULATION CENSUS		
	Statistics Canada, 1982b, 1987b, 1992b, 1997b, 2002b, 2007b, 2012b, 2017b	
FERTILIZER		
	Statistics Canada, 2022d	Metric tonnes of N, P fertilizer at QC level (x1000).
	Statistics Canada, 2013	For 2006 and prior
	Russell et al., 2008	To transform P_2O_5 into P

LIVESTOCK SLAUGHTER		
Number slaughtered cattle, calves	Statistics Canada, 2022b	Number of cattle, calves slaughtered at the national level (Canada)
Number slaughtered hogs, sheep & lamb	Statistics Canada, 2022d	Number of hogs, sheep & lamb slaughtered at the national level (Canada)
Number slaughtered chicken, turkey	Government of Canada, 2021	Number of chicken, turkeys slaughtered at national level (Canada)
Number slaughtered livestock at provincial level	Census of agriculture > Livestock	Total heads cattle, calves, hogs, sheep, lamb, chicken, turkey at national level (Canada)
	Census of agriculture > Livestock	Total heads cattle, calves, hogs, sheep, lamb, chicken, turkey at provincial level (QC)
LIVESTOCK LIVE WEIGHT		
Weight cold carcass cattle, calves	Statistics Canada, 2022b	Average weight, cold carcass
Weight cold carcass hog, sheep & lamb	Statistics Canada, 2022d	Average weight, cold carcass
Conversion factor carcass to live	Government of Canada, 2022	Conversion factor from live weight to cold carcass
Weight live chicken, turkey	Statistics Canada, 2021a	Total kg for chickens, hens + number of heads
Weight live egg	Statistics Canada, 2021b	Egg number per head of layer
Weight live milk	FAO, 2021	Kg of milk produced per cow
EDIBLE PORTION		
Edible portion of animals as % of live weight	Han et al., 2009	What we can eat of the animal
NP CONTENT		
N content	Han et al., 2009	What % of the edible portion is N
	personal communication with JOG	N % for pork, chicken, broiler (all 3.648)
P content	Goyette et al., 2016	What % of the edible portion is P
ANIMAL INTAKE		
Consumtion rates N	Han & Allan, 2008	Consumption rates of N for livestock under dynamic model
Consumtion rates P	Han et al., 2011	Consumption rates of P for livestock under dynamic model
Life cycle (days alive per year)	Han et al., 2009	Duration of livestock life on farm (usually less than 1 year)
	Kellogg et al., 2000	" "
	Goyette et al., 2016	" "
Equations to calculate dynamic life cycle	Goyette et al., 2016 Kellogg et al., 2000 Han et al., 2009	
CROP YIELD		
Provincial yield for certain crops	Statistics Canada, 2022b	Crop yields at provincial level because not found at smaller scale
Provincial yield for potatoes	Statistics Canada, 2022a	Crop yield at prov level for potatoes
	https://www.potatopro.com/quebec/potato-statistics	PotatoPro!
Administrative region crop yield	Institut de la statistique du Québec, 2020	Crop yield at admin level for big cultures
		For the provincial yield, if had no data for region, used average of all instead. Used the provincial average for the following crops to build in missing regional data:

		For Fodder corn: Saguenay, Abitibi, Côte-Nord, Nord-du-Québec For Grain corn : Bas-Saint-Laurent,Abitibi,Nord-du-Québec,Gaspésie For Barley: Estrie,Outaouais, Laurentides For Soya : Bas-Saint-Laurent,Gaspésie,Abitibi,Nord-du-Québec For Oats : Montréal,Laval,Lanaudière,Montérégie For mixed grains : Capitale-Nationale, Mauricie, Montréal, Laval, Lanaudière, Outouais, Laurentides, Abitibi, Nord-du-Québec, Montérégie
Understanding agricultural regions in QC	Statistics Canada, 2021	Codes for each region (not to mix up with administrative codes, they're a little different)
CROP CONTENT		
Kilograms harvested per yield unit (nitrogen)	USDA, 2017	USDA Natural Resources Conservation Service, Technical Resources
Percent Dry Matter, Percent N in Dry Matter (nitrogen)	USDA, 2017	USDA Natural Resources Conservation Service, Technical Resources
Percent N in Dry Matter for Corn grain : updated (nitrogen)	David et al., 2010	% protein in modern corn hybrids is decreasing continuously (from 10 to 8.5% from 1985 to 2006). Assumed 1.36% N for 2006 (assumption: use 2006 data for today too). Toolbox assumes 9.5% protein = 1.5% N (average between 1985 - 2006).
N content for cropland and non cropland pastures (nitrogen)	Hong & Swaney, 2010 (Table 5.1.1.1)	
P content in crops	MacDonald & Bennett, 2009	P content in crop types (kg / kg of crop)
P content for cropland and non cropland pastures	Schaefer & Alber, 2007	P content for pastures
DISTRIBUTION		
% distributed to humans and animals	Boyer et al., 2002	Partition crop yields to humans and animals
	Jordan & Weller, 1996	
% of crop lost during harvest	Boyer et al., 2002	Losses of crops during harvest
		Missing rice and buckwheat for distribution and loss: For buckwheat, in Yieldbased BNF, buckwheat column notes are in red (10% loss and 90% to humans)
	Swaney et al., 2018 (Toolbox v3)	pasture loss : take half leave half
BIOLOGICAL NITROGEN FIXATION		
Yield based for soybean, alfalfa, non-alfalfa	Han & Allan, 2008	Table 4 : proportion of plant N from fixation
Nonalfalfa have 25% leguminous plants	USDA, 2007	Alfalfa fixes nitrogen. Legumes (in non-alfalfa plants) are the ones that fix nitrogen in the non-alfalfa pastures. So, include the legumes from nonalfalfa that fix nitrogen in calculation.
Cropland, area-based	Jordan & Weller, 1996	Named non-wooded pastures, east of Mississippi, eastern pastures
Snap beans, area-based	Boyer et al., 2002 cites Westerman et al. (Agronomy journal) 1981 which is unavailable	
Peanuts, area-based	Jordan & Weller, 1996	They have 86 kg N / ha / yr

	Schaefer & Alber, 2007	They have 8000 kg N / km2 / yr
PROTEIN CONSUMPTION		
Amount of protein consumed per capita, recent average	Hong & Swaney, 2010 (Toolbox 3.1)	6.21 kg / person / yr is data in toolbox. It's an average, and does not say from what years. Only says that data comes from US censuses.
N content in protein	Jones, 1941	N is 16% of protein
	Hong et al., 2012	Conversion factor used in NANI-PI
P content in protein	Hong et al., 2012	P consumption is equivalent to 20% N consumption
	Russell et al., 2008	Don't clearly state in article that N:P is 5, so ref is here because Hong et al., 2012 based themselves off Russel et al., 2008 to calculate N:P of 5
DETERGENT		
For laundry detergent :		
Laundry detergent (kg / capita / yr)	Han et al., 2012	Laundry detergent use (USA proxy because unavailable for Canada)
% of P by weight	Litke, 1999	Detergent industry limits phosphate in detergents to 8.7% by weight as phosphorus in 1970 and to 2.2% in 1972 in Canada (for LAUNDRY)
	Government of Canada, 2019	Limit goes down to 0.5% in 2009 + when click to see previous versions, find the 2.2% limit website last up to date 2019, so use values there for most recent year
For dishwasher detergent :		
Detergent use (Spoons / capita / yr)	Han et al., 2012	dishwasher detergent use
	Goyette et al., 2016	dishwasher detergent use
P content (kg P / spoons)	Han et al., 2012	Has kg P per spoon (0.0009687). Assume this is when limit is at 8.7% P content because in same time range of reglementations (read Litke 1999)
	Government of Canada, 2019	Limit goes down to 0.5% in 2009
		Rule of 3 : if 0.0009687 is for 8.7, what is kg-P for 0.5% (limit of 2.2% in the 1970s only for laundry)
Proportion of households with automatic washers	Goyette et al., 2016	Proportion of households with dishwasher
	Statistics Canada, 2017c	We are looking for DISHWASHER information.
		Calculate trendline for 1997-2009 and get proportion for 2011, 2016 (for Canada) but QC trend unclear for estimation. Spent 40min on the phone with stats can to have updated information, but not available. Got person on the line to send email to analysts. Info does not exist 17-07-2019.
P dishwashing detergent cosumption (kg P / capita / yr)	Equation	= dishwashing detergent use * P content * Proportion of households
ATMOSPHERIC DEPOSITION		
N deposition	www.cmaq-model.org/	Community Multiscale Air Quality model for 2008 (usually kg-N / km²) Used NH_y and NO_x deposition because of small surface areas of municipalities and discrete land use (Dentener & Crutzen, 1994; Boyer et al., 2002).

N emissions, historical	Government of Canada, 2018		Air Pollutant and Black Carbon Emissions Inventories online search (1990 – 2020).
	Asadoorian et al., 2006		Emission trends (Tg) 1890 – 1995.

Supplementary Table 3 Example of loadflex model fit for the three sites along the *Rivière du Nord* mainstem, RKms 4, 58, 101. The best models were chosen for their lowest RRMSE and ARIL. They are in bold and are the ones that were used to interpolate concentration predictions for the years of interest, 1980-2020.

RKm	Variable	Years spanned by data	Model	RRMSE	ARIL
4	TN	1985-2020	interpolation	0	1.1492
			linear model	0.3943	1.3169
			loadReg	0.3389	1.1090
			composite	**0.0006**	**1.1051**
	TP	1979-2020	interpolation	0	2.8505
			linear model	0.9759	3.0094
			loadReg	0.6406	2.1455
			composite	**0.0002**	**1.8968**
	NO_3^-	1979-2020	interpolation	0	1.7262
			linear model	0.7006	2.1615
			loadReg	0.5748	1.5745
			composite	**0.0004**	**1.4519**
	TDP	1979-2009, 2016-2020	interpolation	0	4.5311
			linear model	2.4690	5.9178
			loadReg	1.7205	4.4103
			composite	**0.0008**	**2.6051**
	DOC	1984-1990, 1993-2020	**interpolation***	**0**	**0.7636**
			linear model	2.3623	1.2422
			loadReg	2.1029	1.0697
			composite	0.0002	1.1518
58	TN	1985-1986, 1988-2020	interpolation	0	1.2653
			linear model	0.3298	1.1935
			loadReg	0.2736	0.9943
			composite	**0.0009**	**1.0342**
	TP	1979-1986, 1988-2020	interpolation	0	3.2604
			linear model	1.2368	3.7891
			loadReg	0.8605	2.4154
			composite	**0.0007**	**1.8788**
	NO_3^-	1979-1986, 1988-2020	interpolation	0	2.5651
			linear model	3.5660	4.3018
			loadReg	2.0293	2.9024
			composite	**0.0002**	**2.0617**
	TDP	1979-1986,1988-2009, 2016-2020	interpolation	0	8.2942
			linear model	2.3595	6.8395
			loadReg	1.6016	4.9448
			composite	0.0014	2.6148
	DOC	1984-1986, 1988-1990, 1993-2020	**interpolation**	**0**	**0.70633**
			linear model	0.2179	0.7174
			loadReg	0.1931	0.6003
			composite	0.0001	0.7288
101	TN	1985-1986, 1988-2020	interpolation	0	1.2745
			linear model	0.2708	1.1115
			loadReg	0.2176	0.8988
			composite	**0.0003**	**0.9723**
	TP	1979-1986, 1988-2020	interpolation	0	6.0454
			linear model	1.9940	5.5106
			loadReg	0.9638	2.8503

		composite	**0.0002**	**2.4020**
NO_3^-	1979-1986, 1988-2020	interpolation	0	1.1121
		linear model	0.4419	1.6230
		loadReg	0.2769	0.9850
		composite	**0.0003**	**0.9967**
TDP	1979-1986,1988-2009,	interpolation	0	9.9774
	2016-2020	linear model	3.3331	9.2055
		loadReg	1.1510	4.4743
		composite	**0.0008**	**2.9761**
DOC	1984-1986, 1988-1990,	interpolation	0	0.6890
	1993-2020	linear model	0.1957	0.7490
		loadReg	0.1379	0.5257
		composite	**0.0003**	**0.5913**

RRMSE : relative root mean square error, ARIL : average of the relative 95% prediction interval lengths (Appling et al 2015). Variable acronyms refer to total nitrogen (TN), total phosphorus (TP), nitrate (NO_3^-), total dissolved phosphorus (TDP), and dissolved organic carbon (DOC).

Supplementary Table 4 multiple linear regressions (TN riverine load ~ NANI + precipitation) to determine the relative strength of each predictor variable.

Dataframe structure	RKm	p-value		R^2	lmg*	
5 yr mean around focal census year for both riverine loads and precipitation (8 observations)	5 & 41	NANI	< 0.001	0.59	NANI	0.58
		Precip	0.91		Precip	0.01
	80	NANI	0.2	0.29	NANI	0.27
		Precip	0.7		Precip	0.02
Interpolation of missing years for NANI** (40 observations)	5 & 41	NANI	< 0.001	0.60	NANI	0.33
		Precip	< 0.001		Precip	0.27
	80	NANI	0.72	0.72	NANI	0.02
		Precip	0.02		Precip	0.70

* Relative importance metric (one of the outputs of relaimpo)
** Done using linear regressions for RKms 5 and 41 (NANI ~ Year), and a quadratic for RKm 80 (NANI ~ Year + Year^2). Equations were:
RKm 5: y = 12.736x – 24085.4, p-value < 0.0001, R^2 0.93
RKm 41 : y = 14.036x – 26705.7, p-value < 0.0001, R^2 0.95
RKm 80 (linear): y = 2.63x – 4363.3, p-value = 0.2, R^2 0.24
RKm 80 (quadratic): y = -0.3177x^2 + 1272x – 1273000, p-value x = 0.08, p-value x^2 = 0.08, R^2 0.60

There are multiple ways to compare the relative strength of predictor variables. However, each variable to compare contains a different number of observations. Precipitation has one observation per year (40 years) while NANI or NAPI only has 8 observations. To combine both predictor variables in the same model, we either interpolated the missing data for NANI-NAPI or averaged 5 years around the focal census year for both riverine loads and precipitation. Supplementary Table 4 summarises the outputs of the multiple linear regressions for both new data frames (5yr vs interpolation). The RKm sites 5 and 41 were combined as they were in the manuscript. Using the relaimpo function in R (Grömping, 2006) on the outputs of the multiple linear regression models, we

determined the relative contribution of each predictor variable to the R2. In the 5yr data frame, anthropogenic N inputs to land for RKms 5 & 41 explained the majority of the variation in riverine loads (0.58 of a 0.59 R^2). Although both predictor variables explained less of the variation at RKm 80, NANI was still better than precipitation (0.27 of 0.29 R^2). However, NANI only explained 0.33 of a 0.60 R^2 at RKms 5 & 41 when the data were interpolated to match the original riverine loads and precipitation, and 0.02 of a 0.72 R^2 at RKm 80.

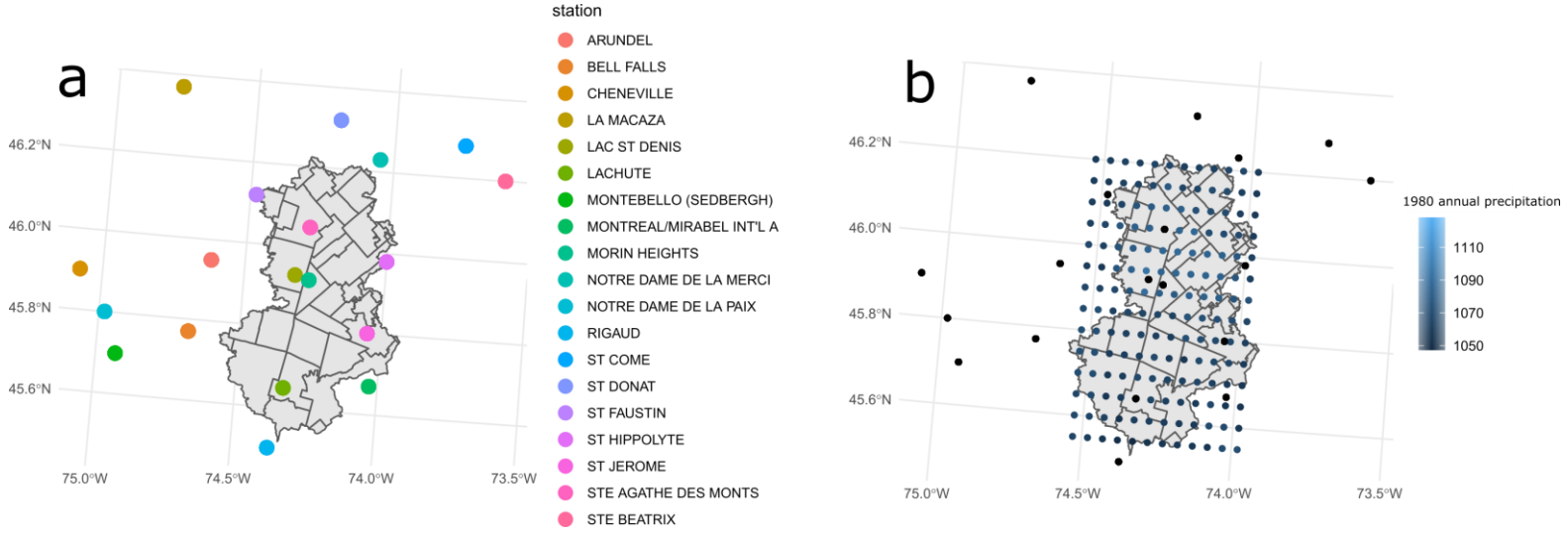

Supplementary Figure S1 a) Location of 19 stations where historical precipitation data is recorded, compared to the *Rivière du Nord* watershed and b) Inverse Distance Weighting interpolation for 1980. The geospatial interpolation is shown with a resolution of 0.05 degrees for visual representation purposes, but the actual data were interpolated using a 0.01 degree resolution.

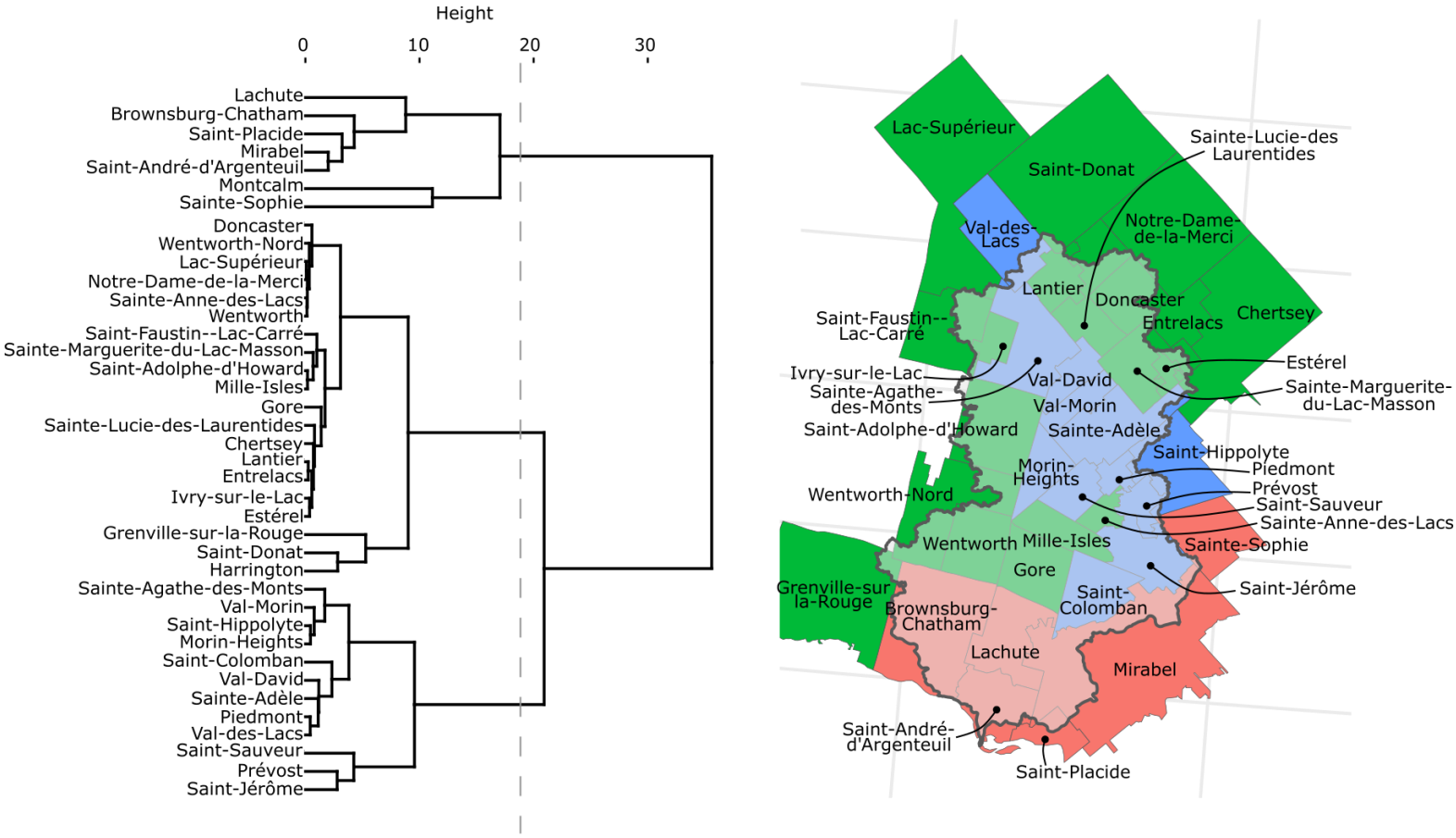

Supplementary Figure S2 On the left, dendrogram resulting from hierarchical agglomerative clustering, using Euclidean distances on scaled data, and ward.D2 as linkage method. The data used to cluster the municipalities were all the categories from the Net Anthropogenic Nitrogen Input (NANI) model. On the right, map of the *Rivière du Nord* watershed and underlying municipalities, coloured according to cluster, and identified. The dotted line helps separate clusters.

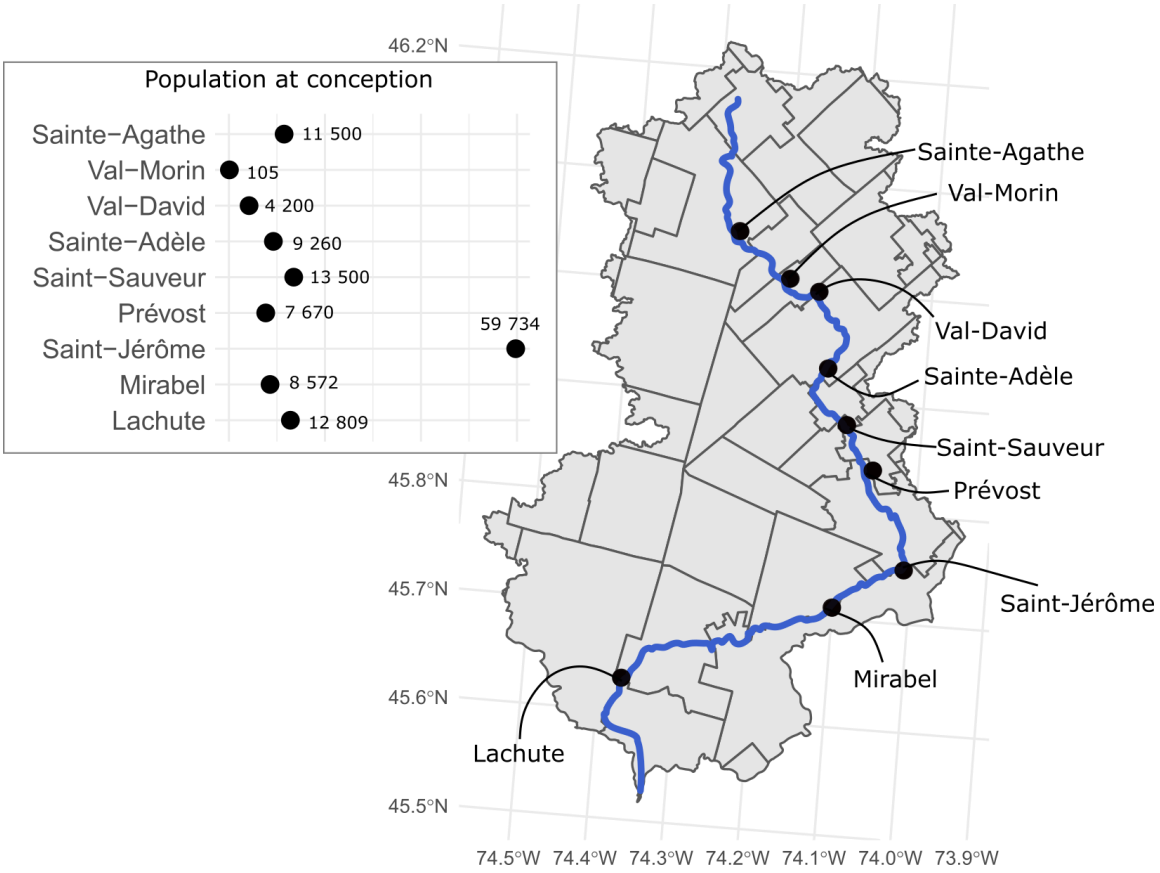

Supplementary Figure S3 Location of wastewater treatment plants in the *Rivière du Nord* watershed with their associated population in the year of conception.

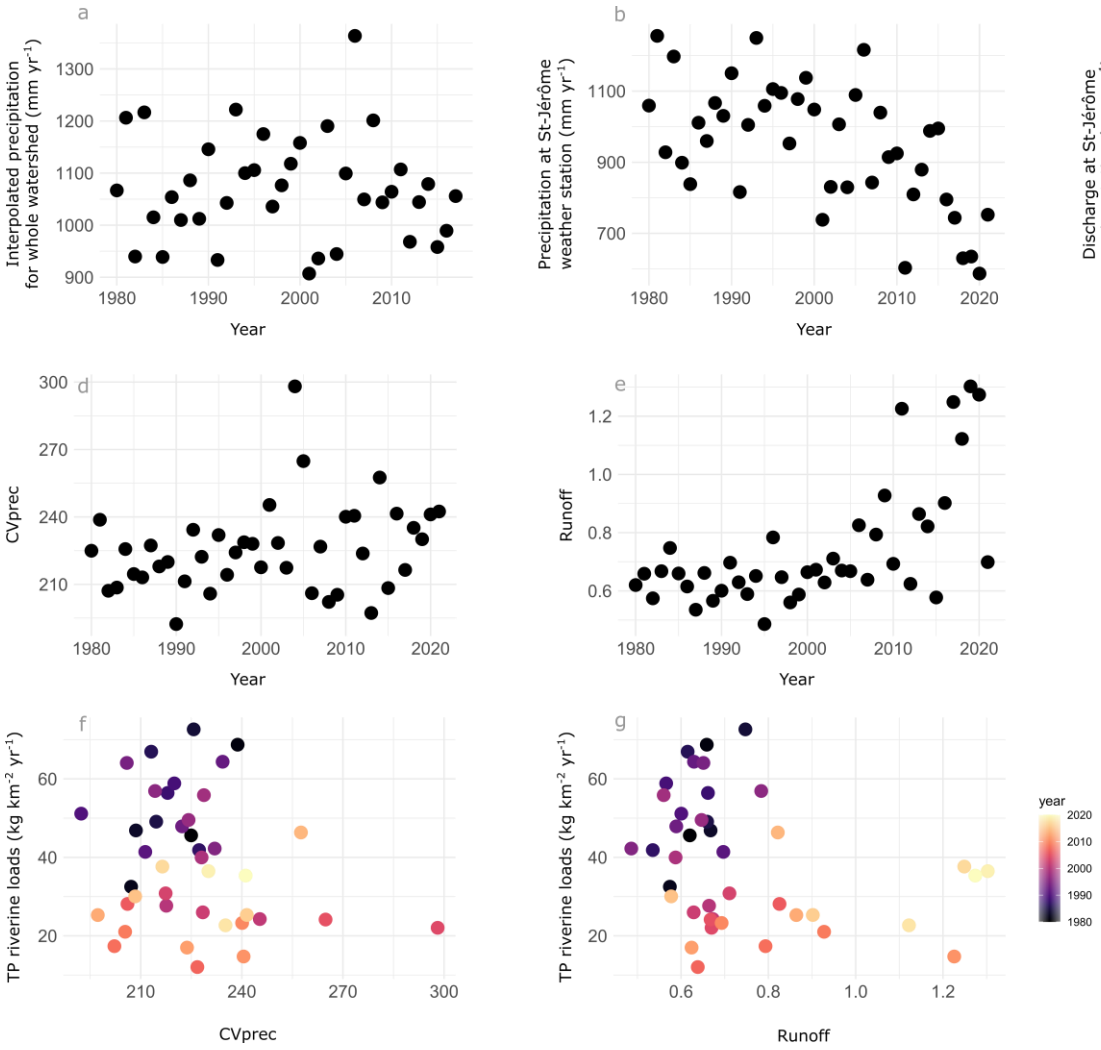

Supplementary Figure S4 Can TP loads (kg km $^{-2}$ yr^{-1}) be explained by hydrological regimes? Panel a and b show precipitation (rain and snow) for each year at the watershed level (interpolated) and at the specific *Saint-Jérôme* weather station. Panel c shows discharge at the *Saint-Jérôme* gauging station. We use CV_{prec} as a proxy for flashiness, with the intent that if a year had a larger coefficient of variation (CV) for its total precipitation, that year had flashier precipitation. Panel e shows that runoff (annual discharge over annual precipitation) has increased in the last 10 years. Panels f and g show no clear relationship between TP riverine loads (at RKm 58, the closest to *Saint-Jérôme*) and flashiness or runoff.

Conclusion générale

Ma thèse avait pour but commun de réunir quatre aspects clés des rivières et des pressions naturelles et anthropiques auxquelles elles sont sujettes sous une approche intégrative au niveau du bassin versant. L'utilisation de la stœchiométrie écosystémique et des formes de C, N, et P selon des gradients climatiques et d'utilisation du territoire dans une même rivière a permis d'unir les connaissances entourant les apports et les pertes des éléments, et de départager l'importance relative des facteurs naturels et anthropiques qui les influencent différentiellement. Il en ressort un patron général où l'activité humaine, spatiale ou historique, éclipse les effets de rétention au niveau de la stœchiométrie écosystémique. Par contre, selon les potentiels de transformation, les formes maintiennent toutefois une certaine variabilité stœchiométrique inter-saisonnière et offrent un aperçu des sources qui contribuent le plus à la stœchiométrie générale des rivières. La Figure 1 résume ces résultats.

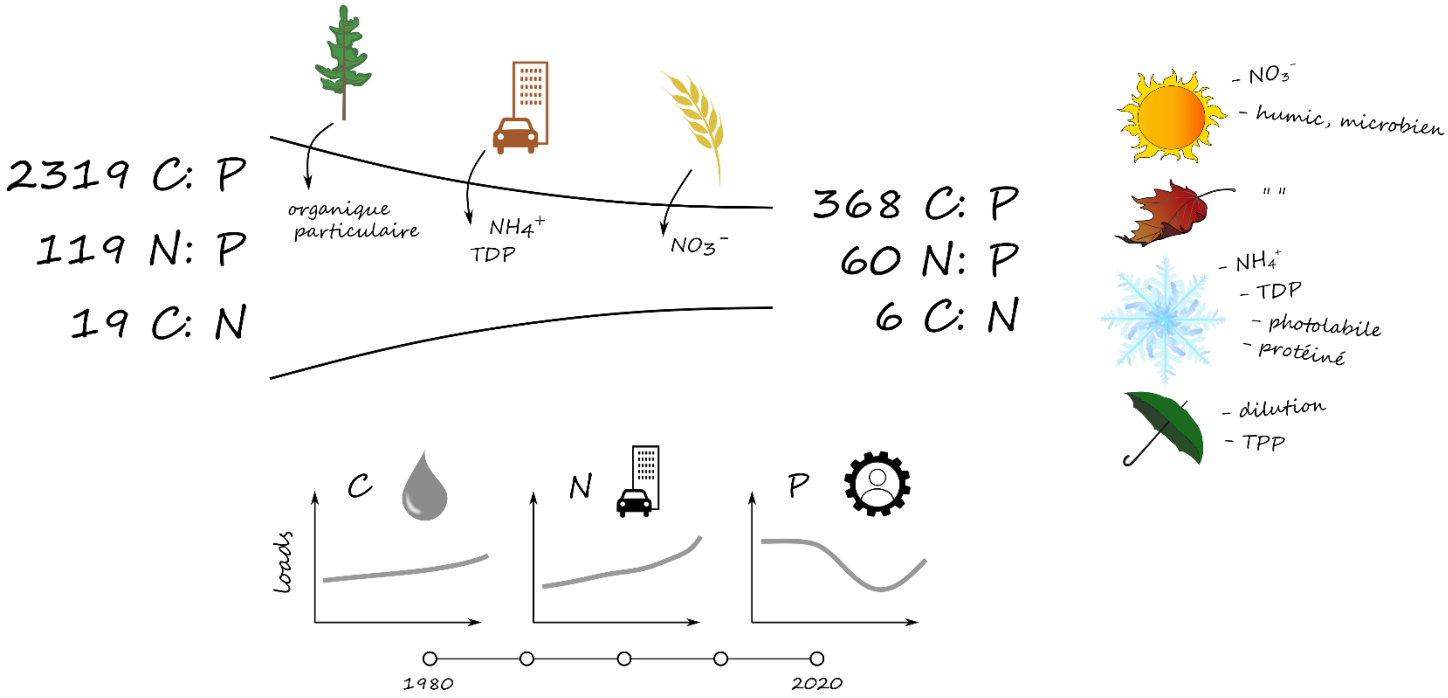

Figure 1 Schéma adapté de la Figure 1 de l'introduction en y apportant les résultats majeurs des trois chapitres de ma thèse. Le long du continuum fluvial, les ratios C : N : P ont diminué à cause d'un apport important de N et de P dû au changement de territoire. Selon les saisons et l'utilisation du territoire, des formes spécifiques contribuent différentiellement aux patrons observés. De 1980 à 2020, les patrons de C, N, et P riverains ont varié à cause de facteurs naturels ou anthropiques.

Particulièrement, au **Chapitre 1**, l'étude simultanée du C, N, et P a montré que peu importe la saison, les concentrations de C restent stables mais les nutriments augmentent le long du continuum, de concert avec une activité humaine plus importante en aval. Due à la différence des réponses du C vs

nutriments en fonction de l'utilisation du territoire, les ratios C : N : P couvrent une étendue spatiale qui se rend presque d'un extrême du continuum terre – océan à l'autre. La saisonnalité apparaît comme fort contrôle sur les formes de N et P, suggérant des contributions d'apports et transformations différentes, mais dont le résultat change peu la stœchiométrie générale.

Puis au **Chapitre 2**, malgré la constance des concentrations de C observée au premier chapitre, la combinaison du gradient anthropique d'utilisation du territoire (peu développé vs plus développé) et de contrastes climatiques utilisés comme proxy pour des potentiels de transformation opposés a révélé un changement clair et abrupt dans la composition de la matière organique dissoute (MOD) qui coïncidait constamment avec le changement d'utilisation du territoire. L'association de certaines formes de nutriments avec certaines molécules de MOD a pu décortiquer la complexité des sources et destins de ces molécules.

Enfin le **Chapitre 3** bâtit sur des efforts provinciaux de récoltes des données décennales de qualité d'eau, et met ainsi en lumière les tendances spatiales et historiques des flux de C, N, et P. Les patrons de précipitation et d'apports en nutriments démontre que le flux de chaque élément est modulé par une combinaison différente de facteurs naturels ou anthropiques. Dans les bassins versants modérément impactés par les activités humaines, la gestion du P urbain constitue presque la cause unique de l'étendue observée dans les ratios historiques de C : N : P.

Malgré l'étendue spatiale restreinte, l'innovation de l'étude accomplie ici se trouve dans la combinaison du gradient anthropique couvert, des contrastes climatiques étudiés, des formes de C, N, et P combinées, et de l'échelle de temps décennale considérée au sein d'un même bassin versant. L'ampleur de ma thèse a permis de mettre en lumière deux pôles dans la réponse d'une même rivière aux variations environnementales et anthropiques l'entourant. Premièrement, il existe un lien fort entre les types d'apports de C, N, et P et l'utilisation du territoire, mais la contribution des formes de n'importe quelle provenance est clairement modulée par les saisons. L'alternance saisonnière de la composition des molécules de C, N, et P exportées par une rivière, dont la biodisponibilité a des conséquences sur le métabolisme des écosystèmes en aval, est en vue de changer à cause des extrêmes climatiques qui seront plus fréquents ou dureront plus ou moins longtemps (été vs hiver) dans les années futures. Deuxièmement, la force des apports de C, N, et P est presqu'entièrement dictée par le développement humain sur le territoire (spatialement et historiquement), mais le mouvement des trois éléments de l'écosystème terrestre à l'écosystème aquatique est découplé. La configuration et la gestion du territoire exercent donc un contrôle important sur l'endroit et la quantité des éléments livrés à une rivière, car le

découplage du C vs nutriments ou N vs P peut avoir des conséquences sur la capacité des rivières à retirer les éléments de l'eau. La pertinence de ma thèse s'inscrit donc à plusieurs niveaux : elle met en lumière les changements de la composition élémentale de trois éléments à la base du fonctionnement des écosystèmes, et les réponses des écosystèmes riverains et conséquemment de la qualité de l'eau face à plusieurs pressions omniprésentes et grandissantes dans les régions tempérées du monde.

Évidemment, quelques limitations ont ponctué ces recherches. Pour les chapitres 1 et 2, si nous avions bien ciblé la saison d'automne, nous aurions probablement discerné une signature très différente de celle reportée. Échantillonner à la tombée des feuilles aurait potentiellement permis de capturer un pouls de matière organique dans l'écosystème aquatique, des concentrations de carbone organique dissous plus élevées et une qualité de la matière organique dissoute plus forestière. L'automne aurait donc servi comme autre extrême à comparer. Pour le chapitre 3, le site le plus en aval (RKm 4) ne capturait pas le tributaire agricole le plus important du bassin versant (chapitre 3, Figure 1). De par le positionnement des sites échantillonnés historiquement et la configuration des tributaires, il est donc impossible de quantifier l'impact des apports anthropiques de N et P au territoire agricole sur la qualité de l'eau dans le bassin versant de la Rivière du Nord. De plus, il m'a toujours été évident de comprendre où les apports anthropiques reliés à l'agriculture étaient stockés sur le territoire. Comme ce n'est pas l'entièreté de ces apports qui sont lessivés à la rivière, j'arrive à imaginer le reste s'emmagasiner sur les champs agricoles. Par contre, lorsque j'imagine un centre urbain, je vois des zones imperméabilisées. J'ai plus de mal à comprendre où sont stockés les apports anthropiques urbains de N et P qui restent sur le territoire. Les données telles qu'elles ont été analysées ne permettent pas de le déterminer. Par exemple, je serais curieuse de voir si l'export fractionnel du NANI urbain d'une ville représente une proportion encore plus élevée dans le N mesuré à l'intrant de l'usine de traitement des eaux usées de cette ville. Aussi, une analyse plus fine de l'expansion des zones imperméabilisées apporterait peut-être des explications quant aux flux de P riverains à la hausse dans la dernière décennie (chapitre 3, Figure 2). Finalement, appliquer l'approche de la stœchiométrie écosystémique et le modèle NANI-NAPI à des bassins versants morphologiquement différents (pente, nombre de lacs, de réservoirs, linéarité des cours d'eau, profondeur du réseau hydrographique) permettrait d'explorer plus en profondeur la capacité de ces bassins à retenir le C, N, et P, anthropique ou naturel, avant qu'ils ne soient exportés.

Le C, N, P, et leurs formes sont des mesures de base relativement simples à récolter et analyser, mais considérées ensembles, elles offrent un aperçu formidable du résultat de la provenance et des transformations des éléments à travers des gradients d'utilisation du territoire et de conditions climatiques qui n'iront qu'en s'aggravant dans les années futures. Le DOC, TN, et TP font déjà partie de plusieurs bases de données d'envergure et l'étude de la stœchiométrie écosystémique pourrait être appliquée à des combinaisons d'écosystèmes (lacs, rivières, sols) et de régions climatiques (tropical vs tempéré vs désert) contrastés. La généralité de ces données permettrait d'approfondir la Figure 6 du chapitre 1 en ajoutant toutes les distributions de ratios de ces combinaisons, qui nous permettrait de découvrir si des endroits « stœchiométriquement impossibles » existent. Ensuite, de par leur nature, les données de recensement agricole et de population utilisées pour le modèle NANI-NAPI continueront à être récoltées par le gouvernement, fournissant une perpétuité possible pour les résultats futurs de NANI-NAPI. Ce modèle est aussi applicable à toute autre région qui contient des données similaires, et a déjà été calculé pour plusieurs bassins versant de l'Europe, de la Chine, des États-Unis, en Ontario, et pour les sous-bassins versants du Fleuve Saint-Laurent. Par contre, l'applicabilité du modèle à un niveau qui est pertinent pour une gestion concrète du territoire est seulement possible à une échelle plus fine, que nous avons réalisée au chapitre 3. Appliquer le modèle pour le Québec où les pressions aux cours d'eau sont de type agricole ou urbain est critique, car la force de l'approche de NANI-NAPI à une échelle régionale réside dans le fait de pouvoir départager entre ces sources de pollution à l'eau. De plus, les bases de données publiques qui existent pour les rivières du Québec permettraient de quantifier l'historique des flux de C, N, et P et de projeter la trajectoire de leurs tendances si le statut quo du développement urbain et de la gestion du territoire est maintenue. Nos méthodes, appliquées à d'autres bassins versants d'utilisation mixte du territoire, à l'échelle des municipalités, en combinaison aux flux historiques des formes des éléments, pourraient donc distinguer entre les sources de pollution (urbaine vs agricole) et justifier les méthodes de contrôles sur le territoire pour diminuer les apports des nutriments vers l'eau à une échelle provinciale.

Références bibliographiques

Aber, J. D., Goodale, C. L., Ollinger, S. V., Smith, M. L., Magill, A. H., Martin, M. E., Hallett, R. A., & Stoddard, J. L. (2003). Is nitrogen deposition altering the nitrogen status of northeastern forests? *BioScience*, *53*(4), 375–389. https://doi.org/10.1641/0006-3568(2003)053[0375:INDATN]2.0.CO;2

Abrinord, O. de bassin versant de la rivière du N. (2015). *Portrait de la zone de gestion intégrée de l'eau d'Abrinord. Saint-Jérôme*.

Adler, D., & Kelly, S. T. (2019). Vioplot: violin plot. R package version 0.3.4.

Aitkenhead-Peterson, J. A., McDowell, W. H., & Neff, J. C. (2003). Sources, Production, and Regulation of Allochthonous Dissolved Organic Matter Inputs to Surface Waters. *Aquatic Ecosystems*, 25–70. https://doi.org/10.1016/b978-012256371-3/50003-2

Alexander, R. B., Smith, R. A., & Schwarz, G. E. (2000). Effect of stream channel size on the delivery of nitrogen to the Gulf of Mexico. *Nature*, *403*(6771), 758–761. https://doi.org/10.1038/35001562

Allard, M., & Painchaud-Francoeur, M. (2017). *Le coeur des Laurentides*.

Arbuckle, K. E., & Downing, J. A. (2001). The influence of watershed land use on lake N : P in a predominantly agricultural landscape. *Limnology and Oceanography*, *46*(4), 970–975. https://doi.org/10.4319/lo.2001.46.4.0970

Arnosti, C. (2011). Microbial Extracellular Enzymes and the Marine Carbon Cycle. *Annu. Rev. Mar. Sci.*, *3*(401–425).

Asadoorian, M. O., Sorofim, M. C., Reilly, J. M., Paltsev, S., & Forest, C. (2006). *MIT Joint Program on the Science and Policy of Global Change: Historical Anthropogenic Emissions Inventories for Greenhouse Gases and Major Criteria Pollutants (Technical Note No. 8)*.

Ashkenas, L. R., Johnson, S. L., Gregory, S. V., Tank, J. L., & Wollheim, W. M. (2004). A stable isotope tracer study of nitrogen uptake and transformation in an old-growth forest stream. *Ecology*. https://doi.org/10.1890/03-0032

Asmala, E., Autio, R., Kaartokallio, H., Stedmon, C. A., & Thomas, D. N. (2014). Processing of humic-rich riverine dissolved organic matter by estuarine bacteria: Effects of predegradation and inorganic nutrients. *Aquatic Sciences*, *76*(3), 451–463. https://doi.org/10.1007/s00027-014-0346-7

Ator, S. W., & Denver, J. M. (2012). Estimating Contributions of Nitrate and Herbicides From

Groundwater to Headwater Streams, Northern Atlantic Coastal Plain, United States. *Journal of the American Water Resources Association*, *48*(6), 1075–1090. https://doi.org/10.1111/j.1752-1688.2012.00672.x

Baken, S., Degryse, F., Verheyen, L., Merckx, R., & Smolders, E. (2011). Metal complexation properties of freshwater dissolved organic matter are explained by its aromaticity and by anthropogenic ligands. *Environmental Science and Technology*, *45*(7), 2584–2590. https://doi.org/10.1021/es103532a

Ballard, T. C., Sinha, E., & Michalak, A. M. (2019). Long-Term Changes in Precipitation and Temperature Have Already Impacted Nitrogen Loading. *Environmental Science and Technology*, *53*(9), 5080–5090. https://doi.org/10.1021/acs.est.8b06898

Basche, A. D., Archontoulis, S. V., Kaspar, T. C., Jaynes, D. B., Parkin, T. B., & Miguez, F. E. (2016). Simulating long-term impacts of cover crops and climate change on crop production and environmental outcomes in the Midwestern United States. *Agriculture, Ecosystems and Environment*, *218*, 95–106. https://doi.org/10.1016/j.agee.2015.11.011

Battin, T. J., Besemer, K., Bengtsson, M. M., Romani, A. M., & Packmann, A. I. (2016). The ecology and biogeochemistry of stream biofilms. *Nature Reviews*, *14*, 251–263.

Bengtsson, M. M., Attermeyer, K., & Catalán, N. (2018). Interactive effects on organic matter processing from soils to the ocean: are priming effects relevant in aquatic ecosystems? *Hydrobiologia*, *822*(1), 1–17. https://doi.org/10.1007/s10750-018-3672-2

Benner, R. (2003). Molecular Indicators of the Bioavailability of Dissolved Organic Matter. *Aquatic Ecosystems*, 121–137. https://doi.org/10.1016/b978-012256371-3/50006-8

Boano, F., Harvey, J. W., Marion, A., Packman, A. I., Revelli, R., Ridolfi, L., & Wörman, A. (2014). Hyporheic flow and transport processes: Mechanisms, models, and biogeochemical implications. *Reviews of Geophysics*, *52*, 603–679. https://doi.org/10.1029/88EO01108

Borges, A. V., Darchambeau, F., Lambert, T., Bouillon, S., Morana, C., Brouyère, S., … Roland, F. A. E. (2018). Effects of agricultural land use on fluvial carbon dioxide, methane and nitrous oxide concentrations in a large European river, the Meuse (Belgium). *Science of the Total Environment*, *610–611*, 342–355. https://doi.org/10.1016/j.scitotenv.2017.08.047

Botrel, M., Bristow, L. A., Altabet, M. A., Gregory-Eaves, I., & Maranger, R. (2017). Assimilation and nitrification in pelagic waters: insights using dual nitrate stable isotopes (δ15N, δ18O) in a shallow lake. *Biogeochemistry*, *135*(3), 221–237. https://doi.org/10.1007/s10533-017-0369-y

Bouchard, I., & Shiab, N. (2022). A Study of Urban Sprawl and Commuting Modes in Canadian

Metropolitan Areas. *CBC/Radio-Canada*. Retrieved from https://ici.radio-canada.ca/info/codesource/code-ouvert/2022/03/etalement-urbain/analysis.nb.html#Q1:_Urban_areas_expansion_and_density

Boyer, E. W., Goodale, C. L., Jaworski, N. A., & Howarth, R. W. (2002). Anthropogenic nitrogen sources and relationships to riverine nitrogen export in the northeastern U.S.A. *Biogeochemistry*, *57–58*, 137–169. https://doi.org/10.1023/A:1015709302073

Butman, D., & Raymond, P. A. (2011). Significant efflux of carbon dioxide from streams and rivers in the United States. *Nature Geoscience*, *4*(12), 839–842. https://doi.org/10.1038/ngeo1294

Caraco, N. F., & Cole, J. J. (1999). Human impact on nitrate export: An analysis using major world rivers. *Ambio*, *28*(2), 167–170. https://doi.org/10.1038/350386b0

Carey, R. O., & Migliaccio, K. W. (2009). Contribution of wastewater treatment plant effluents to nutrient dynamics in aquatic systems. *Environmental Management*, *44*(2), 205–217. https://doi.org/10.1007/s00267-009-9309-5

Carpenter, S. R., Caraco, N. F., Correll, D. L., Howarth, R. W., Sharpley, A. N., & Smith, V. H. (1998). Nonpoint pollution of surface waters with phosphorus and nitrogen. *Ecological Applications*, *8*(3), 559–568. https://doi.org/10.1890/1051-0761(1998)008[0559:NPOSWW]2.0.CO;2

Casas-Ruiz, J. P., Catalán, N., Gómez-Gener, L., von Schiller, D., Obrador, B., Kothawala, D. N., … Marcé, R. (2017). A tale of pipes and reactors: Controls on the in-stream dynamics of dissolved organic matter in rivers. *Limnology and Oceanography*, *62*, S85–S94. https://doi.org/10.1002/lno.10471

Castagno, L. N., I., S. A., Gonzalez, M. E., Pieckenstain, F. L., & Estrella, M. J. (2021). Phosphobacteria as key actors to overcome phosphorus deficiency in plants. *Ann Appl Biol.*, *178*, 256–267.

Catalán, N., Marcé, R., Kothawala, D. N., & Tranvik, L. J. (2016). Organic carbon decomposition rates controlled by water retention time across inland waters. *Nature Geoscience*, *9*(7), 501–504. https://doi.org/10.1038/ngeo2720

Chai, L., Huang, M., Fan, H., Wang, J., Jiang, D., Zhang, M., & Huang, Y. (2019). Urbanization altered regional soil organic matter quantity and quality: Insight from excitation emission matrix (EEM) and parallel factor analysis (PARAFAC). *Chemosphere*, *220*(5), 249–258. https://doi.org/10.1016/j.chemosphere.2018.12.132

Charrier Tremblay, C., Botrel, M., Lapierre, J. F., Franssen, J., & Maranger, R. (2020). Relative

influence of watershed and geomorphic features on nutrient and carbon fluxes in a pristine and moderately urbanized stream. *Science of the Total Environment*, *715*, 136411. https://doi.org/10.1016/j.scitotenv.2019.136411

Chen, B., Huang, W., Ma, S., Feng, M., Liu, C., Gu, X., & Chen, K. (2018). Characterization of chromophoric dissolved organic matter in the littoral zones of eutrophic lakes Taihu and Hongze during the algal bloom season. *Water*, *10*(7). https://doi.org/10.3390/w10070861

Chen, F., Hou, L., Liu, M., Zheng, Y., Yin, G., Lin, X., … Jiang, X. (2016). Net anthropogenic nitrogen inputs (NANI) into the Yangtze River basin and the relationship with riverine nitrogen export. *Journal of Geophysical Research: Biogeosciences*, *121*(2), 451–465. https://doi.org/10.1002/2015JG003186

Chen, M., Kim, S. H., Jung, H. J., Hyun, J. H., Choi, J. H., Lee, H. J., Huh, I. A., & Hur, J. (2017). Dynamics of dissolved organic matter in riverine sediments affected by weir impoundments: Production, benthic flux, and environmental implications. *Water Research*, *121*, 150–161. https://doi.org/10.1016/j.watres.2017.05.022

Cheng, F. Y., Van Meter, K. J., Byrnes, D. K., & Basu, N. B. (2020). Maximizing US nitrate removal through wetland protection and restoration. *Nature*, *588*(7839), 625–630. https://doi.org/10.1038/s41586-020-03042-5

Clark, J. M., Bottrell, S. H., Evans, C. D., Monteith, D. T., Bartlett, R., Rose, R., Newton, R. J., & Chapman, P. J. (2010). The importance of the relationship between scale and process in understanding long-term DOC dynamics. *Science of the Total Environment*, *408*(13), 2768–2775. https://doi.org/10.1016/j.scitotenv.2010.02.046

Climate Data. (2012). Saint-Jérôme Climate (Canada).

Cole, J. J., Prairie, Y. T., Caraco, N. F., McDowell, W. H., Tranvik, L. J., Striegl, R. G., … Melack, J. (2007). Plumbing the global carbon cycle: Integrating inland waters into the terrestrial carbon budget. *Ecosystems*, *10*(1), 171–184. https://doi.org/10.1007/s10021-006-9013-8

Conley, D. J., Paerl, H. W., Howarth, R. W., Boesch, D. F., Seitzinger, S. P., Havens, K. E., Lancelot, C., & Likens, G. E. (2009). Controlling Eutrophication: Nitrogen and Phosphorus. *Science*, *323*(5917), 1014–1015. https://doi.org/10.1126/science.1167755

Cory, R. M., & Kling, G. W. (2018). Interactions between sunlight and microorganisms influence dissolved organic matter degradation along the aquatic continuum. *Limnology and Oceanography Letters*, *3*(3), 102–116. https://doi.org/10.1002/lol2.10060

Cory, R. M., Ward, C. P., Crump, B. C., & Kling, G. W. (2014). Sunlight controls water column

processing of carbon in arctic fresh waters. *Science*, *345*(6199).

Creed, I. F., & Band, L. E. (1998). Export of nitrogen from catchments within a temperate forest: Evidence for a unifying mechanism regulated by variable source area dynamics. *Water Resources Research*, *34*(11), 3105–3120. https://doi.org/10.1029/98WR01924

Cruaud, P., Vigneron, A., Fradette, M. S., Dorea, C. C., Culley, A. I., Rodriguez, M. J., & Charette, S. J. (2020). Annual bacterial community cycle in a seasonally ice-covered river reflects environmental and climatic conditions. *Limnology and Oceanography*, *65*(S1), S21–S37. https://doi.org/10.1002/lno.11130

Dainard, P. G., Guéguen, C., McDonald, N., & Williams, W. J. (2015). Photobleaching of fluorescent dissolved organic matter in Beaufort Sea and North Atlantic Subtropical Gyre. *Marine Chemistry*, *177*, 630–637. https://doi.org/10.1016/j.marchem.2015.10.004

David, M. B., Drinkwater, L. E., & McIsaac, G. F. (2010). Sources of Nitrate Yields in the Mississippi River Basin. *Journal of Environmental Quality*, *39*(5), 1657–1667. https://doi.org/10.2134/jeq2010.0115

Davis, J. C., & Minshall, W. G. (1999). Nitrogen and phosphorus uptake in two Idaho (USA) headwater wilderness streams. *Oecologia*, *199*, 247–255.

De Bonville, J., Amyot, M., del Giorgio, P., Tremblay, A., Bilodeau, F., Ponton, D. E., & Lapierre, J. F. (2020). Mobilization and Transformation of Mercury Across a Dammed Boreal River Are Linked to Carbon Processing and Hydrology. *Water Resources Research*, *56*(10), 1–17. https://doi.org/10.1029/2020WR027951

de Wit, H. A., Valinia, S., Weyhenmeyer, G. A., Futter, M. N., Kortelainen, P., Austnes, K., … Vuorenmaa, J. (2016). Current Browning of Surface Waters Will Be Further Promoted by Wetter Climate. *Environmental Science and Technology Letters*, *3*(12), 430–435. https://doi.org/10.1021/acs.estlett.6b00396

Dentener, F. J., & Crutzen, P. J. (1994). A three-dimensional model of the global ammonia cycle. *Journal of Atmospheric Chemistry*, *19*(4), 331–369. https://doi.org/10.1007/BF00694492

Derrien, M., Lee, M. H., Choi, K., Lee, K. S., & Hur, J. (2020). Tracking the evolution of particulate organic matter sources during summer storm events via end-member mixing analysis based on spectroscopic proxies. *Chemosphere*, *252*, 126445. https://doi.org/10.1016/j.chemosphere.2020.126445

Dittman, J. A., Driscoll, C. T., Groffman, P. M., & Fahey, T. J. (2007). Dynamics of nitrogen and dissolved organic carbon at the Hubbard Brook Experimental Forest. *Ecology*, *88*(5), 1153–1166.

https://doi.org/10.1890/06-0834

Douglas, R. J. W. (1970). *Geology and Economic Minerals of Canada. Geological Survey of Canada, Department of Energy, Mines and Resources, Ottawa, Ontario, Economic Report No. 1*.

Doyle, M. W. (2005). Incorporating hydrologic variability into nutrient spiraling. *Journal of Geophysical Research*, *110*(G01003), 1–11.

ESRI. (2017). ArcGIS Version 10.5.1. Environmental Systems Research Institute, Inc. Redlands, CA.

FAO. (2021). Food and Agriculture Organiztion of the United Nations, FAOSTAT: Crops and livestock products, Livestock primary. Retrieved from https://www.fao.org/faostat/en/#data/QCL

Farjalla, V. F., Marinho, C. C., Faria, B. M., Amado, A. M., Esteves, F. D. A., Bozelli, R. L., & Giroldo, D. (2009). Synergy of fresh and accumulated organic matter to bacterial growth. *Microbial Ecology*, *57*(4), 657–666. https://doi.org/10.1007/s00248-008-9466-8

Fasching, C., Akotoye, C., Bižić, M., Fonvielle, J., Ionescu, D., Mathavarajah, S., … Xenopoulos, M. A. (2020). Linking stream microbial community functional genes to dissolved organic matter and inorganic nutrients. *Limnology and Oceanography*, *65*(S1), S71–S87. https://doi.org/10.1002/lno.11356

Fenn, M. E., Poth, M. A., Aber, J. D., Baron, J. S., Bormann, B. T., Johnson, D. W., … Stottlemyer, R. (1998). Nitrogen excess in North American ecosystems: Predisposing factors, ecosystem responses, and management strategies. *Ecological Applications*, *8*(3), 706–733. https://doi.org/10.1890/1051-0761(1998)008[0706:NEINAE]2.0.CO;2

Findlay, S. E. G., Sinsabaugh, R. L., Sobczak, W. V., & Hoostal, M. (2003). Metabolic and structural response of hyporheic microbial communities to variations in supply of dissolved organic matter. *Limnology and Oceanography*, *48*(4), 1608–1617. https://doi.org/10.4319/lo.2003.48.4.1608

Fisher, S. G., & Likens, G. E. (1973). Energy Flow in Bear Brook, New Hampshire: An Integrative Approach to Stream Ecosystem Metabolism. *Ecological Monographs*, *43*, 421–439.

Gächter, R., Steingruber, S. M., Reinhardr, M., & Wehrli, B. (2004). Nutrient transfer from soil to surface waters: Differences between nitrate and phosphate. *Aquatic Sciences*, *66*(1), 117–122. https://doi.org/10.1007/s00027-003-0661-x

Galantini, L., Lapierre, J. F., & Maranger, R. (2021). How are greenhouse gases coupled across seasons in a large temperate river with differential land use? *Ecosystems*.

Galloway, J. N., Dentener, F. J., Capone, D. G., Boyer, E. W., Howarth, R. W., Seitzinger, S. P., …

Vörösmarty, C. J. (2004). Nitrogen cycles: past, present, and future. *Biogeochemistry*, *70*, 153–226. Retrieved from papers://aa15ed4a-8b41-4036-84a6-41087bba0cd6/Paper/p3387

Garcia, R. D., Diéguez, M. del C., Gerea, M., Garcia, P. E., & Reissig, M. (2018). Characterisation and reactivity continuum of dissolved organic matter in forested headwater catchments of Andean Patagonia. *Freshwater Biology*, *63*(9), 1049–1062. https://doi.org/10.1111/fwb.13114

Glibert, P. M., & Burkholder, J. A. M. (2011). Harmful algal blooms and eutrophication: "strategies" for nutrient uptake and growth outside the Redfield comfort zone. *Chinese Journal of Oceanology and Limnology*, *29*(4), 724–738. https://doi.org/10.1007/s00343-011-0502-z

Glibert, P. M., Maranger, R., Sobota, D. J., & Bouwman, L. (2014). The Haber Bosch-harmful algal bloom (HB-HAB) link. *Environmental Research Letters*, *9*(10). https://doi.org/10.1088/1748-9326/9/10/105001

Gómez-Gener, L., Rocher-Ros, G., Battin, T., Cohen, M. J., Dalmagro, H. J., Dinsmore, K. J., … Sponseller, R. A. (2021). Global carbon dioxide efflux from rivers enhanced by high nocturnal emissions. *Nature Geoscience*, *14*(5), 289–294. https://doi.org/10.1038/s41561-021-00722-3

Gonçalves-Araujo, R., Stedmon, C. A., Heim, B., Dubinenkov, I., Kraberg, A., Moiseev, D., & Bracher, A. (2015). From fresh to marine waters: Characterization and fate of dissolved organic matter in the Lena River Delta Region, Siberia. *Frontiers in Marine Science*, *2*(DEC), 1–13. https://doi.org/10.3389/fmars.2015.00108

Gonsior, M., Schmitt-Kopplin, P., & Bastviken, D. (2013). Depth-dependent molecular composition and photo-reactivity of dissolved organic matter in a boreal lake under winter and summer conditions. *Biogeosciences*, *10*(11), 6945–6956. https://doi.org/10.5194/bg-10-6945-2013

Gouvernement du Québec. (2012). Commission de toponymie: Doncaster. Retrieved from https://toponymie.gouv.qc.ca/ct/toposweb/fiche.aspx?no_seq=82105

Gouvernement du Québec. (2016a). Données Québec: LIDAR - Modèles Numériques (Terrain, Canopée, Pente).

Gouvernement du Québec. (2016b). Données Québec: LIDAR - Modèles Numériques (Terrain, Canopée, Pente).

Government of Canada. (2018). Air Pollutants Emissions Inventory online search. Retrieved from https://pollution-waste.canada.ca/air-emission-inventory

Government of Canada. (2019). Justice Laws Website: Concentration of Phosphorus in Certain Cleaning Products Regulations (SOR/89-501), Canadian Environmental Protection Act, 1999. Retrieved from https://laws-lois.justice.gc.ca/eng/regulations/SOR-89-501/page-1.html

Government of Canada. (2021a). Historical Data : Past weather and climate. Retrieved from https://climate.weather.gc.ca/historical_data/search_historic_data_e.html

Government of Canada. (2021b). Poultry slaughter reports. Retrieved from https://agriculture.canada.ca/en/canadas-agriculture-sectors/animal-industry/poultry-and-egg-market-information/slaughter

Government of Canada. (2022). Agriculture et Agroalimentaire Canada. Retrieved from https://agriculture.canada.ca/fr

Goyette, J.-O., Bennett, E. M., Howarth, R. W., & Maranger, R. (2016). Changes in anthropogenic nitrogen and phosphorus inputs to the St. Lawrence sub-basin over 110 years and impacts on riverine export. *Global Biogeochemical Cycles*, *30*, 1000–1014. https://doi.org/10.1111/1462-2920.13280

Goyette, J.-O., Bennett, E. M., & Maranger, R. (2019). Differential influence of landscape features and climate on nitrogen and phosphorus transport throughout the watershed. *Biogeochemistry*, *142*(1), 155–174. https://doi.org/10.1007/s10533-018-0526-y

Goyette, J. O., Bennett, E. M., & Maranger, R. (2018). Low buffering capacity and slow recovery of anthropogenic phosphorus pollution in watersheds. *Nature Geoscience*, *11*(12), 921–925. https://doi.org/10.1038/s41561-018-0238-x

Graça, M. A. S., Ferreira, V., Canhoto, C., Encalada, A. C., Guerrero-Bolaño, F., Wantzen, K. M., & Boyero, L. (2015). A conceptual model of litter breakdown in low order streams. *International Review of Hydrobiology*, *100*(1), 1–12. https://doi.org/10.1002/iroh.201401757

Graeber, D., Tenzin, Y., Stutter, M., Weigelhofer, G., Shatwell, T., von Tümpling, W., … Borchardt, D. (2021). Bioavailable DOC: reactive nutrient ratios control heterotrophic nutrient assimilation—An experimental proof of the macronutrient-access hypothesis. *Biogeochemistry*, *155*(1), 1–20. https://doi.org/10.1007/s10533-021-00809-4

Groffman, P. M., Law, N. L., Belt, K. T., Band, L. E., & Fisher, G. T. (2004). Nitrogen fluxes and retention in urban watershed ecosystems. *Ecosystems*, *7*(4), 393–403. https://doi.org/10.1007/s10021-003-0039-x

Gücker, B., Brauns, M., & Pusch, M. T. (2006). Effects of wastewater treatment plant discharge on ecosystem structure and function of lowland streams. *Journal of the North American Benthological Society*, *25*(2), 313–329. https://doi.org/10.1899/0887-3593(2006)25[313:EOWTPD]2.0.CO;2

Haggard, B. E., Stanley, E. H., & Storm, D. E. (2005). Nutrient retention in a point-source-enriched stream. *Journal of the North American Benthological Society*, *24*(1), 29–47.

https://doi.org/10.1899/0887-3593(2005)024<0029:NRIAPS>2.0.CO;2

Hall, R. O., Tank, J. L., Sobota, D. J., Mulholland, P. J., O'Brien, J. M., Dodds, W. K., … Arango, C. P. (2009). Nitrate removal in stream ecosystems measured by 15N addition experiments: Total uptake. *Limnol. Oceangr.*, *54*(3), 653–665.

Hampton, S. E., Galloway, A. W. E., Powers, S. M., Ozersky, T., Woo, K. H., Batt, R. D., … Xenopoulos, M. A. (2017). Ecology under lake ice. *Ecology Letters*, *20*(1), 98–111. https://doi.org/10.1111/ele.12699

Han, H., Allan, D. J., & Bosch, N. S. (2012). Historical pattern of phosphorus loading to Lake Erie watersheds. *Journal of Great Lakes Research*, *38*(2), 289–298. https://doi.org/10.1016/j.jglr.2012.03.004

Han, H., & Allan, J. D. (2008). Estimation of nitrogen inputs to catchments: Comparison of methods and consequences for riverine export prediction. *Biogeochemistry*, *91*(2–3), 177–199. https://doi.org/10.1007/s10533-008-9279-3

Han, H., Allan, J. D., & Scavia, D. (2009). Influence of climate and human activities on the relationship between watershed nitrogen input and river export. *Environmental Science and Technology*, *43*(6), 1916–1922. https://doi.org/10.1021/es801985x

Han, H., Bosch, N., & Allan, J. D. (2011). Spatial and temporal variation in phosphorus budgets for 24 watersheds in the Lake Erie and Lake Michigan basins. *Biogeochemistry*, *102*(1), 45–58. https://doi.org/10.1007/s10533-010-9420-y

Han, Y., Yu, X., Wang, X., Wang, Y., Tian, J., Xu, L., & Wang, C. (2013). Net anthropogenic phosphorus inputs (NAPI) index application in Mainland China. *Chemosphere*, *90*(2), 329–337. https://doi.org/10.1016/j.chemosphere.2012.07.023

Harrison, J. A., Maranger, R. J., Alexander, R. B., Giblin, A. E., Jacinthe, P. A., Mayorga, E., … Wollheim, W. M. (2009). The regional and global significance of nitrogen removal in lakes and reservoirs. *Biogeochemistry*, *93*(1–2), 143–157. https://doi.org/10.1007/s10533-008-9272-x

Haygarth, P. M., Jarvie, H. P., Powers, S. M., Sharpley, A. N., Elser, J. J., Shen, J., … Liu, X. (2014). Sustainable Phosphorus Management and the Need for a Long-Term Perspective: The Legacy Hypothesis. *Environmental Science & Technology*, *48*, 8417–8419.

Heath, R. T. (2004). Microbial turnover of organic phosphorus in aquatic systems. In B. L. Turner, E. Frossard, & D. S. Baldwin (Eds.), *Organic Phosphorus in the Environment* (pp. 185–204). Wallingford, UK: CABI Publishing. https://doi.org/10.1079/9780851998220.0185

Heathcote, A. J., Giorgio, P. A., & Prairie, Y. T. (2015). Predicting bathymetric features of lakes from

the topography of their surrounding landscape. *Canadian Journal of Fisheries and Aquatic Sciences*, *72*(5), 643–650. https://doi.org/10.1139/cjfas-2014-0392

Hedin, L. O. (1995). Patterns of nutrient loss from unpolluted, old-growth temperate forests: evaluation of biogeochemical theory. *Ecology*, *76*(2), 493–509.

Hendricks, S. P., & White, D. S. (2000). Stream and Groundwater Influences on Phosphorus Biogeochemistry. In *Influences on Phosphorus Biogeochemistry* (pp. 221–235). Elsevier Inc. https://doi.org/10.1016/B978-0-12-389845-6.50010-7

Hilton, J., O'Hare, M., Bowes, M. J., & Jones, J. I. (2006). How green is my river? A new paradigm of eutrophication in rivers. *Science of the Total Environment*, *365*(1–3), 66–83. https://doi.org/10.1016/j.scitotenv.2006.02.055

Hobara, S., Osono, T., Hirose, D., Noro, K., Hirota, M., & Benner, R. (2014). The roles of microorganisms in litter decomposition and soil formation. *Biogeochemistry*, *118*(1–3), 471–486. https://doi.org/10.1007/s10533-013-9912-7

Hobbie, S. E., Finlay, J. C., Janke, B. D., Nidzgorski, D. A., Millet, D. B., & Baker, L. A. (2017). Contrasting nitrogen and phosphorus budgets in urban watersheds and implications for managing urban water pollution. *Proceedings of the National Academy of Sciences of the United States of America*, *114*(16), 4177–4182. https://doi.org/10.1073/pnas.1618536114

Holtan, H., Kamp-Nielsen, L., & Stuanes, A. O. (1988). Phosphorus in soil, water and sediment: an overview. *Hydrobiologia*, *170*(1), 19–34. https://doi.org/10.1007/BF00024896

Hong, B., & Swaney, D. P. (2010). NANI Calculator Toolbox Documentation, (June), 1–31. Retrieved from http://www.eeb.cornell.edu/biogeo/nanc/nani/NANI_Calculator_Toolbox_Documentation.pdf

Hong, B., Swaney, D. P., & Howarth, R. W. (2013). Estimating net anthropogenic nitrogen inputs to U.S. watersheds: Comparison of methodologies. *Environmental Science and Technology*, *47*(10), 5199–5207. https://doi.org/10.1021/es303437c

Hong, B., Swaney, D. P., McCrackin, M., Svanbäck, A., Humborg, C., Gustafsson, B., Yershova, A., & Pakhomau, A. (2017). Advances in NANI and NAPI accounting for the Baltic drainage basin: spatial and temporal trends and relationships to watershed TN and TP fluxes. *Biogeochemistry*, *133*(3), 245–261. https://doi.org/10.1007/s10533-017-0330-0

Hong, B., Swaney, D. P., Mörth, C. M., Smedberg, E., Eriksson Hägg, H., Humborg, C., Howarth, R. W., & Bouraoui, F. (2012). Evaluating regional variation of net anthropogenic nitrogen and

phosphorus inputs (NANI/NAPI), major drivers, nutrient retention pattern and management implications in the multinational areas of Baltic Sea basin. *Ecological Modelling*, *227*, 117–135. https://doi.org/10.1016/j.ecolmodel.2011.12.002

Hornberger, G. M., Bencala, K. E., & McKnight, D. M. (1994). Hydrological controls on dissolved organic carbon during snowmelt in the Snake River near Montezuma, Colorado. *Biogeochemistry*, *25*(3), 147–165. https://doi.org/10.1007/BF00024390

Hosen, J. D., McDonough, O. T., Febria, C. M., & Palmer, M. A. (2014). Dissolved organic matter quality and bioavailability changes across an urbanization gradient in headwater streams. *Environmental Science and Technology*, *48*(14), 7817–7824. https://doi.org/10.1021/es501422z

Hotchkiss, E. R., Hall, R. O., Sponseller, R. A., Butman, D., Klaminder, J., Laudon, H., Rosvall, M., & Karlsson, J. (2015). Sources of and processes controlling CO2emissions change with the size of streams and rivers. *Nature Geoscience*, *8*(9), 696–699. https://doi.org/10.1038/ngeo2507

Howarth, R., Swaney, D., Billen, G., Garnier, J., Hong, B., Humborg, C., … Marino, R. (2012). Nitrogen fluxes from the landscape are controlled by net anthropogenic nitrogen inputs and by climate. *Frontiers in Ecology and the Environment*, *10*(1), 37–43. https://doi.org/10.1890/100178

Howarth, R. W., Billen, G., Swaney, D., Townsend, A., Jaworski, N., Lajtha, K., … Zhu, Z. L. (1996). Regional nitrogen budgets and riverine N & P fluxes for the drainages to the North Atlantic Ocean: Natural and human influences. *Biogeochemistry*, *35*(1), 75–139. https://doi.org/10.1007/BF02179825

Howarth, R.W., Swaney, D. ., Boyer, E. W., Marino, R., Jaworski, N., & Goodale, C. (2006). The influence of climate on average nitrogen export from large from large watersheds in the Northeastern United States. *Biogeochemistry*, *79*, 163–186.

Howarth, Robert W. (2008). Coastal nitrogen pollution: A review of sources and trends globally and regionally. *Harmful Algae*, *8*(1), 14–20. https://doi.org/10.1016/j.hal.2008.08.015

Hu, M., Liu, Y., Zhang, Y., Shen, H., Yao, M., Dahlgren, R. A., & Chen, D. (2020). Long-term (1980–2015) changes in net anthropogenic phosphorus inputs and riverine phosphorus export in the Yangtze River basin. *Water Research*, *177*, 115779. https://doi.org/10.1016/j.watres.2020.115779

Humborg, C., Mörth, C.-M., Sundbom, M., Borg, H., Blenckner, T., Giesler, R., & Ittekkot, V. (2010). CO2 supersaturation along the aquatic conduit in Swedish watersheds as constrained by terrestrial respiration, aquatic respiration and weathering. *Global Change Biology*, *16*, 1966–1978.

Inamdar, S., Dhillon, G., Singh, S., Parr, T., & Qin, Z. (2015). Particulate nitrogen exports in stream

runoff exceed dissolved nitrogen forms during large tropical storms in a temperate, headwater, forested watershed. *Journal of Geophysical Research G: Biogeosciences*, *120*(8), 1548–1566. https://doi.org/10.1002/2015JG002909

Institut de la statistique du Québec. (2020). Superficie des grandes cultures, rendement à l'hectare et production, par regroupement de régions administratives, Québec. Retrieved from https://statistique.quebec.ca/fr/statistiques/par-themes

Ishii, S. K. L., & Boyer, T. H. (2012). Behavior of Reoccurring PARAFAC Components in Fluorescent Dissolved Organic Matter in Natural and Engineered Systems: A Critical Review. *Environmental Science & Technology*, *46*, 2006–2017. https://doi.org/10.1080/08913819308443310

Jeong, J. J., Bartsch, S., Fleckenstein, J. H., Matzner, E., Tenhunen, J. D., Lee, S. D., Park, S. K., & Park, J. H. (2012). Differential storm responses of dissolved and particulate organic carbon in a mountainous headwater stream, investigated by high-frequency, in situ optical measurements. *Journal of Geophysical Research: Biogeosciences*, *117*(3), 1–13. https://doi.org/10.1029/2012JG001999

Johnson, H. M., & Stets, E. G. (2020). Nitrate in Streams During Winter Low-Flow Conditions as an Indicator of Legacy Nitrate. *Water Resources Research*, *56*(11). https://doi.org/10.1029/2019WR026996

Jones, D. B. (1941). Factors for converting percentages of nitrogen in foods and feeds into percentages of protein. *British Food Journal*. https://doi.org/10.1108/eb011242

Jordan, T. E., & Weller, D. E. (1996). Human Contributions to Terrestrial Nitrogen Flux. *BioScience*, *46*(9), 655–664.

Judd, K. E., Crump, B. C., & Kling, G. W. (2006). Variation in dissolved organic matter controls bacterial production and community composition. *Ecology*, *87*(8), 2068–2079. https://doi.org/10.1890/0012-9658(2006)87[2068:VIDOMC]2.0.CO;2

Kaspar, T. C., & Singer, J. W. (2011). The Use of Cover Crops to Manage Soil. *Soil Management: Building a Stable Base for Agriculture*, 321–337. https://doi.org/10.2136/2011.soilmanagement.c21

Kaushal, S. S., Groffman, P. M., Band, L. E., Elliott, E. M., Shields, C. A., & Kendall, C. (2011). Tracking nonpoint source nitrogen pollution in human-impacted watersheds. *Environmental Science and Technology*, *45*(19), 8225–8232. https://doi.org/10.1021/es200779e

Kaushal, S. S., Lewis, W. M., & McCutchan, J. H. (2006). Land use change and nitrogen enrichment of a rocky mountain watershed. *Ecological Applications*, *16*(1), 299–312. https://doi.org/10.1890/05-0134

Kellogg, R. L., Lander, C. H., Moffitt, D. C., & Gollehon, N. (2000). Manure Nutrients Relative to

The Capacity Of Cropland And Pastureland To Assimilate Nutrients: Spatial and Temporal Trends for the United States. *US Department of Agriculture, NPS00-0579*. https://doi.org/10.2175/193864700784994812

Koehler, B., Landelius, T., Weyhenmeyer, G. A., Machida, N., & Tranvik, L. J. (2014). Sunlight-induced carbon dioxide emissions from inland waters. *Global Biogeochemical Cycles*, *28*(696–711).

Koenig, L. E., Shattuck, M. D., Snyder, L. E., Potter, J. D., & McDowell, W. H. (2017). Deconstructing the Effects of Flow on DOC, Nitrate, and Major Ion Interactions Using a High-Frequency Aquatic Sensor Network. *Water Resources Research*, *53*(12), 10655–10673. https://doi.org/10.1002/2017WR020739

Kortelainen, P., Mattsson, T., Finér, L., Ahtiainen, M., Saukkonen, S., & Sallantaus, T. (2006). Controls on the export of C, N, P and Fe from undisturbed boreal catchments, Finland. *Aquatic Sciences*, *68*(4), 453–468. https://doi.org/10.1007/s00027-006-0833-6

Kothawala, D. N., Stedmon, C. A., Müller, R. A., Weyhenmeyer, G. A., Köhler, S. J., & Tranvik, L. J. (2014). Controls of dissolved organic matter quality: Evidence from a large-scale boreal lake survey. *Global Change Biology*, *20*(4), 1101–1114. https://doi.org/10.1111/gcb.12488

Krause, S., Abbott, B. W., Baranov, V., Bernal, S., Blaen, P., Datry, T., … Zarnetske, J. P. (2022). Organizational Principles of Hyporheic Exchange Flow and Biogeochemical Cycling in River Networks Across Scales. *Water Resources Research*, *58*, 1–25.

Kritzberg, E. S. (2017). Centennial-long trends of lake browning show major effect of afforestation. *Limnology and Oceanography Letters*, *2*, 105–112.

Kritzberg, E. S., Cole, J. J., Pace, M. L., Granéli, W., & Bade, D. L. (2004). Autochthonous versus allochthonous carbon sources of bacteria: Results from whole-lake 13C addition experiments. *Limnology and Oceanography*, *49*(2), 588–596. https://doi.org/10.4319/lo.2004.49.2.0588

Kritzberg, E. S., Hasselquist, E. M., Škerlep, M., Löfgren, S., Olsson, O., Stadmark, J., … Laudon, H. (2020). Browning of freshwaters: Consequences to ecosystem services, underlying drivers, and potential mitigation measures. *Ambio*, *49*(2), 375–390. https://doi.org/10.1007/s13280-019-01227-5

LaBrie, R., Fortin St-Gelais, N., & Bélanger, S. (2017). an R Package to correct EEMs and derive CDOM and FDOM indices. http://doi.org/10.5281/zenodo.833530. Retrieved from https://github.com/RichardLaBrie/paRafac_correction

Lambert, T., Bouillon, S., Darchambeau, F., Massicotte, P., & Borges, A. V. (2016). Shift in the chemical composition of dissolved organic matter in the Congo River network. *Biogeosciences*,

13(18), 5405–5420. https://doi.org/10.5194/bg-13-5405-2016

Lambert, T., Bouillon, S., Darchambeau, F., Morana, C., Roland, F. A. E., Descy, J. P., & Borges, A. V. (2017). Effects of human land use on the terrestrial and aquatic sources of fluvial organic matter in a temperate river basin (The Meuse River, Belgium). *Biogeochemistry*, *136*(2), 191–211. https://doi.org/10.1007/s10533-017-0387-9

Lapierre, J. F., & del Giorgio, P. A. (2014). Partial coupling and differential regulation of biologically and photochemically labile dissolved organic carbon across boreal aquatic networks. *Biogeosciences*, *11*(20), 5969–5985. https://doi.org/10.5194/bg-11-5969-2014

Laurin, S. (1989). *Histoire des Laurentides*. Diffusion Prologue Inc., Québec.

Lewis, W. M. (2002). Yield of nitrogen from minimally disturbed watersheds of the United States. *Biogeochemistry*, *57–58*, 375–385. https://doi.org/10.1023/A:1015709128245

Li, J., Wang, L., Geng, J., Li, S., Yu, Q., Xu, K., & Ren, H. (2020). Distribution and removal of fluorescent dissolved organic matter in 15 municipal wastewater treatment plants in China. *Chemosphere*, *251*(163). https://doi.org/10.1016/j.chemosphere.2020.126375

Litke, D. W. (1999). Review of Phosphorus Control Measures in the United States and Their Effects on Water Quality. *Water-Resources Investigations Report 99-4007*, 1–38. Retrieved from http://www.msue.msu.edu/waterqual/WQWEB/ReviewPUSGS.pdf

Lu, Y., Bauer, J. E., Canuel, E. A., Yamashita, Y., Chambers, R. M., & Jaffé, R. (2013). Photochemical and microbial alteration of dissolved organic matter in temperate headwater streams associated with different land use. *Journal of Geophysical Research: Biogeosciences*. https://doi.org/10.1002/jgrg.20048

Lu, Y., Li, X., Mesfioui, R., Bauer, J. E., Chambers, R. M., Canuel, E. A., & Hatcher, P. G. (2015). Use of ESI-FTICR-MS to Characterize Dissolved Organic Matter in Headwater Streams Draining Forest-Dominated and Pasture-Dominated Watersheds. *PLoS ONE*, *10*(12), 1–21. https://doi.org/10.1371/journal.pone.0145639

Luo, J., Li, S., Ni, M., & Zhang, J. (2019). Large spatiotemporal shifts of CO2 partial pressure and CO2 degassing in a monsoonal headwater stream. *Journal of Hydrology*, *579*(July), 124135. https://doi.org/10.1016/j.jhydrol.2019.124135

Maavara, T., Parsons, C. T., Ridenour, C., Stojanovic, S., Dürr, H. H., Powley, H. R., & Van Cappellen, P. (2015). Global phosphorus retention by river damming. *Proceedings of the National Academy of Sciences of the United States of America*, *112*(51), 15603–15608. https://doi.org/10.1073/pnas.1511797112

MacDonald, G. K., & Bennett, E. M. (2009). Phosphorus accumulation in saint lawrence river watershed soils: A century-long perspective. *Ecosystems*, *12*(4), 621–635. https://doi.org/10.1007/s10021-009-9246-4

Manning, D. W. P., Rosemond, A. D., Benstead, J. P., Bumpers, P. M., & Kominoski, J. S. (2020). Transport of N and P in U.S. streams and rivers differs with land use and between dissolved and particulate forms. *Ecological Applications*, *0*(0). https://doi.org/10.1002/eap.2130

Maranger, R., Jones, S. E., & Cotner, J. B. (2018). Stoichiometry of carbon, nitrogen, and phosphorus through the freshwater pipe. *Limnology and Oceanography Letters*, *3*(3), 89–101. https://doi.org/10.1002/lol2.10080

Martí, E., & Sabater, F. (1996). High variability in temporal and spatial nutrient retention in mediterranean streams. *Ecology*, *77*(3), 854–869. https://doi.org/10.2307/2265506

Massé, S., Botrel, M., Walsh, D. A., & Maranger, R. (2019). Annual nitrification dynamics in a seasonally ice-covered lake. *PLoS ONE*, *14*(3), 1–21. https://doi.org/10.1371/journal.pone.0213748

Massicotte, P., & Frenette, J. J. (2011). Spatial connectivity in a large river system: Resolving the sources and fate of dissolved organic matter. *Ecological Applications*, *21*(7), 2600–2617. https://doi.org/10.1890/10-1475.1

McGroddy, M. E., Baisden, W. T., & Hedin, L. O. (2008). Stoichiometry of hydrological C, N, and P losses across climate and geology: An environmental matrix approach across New Zealand primary forests. *Global Biogeochemical Cycles*, *22*, 1–14. https://doi.org/10.1029/2007GB003005

McGroddy, Megan E., Daufresne, T., & Hedin, L. O. (2004). Scaling of C:N:P stoichiometry in forests worldwide: Implications of terrestrial redfield-type ratios. *Ecology*, *85*(9), 2390–2401. https://doi.org/10.1890/03-0351

McIsaac, G. F., & Hu, X. (2004). Net N input and riverine N export from Illinois agricultural watersheds with and without extensive tile drainage. *Biogeochemistry*, *70*(2), 251–271. https://doi.org/10.1023/B:BIOG.0000049342.08183.90

McKnight, D. M., Boyer, E. W., Westerhoff, P. K., Doran, P. T., Kulbe, T., & Andersen, D. T. (2001). Spectrofluorometric characterization of dissolved organic matter for indication of precursor organic material and aromaticity. *Limnology and Oceanography*, *46*(1), 38–48. https://doi.org/10.4319/lo.2001.46.1.0038

MDDELC. (2021). M. du D. durable de l'Environnement et de la L. contre les changements Climatiques. Portail des connaissances de l'eau - Suivi des ouvrages municipaux

d'assainissement des eaux usées. Retrieved from https://www.environnement.gouv.qc.ca/eau/portail/index.htm

MDDELCC. (2018a). M. du D. durable de l'Environnement et de la L. contre les changements Climatiques. Centre d'expertise hydrique du Québec: Fiche signalétique de la station.

MDDELCC. (2018b). Ministère du Développement durable de l'Environnement et de la Lutte contre les changements climatiques. Centre d'expertise hydrique du Québec: Fiche signalétique de la station.

MELCC. (2011). Eaux usées domestiques, communautaires et municipales.

MELCC. (2021). *Ministère de l'Environnement et de la Lutte contre les changements climatiques. Bilan de performance des ouvrages municipaux d'assainissement des eaux usées pour l'année 2019*. Retrieved from www.environnement.gouv.qc.ca/formulaires/renseignements.asp

MELCC. (2022a). Ministère de l'Environnement et de la Lutte contre les changements climatiques. 25 ans d'assainissement des eaux usées industrielles au Québec : un bilan. Retrieved from https://www.environnement.gouv.qc.ca/eau/eaux-usees/industrielles/

MELCC. (2022b). Ministère de l'Environnement et de la Lutte contre les changements climatiques. Règlement sur l'évacuation et le traitement des eaux usées des résidences isolées. Retrieved from https://www.environnement.gouv.qc.ca/eau/eaux-usees/residences_isolees/reglement.htm

Merseburger, G. C., Martí, E., & Sabater, F. (2005). Net changes in nutrient concentrations below a point source input in two streams draining catchments with contrasting land uses. *Science of the Total Environment*, *347*(1–3), 217–229. https://doi.org/10.1016/j.scitotenv.2004.12.022

Meyer, J. L., & Likens, G. E. (1979). Transport and Transformation of Phosphorus in a Forest Stream Ecosystem. *Ecology*, *60*(6), 1255–1269.

Mitchell, M. J., Driscoll, C. T., Kahl, J. S., Likens, G. E., Murdoch, P. S., & Pardo, L. H. (1996). Climatic control of nitrate loss from forested watersheds in the northeast United States. *Environmental Science and Technology*, *30*(8), 2609–2612. https://doi.org/10.1021/es9600237

Monteith, D. T., Stoddard, J. L., Evans, C. D., De Wit, H. A., Forsius, M., Høgåsen, T., … Vesely, J. (2007). Dissolved organic carbon trends resulting from changes in atmospheric deposition chemistry. *Nature*, *450*, 537–541.

Moran, M. A., & Zepp, R. G. (1997). Role of photoreactions in the formation of biologically labile compounds from dissolved organic matter. *Limnology and Oceanography*, *42*(6), 1307–1316. https://doi.org/10.4319/lo.1997.42.6.1307

Morris, D. P., & Hargreaves, B. R. (1997). The role of photochemical degradation of dissolved organic carbon in regulating the UV transparency of three lakes on the Pocono Plateau. *Limnol. Oceangr.*, *42*(2), 239–249.

Mostofa, K. M. G., Wu, F., Liu, C. Q., Fang, W. L., Yuan, J., Ying, W. L., Wen, L., & Yi, M. (2010). Characterization of Nanming River (southwestern China) sewerage-impacted pollution using an excitation-emission matrix and PARAFAC. *Limnology*, *11*(3), 217–231. https://doi.org/10.1007/s10201-009-0306-4

MRC d'Argenteuil. (2011). Évaluation géophysique des sols de la zone agricole de la MRC d'Argenteuil pour la diversification des productions végétales et la remise en culture des terres sous-occupées.

MTESS. (2020). Règlement sur les ouvrages municipaux d'assainissement des eaux usées. https://doi.org/10.1163/156852879x00063

MTESS. (2021a). Ministère du Travail, de l'Emploi et de la Solidarité sociale. Règlement sur l'évacuation et le traitement des eaux usées des résidences isolées (Q-2, r. 22). Retrieved from https://www.legisquebec.gouv.qc.ca/fr/document/rc/Q-2, r. 22

MTESS. Ministère du Travail, de l'Emploi et de la Solidarité sociale. Règlement sur les ouvrages municipaux d'assainissement des eaux usées (Q-2, r. 34.1) (2021).

Mulholland, P. J., Hall, R. O., Sobota, D. J., Dodds, W. K., Findlay, S. E. G., Grimm, N. B., … Thomasn, S. M. (2009). Nitrate removal in stream ecosystems measured by 15N addition experiments: Denitrification. *Limnology and Oceanography*, *54*(3), 666–680. https://doi.org/10.4319/lo.2009.54.3.0666

Müller, A., Österlund, H., Marsalek, J., & Viklander, M. (2020). The pollution conveyed by urban runoff: A review of sources. *Science of the Total Environment*, *709*. https://doi.org/10.1016/j.scitotenv.2019.136125

Murphy, K. R., Timko, S. A., Gonsior, M., Powers, L. C., Wünsch, U. J., & Stedmon, C. A. (2018). Photochemistry Illuminates Ubiquitous Organic Matter Fluorescence Spectra. *Environmental Science and Technology*, *52*(19), 11243–11250. https://doi.org/10.1021/acs.est.8b02648

Murphy, Kathleen R., Stedmon, C. A., Wenig, P., & Bro, R. (2014). OpenFluor- An online spectral library of auto-fluorescence by organic compounds in the environment. *Analytical Methods*, *6*(3), 658–661. https://doi.org/10.1039/c3ay41935e

Natural Resources Canada. (2009). Land Cover, circa 2000-Vector: Feature Catalogue - Edition 1.0.

Newbold, J. D., Bott, T. L., Kaplan, L. A., Dow, C. L., Jackson, J. K., Aufdenkampe, A. K., … De

Long, A. A. (2006). Uptake of nutrients and organic C in streams in New York City drinking-water-supply watersheds. *Journal of the North American Benthological Society*, *25*(4), 998–1017. https://doi.org/10.1899/0887-3593(2006)025[0998:UONAOC]2.0.CO;2

Newbold, J. D., Elwood, J. W., O'Neill, R. V., & Winkle, W. Van. (1981). Measuring Nutrient Spiralling in Streams. *Canadian Journal of Fisheries and Aquatic Sciences*, *38*(7), 860–863. https://doi.org/10.1139/f81-114

Niloy, N. M., Haque, M. M., & Tareq, S. M. (2021). Characteristics, Sources, and Seasonal Variability of Dissolved Organic Matter (DOM) in the Ganges River, Bangladesh. *Environmental Processes*, *8*(2), 593–613. https://doi.org/10.1007/s40710-021-00499-y

O'Donnell, J. A., Aiken, G. R., Kane, E. S., & Jones, J. B. (2010). Source water controls on the character and origin of dissolved organic matter in streams of the Yukon River basin, Alaska. *Journal of Geophysical Research: Biogeosciences*, *115*(3), 1–12. https://doi.org/10.1029/2009JG001153

Ohno, T. (2002). Fluorescence inner-filtering correction for determining the humification index of dissolved organic matter. *Environmental Science and Technology*, *36*(4), 742–746. https://doi.org/10.1021/es0155276

Oksanen, J., Blanchet, F. G., Friendly, M., Kindt, R., Legendre, P., McGlinn, D., … Wagner, H. (2019). vegan: Community Ecology Package. R package version 2.5-6.

Osburn, C. L., Boyd, T. J., Montgomery, M. T., Bianchi, T. S., Coffin, R. B., & Paerl, H. W. (2016). Optical proxies for terrestrial dissolved organic matter in estuaries and coastal waters. *Frontiers in Marine Science*, *2*(JAN), 1–11. https://doi.org/10.3389/fmars.2015.00127

Osburn, C. L., Wigdahl, C. R., Fritz, S. C., & Saros, J. E. (2011). Dissolved organic matter composition and photoreactivity in prairie lakes of the U.S. Great Plains. *Limnology and Oceanography*, *56*(6), 2371–2390. https://doi.org/10.4319/lo.2011.56.6.2371

Paerl, H. W., & Scott, J. T. (2010). Throwing fuel on the fire: Synergistic effects of excessive nitrogen inputs and global warming on harmful algal blooms. *Environmental Science and Technology*, *44*(20), 7756–7758. https://doi.org/10.1021/es102665e

Paerl, H. W., Valdes, L. M., Joyner, A. R., Piehler, M. F., & Lebo, M. E. (2004). Solving problems resulting from solutions: Evolution of a dual nutrient management strategy for the eutrophying Neuse River Estuary, North Carolina. *Environmental Science and Technology*, *38*(11), 3068–3073. https://doi.org/10.1021/es0352350

Pagilla, K. R., Urgun-Demirtas, M., & Ramani, R. (2006). Low effluent nutrient technologies for wastewater treatment. *Water Science and Technology*, *53*(3), 165–172.

https://doi.org/10.2166/wst.2006.089

Parr, T. B., Cronan, C. S., Ohno, T., Findlay, S. E. G., Smith, S. M. C., & Simon, K. S. (2015). Urbanization changes the composition and bioavailability of dissolved organic matter in headwater streams. *Limnology and Oceanography*, *60*(3), 885–900. https://doi.org/10.1002/lno.10060

Paytan, A., & McLaughlin, K. (2011). Tracing the Sources and Biogeochemical Cycling of Phosphorus in Aquatic Systems Using Isotopes of Oxygen in Phosphate. In M. Baskaran (Ed.), *Handbook of Environmental Isotope Geochemistry* (pp. 419–436).

Peralta-Tapia, A., Sponseller, R. A., Agren, A., Tetzlaff, D., Soulsby, C., & Laudon, H. (2015). Scale-dependent groundwater contributions influence patterns of winter baseflow stream chemistry in boreal catchments. *Journal of Geophysical Research: Biogeosciences*, 847–858. https://doi.org/10.1002/2014JG002878.Received

Pielke Sr., R. A., Pitman, A., Niyogi, D., Mahmood, R., McAlpine, C., Hossain, F., … de Noblet, N. (2011). Land use/land cover changes and climate: modeling analysis and observational evidence. *WIREs Climate Change*, *828–850*.

Piña-Ochoa, E., & Álvarez-Cobelas, M. (2006). Denitrification in aquatic environments: A cross-system analysis. *Biogeochemistry*, *81*(1), 111–130. https://doi.org/10.1007/s10533-006-9033-7

Powers, S. M., Labou, S. G., Baulch, H. M., Hunt, R. J., Lottig, N. R., Hampton, S. E., & Stanley, E. H. (2017). Ice duration drives winter nitrate accumulation in north temperate lakes. *Limnology and Oceanography Letters*, *2*(5), 177–186. https://doi.org/10.1002/lol2.10048

R Core Team. (2019). R: A language and environment for statistical computing. R Foundation for Statistical Computing, Vienna, Austria.

Rabalais, N. N., Turner, R. E., & Wiseman, W. J. (2001). Hypoxia in the Gulf of Mexico. *Journal of Environmental Quality*, *30*(2), 320–329. https://doi.org/10.2134/jeq2001.302320x

Rahimi, S., Modin, O., & Mijakovic, I. (2020). Technologies for biological removal and recovery of nitrogen from wastewater. *Biotechnology Advances*, *43*(June), 107570. https://doi.org/10.1016/j.biotechadv.2020.107570

Raymond, P. A., Hartmann, J., Lauerwald, R., Sobek, S., McDonald, C., Hoover, M., … Guth, P. (2013). Global carbon dioxide emissions from inland waters. *Nature*, *503*(7476), 355–359. https://doi.org/10.1038/nature12760

Raymond, P. A., Saiers, J. E., & Sobczak, W. V. (2016). Hydrological and biogeochemical controls on watershed dissolved organic matter transport: pulse- shunt concept. *Ecology*, *97*(1), 5–16.

Redfield, A. C., Ketchum, B. H., & Richards, F. A. (1963). The Influence of Organisms on the Composition of Sea Water.

Retelletti Brogi, S., Balestra, C., Casotti, R., Cossarini, G., Galletti, Y., Gonnelli, M., Vestri, S., & Santinelli, C. (2020). Time resolved data unveils the complex DOM dynamics in a Mediterranean river. *Science of the Total Environment*, *733*, 139212. https://doi.org/10.1016/j.scitotenv.2020.139212

Retelletti Brogi, S., Casotti, R., Misson, B., Balestra, C., Gonnelli, M., Vestri, S., & Santinelli, C. (2021). DOM biological lability in an estuarine system in two contrasting periods. *Journal of Marine Science and Engineering*, *9*(2), 1–13. https://doi.org/10.3390/jmse9020172

Ribot, M., Martí, E., Von Schiller, D., Sabater, F., Daims, H., & Battin, T. J. (2012). Nitrogen processing and the role of epilithic biofilms downstream of a wastewater treatment plant. *Freshwater Science*, *31*(4), 1057–1069. https://doi.org/10.1899/11-161.1

Riedel, T., Zark, M., Vähätalo, A. V., Niggemann, J., Spencer, R. G. M., Hernes, P. J., & Dittmar, T. (2016). Molecular signatures of biogeochemical transformations in dissolved organic matter from ten world rivers. *Frontiers in Earth Science*, *4*(September), 1–16. https://doi.org/10.3389/feart.2016.00085

Russell, M. J., Weller, D. E., Jordan, T. E., Sigwart, K. J., & Sullivan, K. J. (2008). Net anthropogenic phosphorus inputs: Spatial and temporal variability in the Chesapeake Bay region. *Biogeochemistry*, *88*(3), 285–304. https://doi.org/10.1007/s10533-008-9212-9

Russell, P. A. (2012). *How Agriculture Made Canada: Farming in the Nineteenth Century*. MQUP.

Saunders, D. L., & Kalff, J. (2001). Nitrogen retention in wetlands, lakes and rivers. *Hydrobiologia*, *443*, 205–212. https://doi.org/10.1023/A:1017506914063

Schaefer, S. C., & Alber, M. (2007). Temporal and spatial trends in nitrogen and phosphorus inputs to the watershed of the Altamaha River, Georgia, USA. *Biogeochemistry*, *86*(3), 231–249. https://doi.org/10.1007/s10533-007-9155-6

Scott, J. T., McCarthy, M. J., Otten, T. G., Steffen, M. M., Baker, B. C., Grantz, E. M., Wilhelm, S. W., & Paerl, H. W. (2013). Comment: An alternative interpretation of the relationship between TN:TP and microcystins in Canadian lakes. *Canadian Journal of Fisheries and Aquatic Sciences*, *70*(8), 1265–1268. https://doi.org/10.1139/cjfas-2012-0490

Sebilo, M., Billen, G., Mayer, B., Billiou, D., Grably, M., Garnier, J., & Mariotti, A. (2006). Assessing nitrification and denitrification in the seine river and estuary using chemical and isotopic techniques. *Ecosystems*, *9*(4), 564–577. https://doi.org/10.1007/s10021-006-0151-9

Seekell, D. A., Lapierre, J.-F., & Cheruvelil, K. S. (2018). A geography of lake carbon cycling. *Limnology and Oceanography Letters*, *3*(3), 49–56. https://doi.org/10.1002/lol2.10078

Seitzinger, S., Harrison, J., Bohlke, J., Bouwman, A., Lowrance, R., Peterson, B., Tobias, C., & Van Drecht, G. (2006). Denitrification across landscapes and waterscapes: a synthesis. *Ecological Applications*, *16*(6), 2064–2090. https://doi.org/10.1890/1051-0761(2006)016[2064:DALAWA]2.0.CO;2

Sharpley, A., Jarvie, H. P., Buda, A., May, L., Spears, B., & Kleinman, P. (2013). Phosphorus Legacy: Overcoming the Effects of Past Management Practices to Mitigate Future Water Quality Impairment. *Journal of Environmental Quality*, *42*, 1308–1326.

Shen, Y., Chapelle, F. H., Strom, E. W., & Benner, R. (2015). Origins and bioavailability of dissolved organic matter in groundwater. *Biogeochemistry*, *122*(1), 61–78. https://doi.org/10.1007/s10533-014-0029-4

Shousha, S., Maranger, R., & Lapierre, J. (2021). Different forms of carbon, nitrogen, and phosphorus influence ecosystem stoichiometry in a north temperate river across seasons and land uses. *Limnology and Oceanography*, 1–14. https://doi.org/10.1002/lno.11960

Sikora, A., Detman, A., Chojnacka, A., & Blaszczyk, M. K. (2017). Anaerobic Digestion: I. A Common Process Ensuring Energy Flow and the Circulation of Matter in Ecosystems. II. A Tool for the Production of Gaseous Biofuels. In *Fermentation Processes*. https://doi.org/10.5772/64645

Skiba, U. (2008). Denitrification. In S. E. Jørgensen & B. D. Fath (Eds.), *Encyclopedia of Ecology* (pp. 866–871).

Smith, V. H., & Schindler, D. W. (2009). Eutrophication science: where do we go from here? *Trends in Ecology and Evolution*, *24*(4), 201–207. https://doi.org/10.1016/j.tree.2008.11.009

Søndergaard, M., Stedmon, C. A., & Borch, N. H. (2003). Fate of terrigenous dissolved organic matter (DOM) in estuaries: Aggregation and bioavailability. *Ophelia*, *57*(3), 161–176. https://doi.org/10.1080/00785236.2003.10409512

Soto Cárdenas, C., Gerea, M., Garcia, P. E., Pérez, G. L., Diéguez, M. C., Rapacioli, R., Reissig, M., & Queimaliños, C. (2017). Interplay between climate and hydrogeomorphic features and their effect on the seasonal variation of dissolved organic matter in shallow temperate lakes of the Southern Andes (Patagonia, Argentina): a field study based on optical properties. *Ecohydrology*, *10*(7), 1–19. https://doi.org/10.1002/eco.1872

Stan Development Team. (2019a). RStan: the R interface to Stan. R package version 2.19.2.

http://mc-stan.org/.

Stan Development Team. (2019b). Stan Modeling Language Users Guide and Reference Manual, VERSION 2.19.1. https://mc-stan.org.

Stanley, E. H., & Maxted, J. T. (2008). Changes in the dissolved nitrogen pool across land cover gradients in wisconsin streams. *Ecological Applications*, *18*(7), 1579–1590. https://doi.org/10.1890/07-1379.1

Stanley, E. H., Powers, S. M., Lottig, N. R., Buffam, I., & Crawford, J. T. (2012). Contemporary changes in dissolved organic carbon (DOC) in human-dominated rivers: Is there a role for DOC management? *Freshwater Biology*, *57*(SUPPL. 1), 26–42. https://doi.org/10.1111/j.1365-2427.2011.02613.x

Statistics Canada. (1982a). Census of Agriculture, 1981. Retrieved from http://odesi2.scholarsportal.info/webview/index.jsp?v=2&submode=abstract&study=http%3A%2F%2F142.150.190.128%3A80%2Fobj%2FfStudy%2Fagcensus-95640XWE-E-2011&mode=documentation&top=yes

Statistics Canada. (1982b). Census of Population, 1981: Profile for Quebec, Census Divisions, Census Subdivisions. Retrieved from http://dc.chass.utoronto.ca/census/

Statistics Canada. (1987a). Census of Agriculture, 1986. Retrieved from http://odesi2.scholarsportal.info/webview/index.jsp?v=2&submode=abstract&study=http%3A%2F%2F142.150.190.128%3A80%2Fobj%2FfStudy%2Fagcensus-95640XWE-E-2011&mode=documentation&top=yes

Statistics Canada. (1987b). Census of Population, 1986: Profile for Quebec, Census Divisions, Census Subdivisions. Retrieved from http://dc.chass.utoronto.ca/census/

Statistics Canada. (1992a). Census of Agriculture, 1991. Retrieved from http://odesi2.scholarsportal.info/webview/index.jsp?v=2&submode=abstract&study=http%3A%2F%2F142.150.190.128%3A80%2Fobj%2FfStudy%2Fagcensus-95640XWE-E-2011&mode=documentation&top=yes

Statistics Canada. (1992b). Census of Population, 1991: Profile for Quebec, Census Divisions, Census Subdivisions. Retrieved from http://dc.chass.utoronto.ca/census/

Statistics Canada. (1997a). Census of Agriculture, 1996. Retrieved from http://odesi2.scholarsportal.info/webview/index.jsp?v=2&submode=abstract&study=http%3A%2F%2F142.150.190.128%3A80%2Fobj%2FfStudy%2Fagcensus-95640XWE-E-2011&mode=documentation&top=yes

Statistics Canada. (1997b). Census of Population, 1996: Profile for Quebec, Census Divisions, Census Subdivisions. Retrieved from http://dc.chass.utoronto.ca/census/

Statistics Canada. (2002a). Census of Agriculture, 2001: Farm Data and Farm Operator Data, Full Release. Retrieved from http://odesi2.scholarsportal.info/webview/index.jsp?v=2&submode=abstract&study=http%3A%2F%2F142.150.190.128%3A80%2Fobj%2FfStudy%2Fagcensus-95640XWE-E-2011&mode=documentation&top=yes

Statistics Canada. (2002b). Census of Population, 2001: Profile for Quebec, Census Divisions, Census Subdivisions. Retrieved from http://dc.chass.utoronto.ca/census/

Statistics Canada. (2007a). Census of Agriculture, 2006: Farm Data and Farm Operator Data, Initial Release. Retrieved from http://odesi2.scholarsportal.info/webview/index.jsp?v=2&submode=abstract&study=http%3A%2F%2F142.150.190.128%3A80%2Fobj%2FfStudy%2Fagcensus-95640XWE-E-2011&mode=documentation&top=yes

Statistics Canada. (2007b). Census of Population, 2006: Profile for Quebec, Census Divisions, Census Subdivisions. Retrieved from http://dc.chass.utoronto.ca/census/

Statistics Canada. (2012a). Census of Agriculture, 2011: Farm Data and Farm Operator Data. Retrieved from http://odesi2.scholarsportal.info/webview/index.jsp?v=2&submode=abstract&study=http%3A%2F%2F142.150.190.128%3A80%2Fobj%2FfStudy%2Fagcensus-95640XWE-E-2011&mode=documentation&top=yes

Statistics Canada. (2012b). Census of Population, 2011: Profile for Quebec, Census Divisions, Census Subdivisions. Retrieved from http://dc.chass.utoronto.ca/census/

Statistics Canada. (2013). Fertilizer shipments to Canadian agriculture markets, by nutrient content and fertilizer year - Archived [Table 32-10-0274-01 (formerly CANSIM 001-0065)]. Retrieved from https://www150.statcan.gc.ca/t1/tbl1/en/cv!recreate.action?pid=3210027401&selectedNodeIds=1D4&checkedLevels=1D1&refPeriods=19810101,20050101&dimensionLayouts=layout2,layout3,layout2&vectorDisplay=false

Statistics Canada. (2017a). Average annual runoff in Canada, 1971 to 2013, Map 1.

Statistics Canada. (2017b). Census of Agriculture, 2016: Farm Data and Farm Operator Data, [Tables 004-0203, 004-0235, 004-0213, 004-0221/0222/0223/0224/0225/0226/0227/0228]. Retrieved

from http://odesi2.scholarsportal.info/webview/index.jsp?v=2&submode=abstract&study=http%3A%2F%2F142.150.190.128%3A80%2Fobj%2FfStudy%2Fagcensus-95640XWE-E-2011&mode=documentation&top=yes

Statistics Canada. (2017c). Census of Population, 2016: Profile for Quebec, Census Divisions, Census Subdivisions. Retrieved from http://dc.chass.utoronto.ca/census/

Statistics Canada. (2017d). Saint-Jérôme [Population centre], Quebec and Quebec [Province] (table). Census Profile.

Statistics Canada. (2017e). Survey of household spending (SHS), household equipment at the time of interview, by province, territory and selected metropolitan areas - Archived [Table 11-10-0216-01 (formerly CANSIM 203-0020)]. Retrieved from https://www150.statcan.gc.ca/t1/tbl1/en/tv.action?pid=1110021601&pickMembers%5B0%5D=1.1&pickMembers%5B1%5D=3.3

Statistics Canada. (2021a). Production, disposition and farm value of poultry meat (x1000) [Table 32-10-0117-01 (formerly CANSIM 003-0018)]. Retrieved from https://www150.statcan.gc.ca/t1/tbl1/en/cv.action?pid=3210011701#timeframe

Statistics Canada. (2021b). Production and disposition of eggs, annual [Table 32-10-0119-01 (formerly CANSIM 003-0020)]. Retrieved from https://www150.statcan.gc.ca/t1/tbl1/en/cv.action?pid=3210011901#timeframe

Statistics Canada. (2021c). Régions agricoles, Variante de la CGT 2016. Retrieved from https://www23.statcan.gc.ca/imdb/p3VD_f.pl?Function=getVD&TVD=318036&CVD=318038&CPV=24&CST=01012016&CLV=2&MLV=6

Statistics Canada. (2022a). Area, production and farm value of potatoes [Table 32-10-0358-01 (formerly CANSIM 001-0014)]. Retrieved from https://www150.statcan.gc.ca/t1/tbl1/en/cv.action?pid=3210035801

Statistics Canada. (2022b). Cattle and calves, farm and meat production [Table 32-10-0125-01 (formerly CANSIM 003-0026)]. Retrieved from https://www150.statcan.gc.ca/t1/tbl1/en/cv.action?pid=3210012501

Statistics Canada. (2022c). Estimated areas, yield, production, average farm price and total farm value of principal field crops, in metric and imperial units [Table 32-10-0359-01 (formerly CANSIM 001-0017)]. Retrieved from https://www150.statcan.gc.ca/t1/tbl1/en/cv.action?pid=3210035901

Statistics Canada. (2022d). Fertilizer shipments to Canadian agriculture markets, by nutrient content and fertilizer year, cumulative data (x 1,000) [Table 32-10-0039-01 (formerly CANSIM 001-0069)]. Retrieved from https://www150.statcan.gc.ca/t1/tbl1/en/cv.action?pid=3210003901

Statistics Canada. (2022e). Hogs, sheep and lambs, farm and meat production [Table 32-10-0126-01 (formerly CANSIM 003-0028)]. Retrieved from https://www150.statcan.gc.ca/t1/tbl1/en/cv.action?pid=3210012601#timeframe

Stedmon, C. A., & Bro, R. (2008). Characterizing dissolved organic matter fluorescence with parallel factor analysis: A tutorial. *Limnology and Oceanography: Methods*, *6*(11), 572–579. https://doi.org/10.4319/lom.2008.6.572

Stedmon, C. A., Markager, S., & Bro, R. (2003). Tracing dissolved organic matter in aquatic environments using a new approach to fluorescence spectroscopy. *Marine Chemistry*, *82*(3–4), 239–254. https://doi.org/10.1016/S0304-4203(03)00072-0

Sterner, R. W., & Elser, J. J. (2002). *Ecological Stoichiometry: The Biology of Elements from Molecules to the Biosphere*. Oxfordshire, UK: Princeton University Press.

Strauss, E. A., Richardson, W. B., Bartsch, L. A., Cavanaugh, J. C., Bruesewitz, D. A., Imker, H., Heinz, J. A., & Soballe, D. M. (2004). Nitrification in the Upper Mississippi River: Patterns, controls, and contribution to the NO3- budget. *Journal of the North American Benthological Society*, *23*(1), 1–14. https://doi.org/10.1899/0887-3593(2004)023<0001:NITUMR>2.0.CO;2

Stubbins, A., Lapierre, J. F., Berggren, M., Prairie, Y. T., Dittmar, T., & Del Giorgio, P. A. (2014). What's in an EEM? Molecular signatures associated with dissolved organic fluorescence in boreal Canada. *Environmental Science and Technology*, *48*(18), 10598–10606. https://doi.org/10.1021/es502086e

Stutter, M. I., Graeber, D., Evans, C. D., Wade, A. J., & Withers, P. J. A. (2018). Balancing macronutrient stoichiometry to alleviate eutrophication. *Science of the Total Environment*, *634*, 439–447. https://doi.org/10.1016/j.scitotenv.2018.03.298

Swaney, D. P., Hong, B., & Howarth, R. W. (2018). NANI/NAPI Calculator Toolbox Version 3.1 Documentation, 1–46. Retrieved from http://www.balticnest.org/balticnest/research/publications/

Talluto, M. V. (2020). WatershedTools: An R package for the spatial analysis of watersheds. Version 1.2.0.

Teodoru, C., & Wehrli, B. (2005). Retention of sediments and nutrients in the Iron Gate I Reservoir on the Danube River. *Biogeochemistry*, *76*(3), 539–565. https://doi.org/10.1007/s10533-005-

0230-6

Thornton, D. C. O. (2014). Dissolved organic matter (DOM) release by phytoplankton in the contemporary and future ocean. *European Journal of Phycology*, *49*(1), 20–46.

Tiwari, T., Buffam, I., Sponseller, R. A., & Laudon, H. (2017). Inferring scale-dependent processes influencing stream water biogeochemistry from headwater to sea. *Limnology and Oceanography*, *62*, S58–S70. https://doi.org/10.1002/lno.10738

USDA. (2007). Profitable Grazing-Based Dairy Systems. *Range and Pasture Technical Note No. 1*, (1), 1–40. Retrieved from https://www.nrcs.usda.gov/Internet/FSE_DOCUMENTS/stelprdb1044245.pdf

USDA. (2017). United States Department of Agriculture: Natural Resources Conservation Service, Technical Resources, Appendix 1 : Nutrient Uptake and Removal. Retrieved from https://www.nrcs.usda.gov/wps/portal/nrcs/main/national/technical/nra/nri/results/

USEPA-350.1. (1993). Method 350.1, Revision 2.0: Determination of Ammonia Nitrogen by Semi-Automated Colorimetry. In: Agency USEP, editor. 15.

USEPA-352.3. (1993). Method 352.3, Revision 2.0: Determination of Nitrate-Nitrite Nitrogen by Automated Colorimetry. In: Agency USEP, editor. 13.

USEPA-365.1. (1993). Method 365.1, Revision 2.0: Determination of Phosphorus by Semi-Automated Colorimetry. In: Agency USEP, editor. 18.

USEPA-415.1. (1974). Method 415.1 : Organic Carbon, Total (Combustion or Oxidation). In: Agency USEP, editor. 3.

Van Breemen, N., Boyer, E. W., Goodale, C. L., Jaworski, N. A., Paustian, K., Seitzinger, S. P., … Billen, G. (2002). Where did all the nitrogen go? Fate of nitrogen inputs to large watersheds in the northeastern U.S.A. *Biogeochemistry*, *57–58*, 267–293. https://doi.org/10.1023/A:1015775225913

Van Meter, K. J., Basu, N. B., Veenstra, J. J., & Burras, C. L. (2016). The nitrogen legacy: Emerging evidence of nitrogen accumulation in anthropogenic landscapes. *Environmental Research Letters*, *11*(3). https://doi.org/10.1088/1748-9326/11/3/035014

Van Meter, K. J., McLeod, M. M., Liu, J., Tenkouano, G. T., Hall, R. I., Van Cappellen, P., & Basu, N. B. (2021). Beyond the Mass Balance: Watershed Phosphorus Legacies and the Evolution of the Current Water Quality Policy Challenge. *Water Resources Research*, *57*, 1–22.

Van Staden, T. L., Van Meter, K. J., Basu, N. B., Parsons, C. T., Akbarzadeh, Z., & Van Cappellen, P. (2021). Agricultural phosphorus surplus trajectories for Ontario, Canada (1961–2016), and

erosional export risk. *Science of the Total Environment*, (xxxx). https://doi.org/10.1016/j.scitotenv.2021.151717

Vanni, M. J., Renwick, W. H., Headworth, J. L., Auch, J. D., & Schaus, M. H. (2001). Dissolved and particulate nutrient flux from three adjacent agricultural watersheds: A five-year study. *Biogeochemistry*, *54*(1), 85–114. https://doi.org/10.1023/A:1010681229460

Vidon, P., Wagner, L. E., & Soyeux, E. (2008). Changes in the character of DOC in streams during storms in two Midwestern watersheds with contrasting land uses. *Biogeochemistry*, *88*(3), 257–270. https://doi.org/10.1007/s10533-008-9207-6

Vitousek, P. M., & Howarth, R. W. (1991). Nitrogen limitation on land and in the sea: How can it occur? *Biogeochemistry*, *13*(5), 87–115.

Vitousek, P. M., Porder, S., Houlton, B. Z., & Chadwick, O. A. (2010). Terrestrial phosphorus limitation: Mechanisms, implications, and nitrogen-phosphorus interactions. *Ecological Applications*, *20*(1), 5–15. https://doi.org/10.1890/08-0127.1

von Schiller, D., Acuña, V., Aristi, I., Arroita, M., Basaguren, A., Bellin, A., … Elosegi, A. (2017). River ecosystem processes: A synthesis of approaches, criteria of use and sensitivity to environmental stressors. *Science of the Total Environment*, *596–597*(April), 465–480. https://doi.org/10.1016/j.scitotenv.2017.04.081

Von Wachenfeldt, E., & Tranvik, L. J. (2008). Sedimentation in boreal lakes - The role of flocculation of allochthonous dissolved organic matter in the water column. *Ecosystems*, *11*(5), 803–814. https://doi.org/10.1007/s10021-008-9162-z

Waiser, M. J., Tumber, V., & Holm, J. (2011). Effluent-dominated streams. Part 1: Presence and effects of excess nitrogen and phosphorus in Wascana Creek, Saskatchewan, Canada. *Environmental Toxicology and Chemistry*, *30*(2), 496–507.

Wauthy, M., Rautio, M., Christoffersen, K. S., Forsström, L., Laurion, I., Mariash, H. L., Peura, S., & Vincent, W. F. (2018). Increasing dominance of terrigenous organic matter in circumpolar freshwaters due to permafrost thaw. *Limnology and Oceanography Letters*, *3*(3), 186–198. https://doi.org/10.1002/lol2.10063

Weishaar, J., Aiken, G., Bergamaschi, B., Fram, M., Fujii, R., & Mopper, K. (2003). Evaluation of specific ultra-violet absorbance as an indicator of the chemical content of dissolved organic carbon. *Environmental Science and Technology*, *37*(20), 4702–4708. https://doi.org/10.1021/es030360x

Wetzel, R. G. (1995). Death, detritus, and energy flow in aquatic ecosystems. *Freshwater Biology*, *33*(1),

83–89. https://doi.org/10.1111/j.1365-2427.1995.tb00388.x

Weyhenmeyer, G. A., & Conley, D. J. (2017). Large differences between carbon and nutrient loss rates along the land to ocean aquatic continuum-implications for energy:nutrient ratios at downstream sites. *Limnology and Oceanography*, (Prairie 2008). https://doi.org/10.1002/lno.10589

Weyhenmeyer, G. A., Fröberg, M., Karltun, E., Khalili, M., Kothawala, D., Temnerud, J., & Tranvik, L. J. (2012). Selective decay of terrestrial organic carbon during transport from land to sea. *Global Change Biology*, *18*(1), 349–355. https://doi.org/10.1111/j.1365-2486.2011.02544.x

Wickland, K. P., Aiken, G. R., Butler, K., Dornblaser, M. M., Spencer, R. G. M., & Striegl, R. G. (2012). Biodegradability of dissolved organic carbon in the Yukon River and its tributaries: Seasonality and importance of inorganic nitrogen. *Global Biogeochemical Cycles*, *26*(3), 1–14. https://doi.org/10.1029/2012GB004342

Wiegner, T. N., Tubal, R. L., & MacKenzie, R. A. (2009). Bioavailability and export of dissolved organic matter from a tropical river during base- And stormflow conditions. *Limnology and Oceanography*, *54*(4), 1233–1242. https://doi.org/10.4319/lo.2009.54.4.1233

Wiken, E. B., Gauthier, D., Marshall, I., Lawton, K., & Hirvonen, H. (1996). A Perspective on Canada's Ecosystems. *Canadian Council on Ecological Areas*, *14*.

Williams, C. J., Yamashita, Y., Wilson, H. F., Jaffé, R., & Xenopoulos, M. A. (2010). Unraveling the role of land use and microbial activity in shaping dissolved organic matter characteristics in stream ecosystems. *Limnology and Oceanography*, *55*(3), 1159–1171. https://doi.org/10.4319/lo.2010.55.3.1159

Wilson, H. F., & Xenopoulos, M. A. (2009). Effects of agricultural land use on the composition of fluvial dissolved organic matter. *Nature Geoscience*, *2*(1), 37–41. https://doi.org/10.1038/ngeo391

Winterdahl, M., Erlandsson, M., Futter, M. N., Weyhenmeyer, G. A., & Bishop, K. H. (2014). Intra-annual variability of organic carbon concentrations in running waters: Drivers along a climatic gradient. *Global Biogeochemical Cycles*, *28*, 451–464. https://doi.org/10.1002/2013GB004770.Received

Withers, P. J. A., & Jarvie, H. P. (2008). Delivery and cycling of phosphorus in rivers: A review. *Science of the Total Environment*, *400*(1–3), 379–395. https://doi.org/10.1016/j.scitotenv.2008.08.002

Wollheim, W. M., Harms, T. K., Robison, A. L., Koenig, L. E., Helton, A. M., Song, C., Bowden, W. B., & Finlay, J. C. (2022). Superlinear scaling of riverine biogeochemical function with

watershed size. *Nature Communications*, *13*(1), 1–9. https://doi.org/10.1038/s41467-022-28630-z

Wu, H., Xu, X., Fu, P., Cheng, W., & Fu, C. (2021). Responses of soil WEOM quantity and quality to freeze–thaw and litter manipulation with contrasting soil water content: A laboratory experiment. *Catena*, *198*(April 2020), 105058. https://doi.org/10.1016/j.catena.2020.105058

Wu, K., Lu, K., Dai, M., & Liu, Z. (2019). The bioavailability of riverine dissolved organic matter in coastal marine waters of southern Texas. *Estuarine, Coastal and Shelf Science*, *231*.

Wünsch, U. J., Murphy, K. R., & Stedmon, C. A. (2017). The One-Sample PARAFAC Approach Reveals Molecular Size Distributions of Fluorescent Components in Dissolved Organic Matter. *Environmental Science and Technology*, *51*(20), 11900–11908. https://doi.org/10.1021/acs.est.7b03260

Xenopoulos, M. A., Barnes, R. T., Boodoo, K. S., Butman, D., Catalán, N., D'Amario, S. C., … Wilson, H. F. (2021). How humans alter dissolved organic matter composition in freshwater: relevance for the Earth's biogeochemistry. *Biogeochemistry*, *3*. https://doi.org/10.1007/s10533-021-00753-3

Yang, Y. Y., & Toor, G. S. (2018). Stormwater runoff driven phosphorus transport in an urban residential catchment: Implications for protecting water quality in urban watersheds. *Scientific Reports*, *8*(1), 1–10. https://doi.org/10.1038/s41598-018-29857-x

Yuan, L. L., Pollard, A. I., Pather, S., Oliver, J. L., & D'Anglada, L. (2014). Managing microcystin: Identifying national-scale thresholds for total nitrogen and chlorophyll a. *Freshwater Biology*, *59*(9), 1970–1981. https://doi.org/10.1111/fwb.12400

Zarnetske, J. P., Bouda, M., Abbott, B. W., Saiers, J., & Raymond, P. A. (2018). Generality of Hydrologic Transport Limitation of Watershed Organic Carbon Flux Across Ecoregions of the United States. *Geophysical Research Letters*, *45*(21), 11,702-11,711. https://doi.org/10.1029/2018GL080005

Zhou, Yongli, Martin, P., & Müller, M. (2019). Composition and cycling of dissolved organic matter from tropical peatlands of coastal Sarawak, Borneo, revealed by fluorescence spectroscopy and parallel factor analysis. *Biogeosciences*, *16*(13), 2733–2749. https://doi.org/10.5194/bg-16-2733-2019

Zhou, Yongqiang, Yao, X., Zhou, L., Zhao, Z., Wang, X., Jang, K., … Wu, F. (2021). How hydrology and anthropogenic activity in fl uence the molecular composition and export of dissolved organic matter : Observations along a large river continuum. *Limnology*, (66), 1730–1742. https://doi.org/10.1002/lno.11716

Zimmermann, C. F., Keefe, C. W., Bashe, J., Luther, W. M., Drive, K., Arar, E. J., & Agency, U. S. E. P. (1997). Determination of Carbon and Nitrogen in Sediments and Particulates of Estuarine / Coastal Waters Using Elemental Analysis University of Maryland System Center for Environmental Estuarine Studies Chesapeake Biological Laboratory and Work Assignment Manager. *EPA Method 440.0*, 1–10.

Zsolnay, A., Baigar, E., & Jimenez, M. (1998). Differentiating With Fluorescence Spectroscopy the Sources of. *Chemosphere*, *38*(1), 45–50.